OBSERVING VARIATION OF ACOUSTICAL CHARACTERISTICS OF SEVERAL COMMON FIREARMS IN A QUASI ANECHOIC ENVIRONMENT AT A HIGH SAMPLING RATE

by

Tushar Kanti Routh

A thesis submitted in partial fulfillment
of the requirements for the degree

of

Master of Science

in

Electrical & Computer Engineering

MONTANA STATE UNIVERSITY
Bozeman, Montana

August 2016

ACKNOWLEDGEMENTS

First, praises and thanks to the God, the Almighty, for His showers of blessings to complete the research successfully.

I would like to express my deep and sincere gratitude to my research supervisor, Dr. Robert C Maher, Ph.D., P.E., Professor, and Head, Department of Electrical & Computer Engineering, Montana State University, Bozeman, Montana, for providing the opportunity and invaluable guidance throughout this research. His dynamism, vision, sincerity and motivation have deeply inspired me. It was a great privilege and honor to carry out my work under his guidance. I am extremely grateful for what he has offered me not only as a mentor but also as a human being. I would also like to thank him for his patience, empathy, and most importantly, understanding me as a person.

My Special thanks go to Prof. Steven Shaw for his support in gunshot recordings. I am extremely grateful to Angelo Borzino, for his support in the interpretation of recorded signals. I am extending my gratitude to Tyler Davis, for his assistance during the whole period.

Finally, my thanks go to my parents and all my friends and staff of this department, who has directly and indirectly, supported me to complete the research work.

TABLE OF CONTENTS

TABLE OF CONTENTS CONTINUED

TABLE OF CONTENTS CONTINUED

LIST OF TABLES

LIST OF FIGURES

LIST OF FIGURES CONTINUED

Figure Page

LIST OF FIGURES CONTINUED

Figure Page

LIST OF FIGURES CONTINUED

Figure Page

LIST OF FIGURES CONTINUED

Figure Page

LIST OF FIGURES CONTINUED

Figure Page

LIST OF FIGURES CONTINUED

Figure Page

LIST OF FIGURES CONTINUED

Figure Page

LIST OF FIGURES CONTINUED

Figure Page

LIST OF FIGURES CONTINUED

Figure Page

LIST OF FIGURES CONTINUED

Figure Page

LIST OF FIGURES CONTINUED

Figure Page

LIST OF FIGURES CONTINUED

Figure Page

LIST OF FIGURES CONTINUED

NOMENCLATURE

Short from	***Full form***
22LR, 22lr, 22r	0.22 caliber long rifle
308, 308r	Winchester rifle with 0.308 caliber ammunition
Colt 1911A1 (45ACP)	0.45 caliber Automatic Colt pistol
AR 15, AR 15r	Stag Arms ArmaLite 15 rifle
C45	1911A1 series 70 made by Colt, chambered in 45 ACP
G19	Glock 19 pistol
G23	Glock 23 pistol
Glock 19/135 JHP	Glock 19 pistol with 135 Jacketed Hollow Point ammunition
Glock 23-40	Glock 23 pistol with 0.40 caliber ammunition
ms	Milliseconds
Shot, S	Gunshot
Mic, M	Microphone
Pa	Pascal
Ruger SP101-357, R357	Ruger SP 101 pistol with 0.357 caliber magnum ammunition
Ruger SP101-38, R38	Ruger SP 101 pistol with 0.38 caliber special ammunition
Sig 239	Sig Sauer p239 pistol
Sig 239-357	Sig Sauer P239 pistol with 0.357 caliber ammunition

ABSTRACT

Audio recordings from a shooting incident may provide crucial information for a criminal investigation. A typical gunshot signal includes two high amplitude and short duration impulsive signature sounds, the muzzle blast, observed in all the gunshot waveforms, and the bullet's shock wave, which can only be detected if the bullet travels at supersonic speed. Acoustic gunshot analysis generally focuses on the study of muzzle blast signals, which last only a few milliseconds. Ideally, gunshot signals needed to be record at a very high sampling rate to reveal the muzzle blast details. Real life gunshot recordings are record with equipment not designed for these high-amplitude sounds. Moreover, the recordings contain the direct sound of the gun along with multiple overlapping signals due to sound reflections from the ground, nearby surfaces, and other obstacles. The resulting reverberant recording may be difficult to interpret. To study the details of these signals in a scientific manner, we have developed a quasi-anechoic procedure to capture gunshot signals at a very high sampling rate (500 kHz samples per second) using 12 microphones covering 180° in azimuth. The recordings are made in an open air environment with a raised shooting platform and microphone position, resulting in sufficient delay between the arrival of the direct sound at the microphones and the arrival of the first reflection (from the ground). The firearms used in this experiment include a Remington 870 shotgun, 308 Winchester rifle, AR15 rifle, and a 22LR rifle. Handguns tested include a Colt 1911A1, Glock 19 with 9mm ammunition, Glock 23, Sig 239, and a Ruger SP101 with both 357 Magnum and 38 Special ammunition. A number of successive shots were record for each of the firearm type. Based on analysis of the recorded data, we find that acoustic gunshot signals vary from one firearm to another in terms of peak sound pressure and Muzzle blast duration. For a given firearm, we observe significant differences in sound level and also Muzzle blast duration as a function of azimuth and find that there is measurable variation in signal details among successive shots from the same firearm.

1. INTRODUCTION

1.1 Introduction

Although human civilization invented the techniques of recording audio signals nearly hundred years ago, utilization of the invention in the field of forensics is relatively new (Maher 2010) . Since the 1960's, different agencies have engaged themselves in audio forensics, including improving audio intelligibility of recordings from different sources. One accepted definition of the field is: "Audio forensics refers to the acquisition, analysis, and evaluation of audio recordings that may ultimately be presented as admissible evidence in a court of law or some other official venue"(Maher, 2009a). Nowadays, recorded gunshot signals are often considered to be an important source of information regarding a shooting incident, and may provide conclusive evidence in a case which can be presented before the court (Maher, 2009b).

1.2 Motivation

Acoustic gunshot signals can play an important role in audio forensic investigations involving gunfire. Gunshot signals, captured from some sort of recording systems placed near a crime scene, can answer questions which are crucial for a judgement (Maher and Shaw, 2014). There is a general perception regarding any kind of recorded gunshot signal that the sound can unmask facts about the firearm and the ammunition. Unfortunately, this has not been the case in reality. A recorded gunshot signal fired from a specific firearm with a specific type of ammunition will theoretically exhibit differences depending on the recording medium, the environment around the

source and many other factors. Moreover, these small duration signals produce reflections from surrounding structures and from the ground. In addition to the direct sound path, these reflected signals result in a complicated received signal at the measurement position which is difficult to analyze (American Private Inverstigator 2013).

In recent years there has been increased interest in gunshot acoustics due to the fact that law enforcement agencies are now largely equipped with devices that are capable of capturing gunshot signals. Audio forensic experts are often called for to provide their expert opinions before the court regarding gunshot incidents. Commonly raised questions include who started the firing, how many shots were there, what was the position of the shooter at that particular time, etc. Despite the importance of these questions, the acoustic characteristics of gunshot recordings is currently little understood in an objective sense; often subject to unscientific physical misunderstanding and subjective interpretation. Moreover, the limitations of commonly available audio recorders can seriously affect the expert's ability to reach a reliable conclusion.

The present state of knowledge of gunshot audio forensics indicates a need for systematic study in this area to explore these answers. This current research studies several aspects of gunshot acoustics in an organized manner. The findings are expected to increase the present knowledge of gunshot acoustical characterization and to understand the strengths and weaknesses of gunshot recordings for forensic interpretation.

The following goals are to be achieved by this research.

Goal 1: To study the acoustical characteristics of different firearms

In this study, we have selected a group of commonly used firearms covering pistols, rifles, and a shotgun. We studied several acoustical features of each firearm, including peak pressure level from the muzzle blast, Muzzle blast duration, total sound power, etc. Our goal was to observe the acoustical behavior of a particular firearm from the captured signal and make a comparative study of the different types.

Goal 2: To study the directional aspect of gunshots

One of the common questions in investigations involving recorded gunshots has been the position and orientation of the firearm with respect to the recording microphone. Previous studies revealed that gunshot signals vary significantly when the firearm is pointed in different directions. Furthermore, as acoustic gunshot analysis deals with the interpretation of very brief, impulsive signal events, the need to identify and to interpret subtle details demands higher sampling rates of the recorded signals. Therefore, one of the objectives of our present work is to study the azimuthal variation at a very high sampling rate. We also develop means to predict the nature of a selected gunshot signal observed in a particular direction.

Goal 3: Deciphering real life recordings

Real life gunshot signals contain background noise, reflections, and reverberation, which complicate interpretation of the signals. Moreover, gunshot-recording devices in real life have limited bandwidth, relatively low sampling rates, and other issues, which limit the intelligibility of the recorded data. Our final goal is to compare real life recordings with our experimental recordings obtained under relatively controlled conditions.

1.3 Broader Impacts

Over the last two decades, dashboard-mounted video camera systems have become widespread in police cruisers. Moreover, with the advancement of technology, the use of lightweight audio capturing devices has become very common. As these portable recording devices are becoming omnipresent, gunshot audio evidence from such equipment is drawing more attention for researchers (Maher and Shaw, 2014). There is no doubt that the availability of such recordings will lead to requests for forensic conclusions that were not possible before. For cases in which the court has audio recordings as evidence, the forensic experts are asked to identify the particular type of firearm and the shooting position, or to discriminate between different firearm types based on those recordings. These problems are difficult to solve without understanding acoustical differences between firearms and differences due to the spatial position and orientation of the firearm with respect to the recording microphone (Maher and Shaw, 2010).

The broader impacts of this work will aid forensic examiners to gather knowledge about the acoustical characteristics of firearms and to determine the type, location, and orientation of firearms at a shooting scene, enabling them to draw legitimate conclusions. In addition, this work is expected to be beneficial for increasing the acceptance of audio gunshot recording as legitimate and reliable forensic evidence.

2. LITERATURE REVIEW

2.1 Formation of Gunshot Wave

Traditional firearms use gunpowder and a projectile mounted inside an ammunition cartridge. The firing mechanism of a conventional firearm can be described as follows: once the trigger is pulled, the firing pin strikes the base of the cartridge, igniting the primer inside the cartridge. The primer generates a spark which rapidly burns the gunpowder and pressurizes the cartridge casing, forcing the bullet to move down the bore of the barrel at high speed.

Only a portion of the blast energy drives the bullet. Some of the energy from gunpowder combustion is lost as heat, and some of the energy escapes through the muzzle opening as a pressure disturbance (Klingenberg 1989). This rapid emission creates a pressure imbalance and acoustic shock outside the barrel that travels through the air at the speed of sound. This acoustic pressure disturbance is known as the *muzzle blast* (Hamernik & Hsueh 1991).

In addition to the muzzle blast, the gunshot signal may also include a ballistic shockwave if the bullet travels faster than the speed of sound. If the bullet leaves the muzzle at supersonic speed, air molecules in front of the bullet cannot dissipate the energy as a normal acoustical pressure wave. As a result, a *shock wave* occurs (Needham, 2010). The nonlinear nature of the shock wave results in rapid conversion of the pressure disturbance into heat, so the effect dissipates more quickly when propagating through the air than for a conventional sound wave (Snow 1967) .

Strength of any bullet shock wave is determined by the cone along the path; known as the *Mach angle*. The angle, α_M, is related to the bullet velocity as follows:

$$\propto_M = \arcsin\frac{1}{M}$$

Where,

$$M = \frac{Velocity\ of\ the\ bullet}{Velocity\ of\ Sound} \quad (2.1)$$

M is known as the *Mach number*.

As the trajectory of the bullet depends on factors like firearm structure, bullet mass, and other features, the study of shock waves is crucial for forensic gunshot analysis (Maher, 2009b).

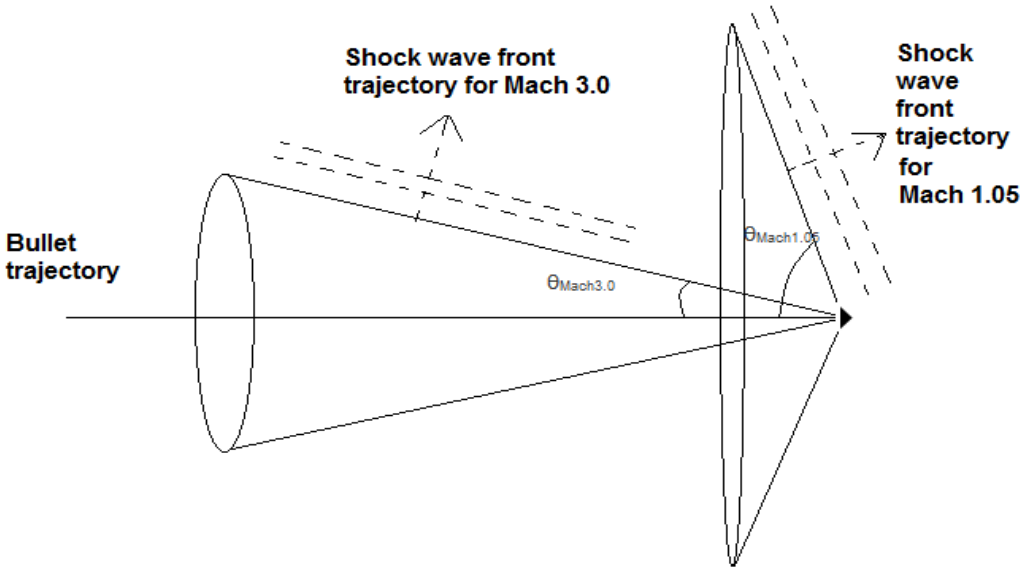

Figure 2.1.1: Shockwave generation by a supersonic bullet (Maher, 2009b)

The following figure shows the series of important elements of a typical gunshot recording. A .308 Winchester rifle gunshot has been chosen to demonstrate the features

as the ammunition used in this example was supersonic. With a particular type of ammunition (175 gr Sierra MK), the muzzle velocity is expected to be 2800 feet per second (853 meters per second). This speed corresponds to a Mach number of 2.53 (sound velocity was considered to be 337 m/s at 10°C) and thereby, with a Mach angle of 23.28°.

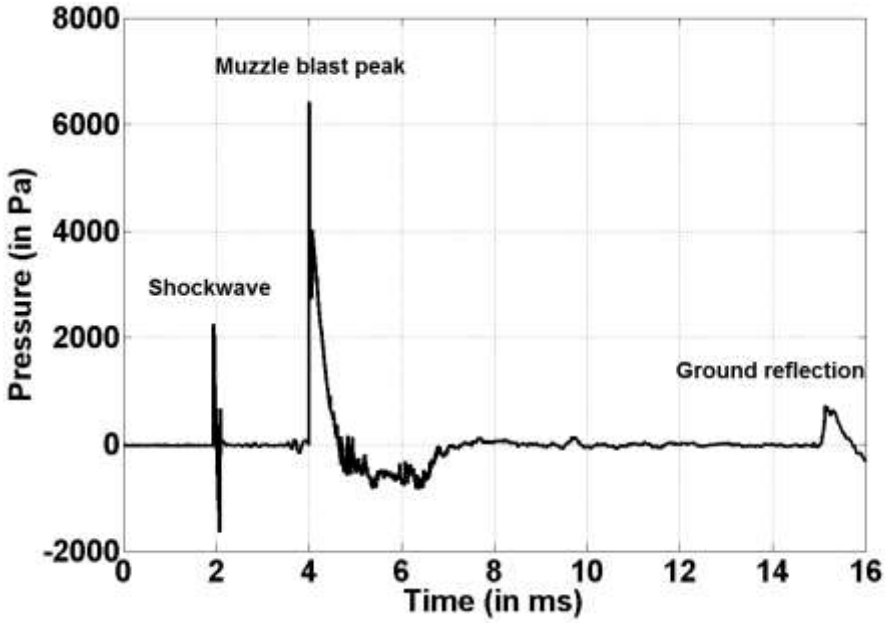

Figure 2.1.2: Pressure variation due to firing from Winchester rifle with 0.308 caliber. Microphone was nearly located at 3 m distance at the line of fire and at a height 3m above the ground

As seen from figure 2.1.2, the ballistic shock wave due to the supersonic projectile appears much before muzzle blast as expected (nearly 2 milliseconds in this case) because the bullet traveling at 853 m/s reaches the vicinity of the microphone before the sound of the muzzle blast (337 m/s). The duration of this shock wave is much shorter than the muzzle blast and much lower in amplitude. Immediately after that, the

muzzle blast wave appears with an abrupt pressure rise, which lasts for approximately 4 milliseconds. Finally, the ground reflected muzzle blast reaches the receiver roughly 7-8 ms later. This time gap in between the direct and reflected sound will depend on the surroundings of the shot. The study of acoustic gunshot signals largely includes the study of the ballistic shock wave and the muzzle blast waves.

2.2 Ground Reflection of Gunshot Signals

In this work, the goal was to analyze the muzzle blast and ballistic shockwave with as little interference as possible. In order to separate the signal of interest from the reflections, it was important to create a relative delay between the direct and reflected signals so that they would not overlap at the microphone.

A prior study by Beck, Nakasone, and Marr (2011) described what happens when a person shoots from a standing position. If firing takes place at the ground level, reflection from the ground overlaps the direct signal quite early, so the information of interest about the muzzle blast waveform is disturbed. The direct sound and the ground reflection sound, both are shown in figure 2.2.1.

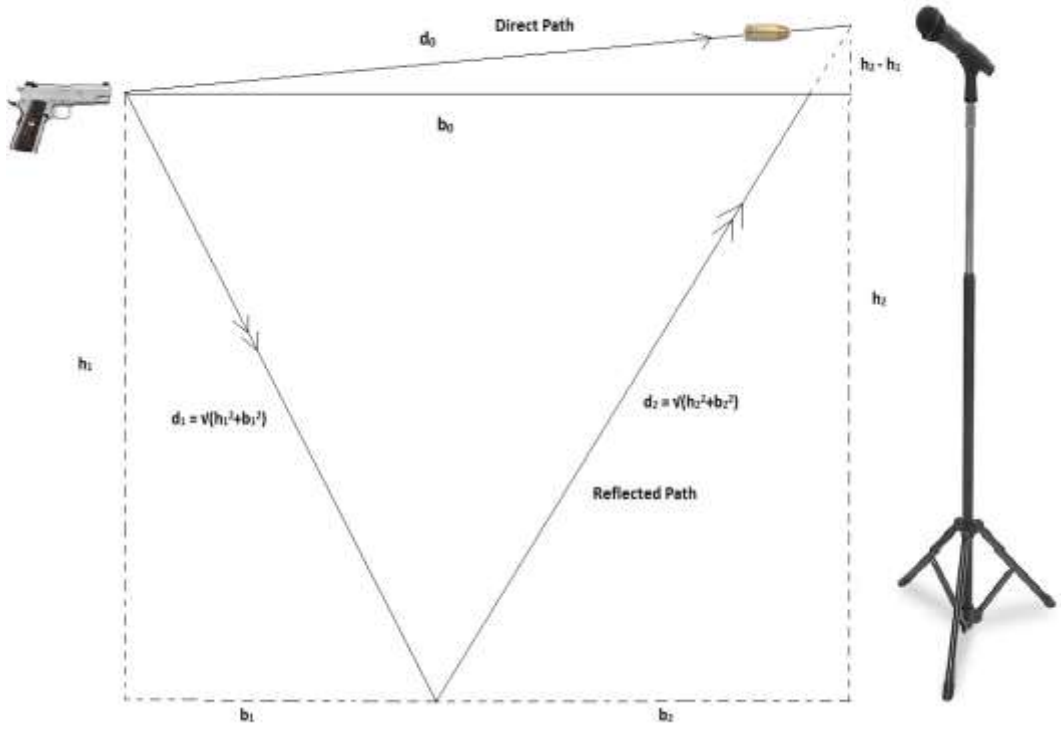

Figure 2.2.1: Path length difference in between the direct and the ground reflected wave (Beck et al. 2011)

Beck, Nakasone, and Marr showed that the calculation for the direct and indirect path will be

$$d_1 = \sqrt{{h_1}^2 + {b_1}^2} \quad , d_2 = \sqrt{{h_2}^2 + {b_2}^2} \quad \text{and} \quad d_0 = \sqrt{(h_1 - h_2)^2 + {b_0}^2} \tag{2.2}$$

Where,
d_1= source to point direct path distance;

d_2= source to point direct path distance;

h_1= height of source above ground; h_2= height of microphone above ground;

b_1= projected distance of d_1 along ground; b_2= projected distance of d_2 along ground;

b_0= surface distance in between source and microphone;

Formula for the time lag was,

$$t_{lag} = \frac{2h_1h_2}{v_0b_0} \quad (2.3)$$

Where, v_0 = velocity of sound

It has been shown in the model that if the firearm is held h_1 = 1.5 meters above the ground and the microphone is b_0 = X meters distant, the time lag will be approximately 8.7ms between the direct and ground- reflected waves if the sound velocity is 344m/s at 20° C (Beck et al. 2011).

In 2010, an elevated arrangement was proposed to capture the variation of gunshot sounds with respect to the azimuth (Maher and Shaw, 2010). In order to capture the total range of azimuth angles, several successive shots were used and a pair of microphone was shifted to a new azimuth position between each shot. The geometry (shown in figure 2.2.3) was termed *quasi-anechoic* because signals were not entirely free from reflections. Rather, the reflections arrived at the microphones with sufficient time delay so that the reflected sound did not overlap the direct sound of the muzzle blast. Reflections from the metal frame and other nearby bodies were ignored.

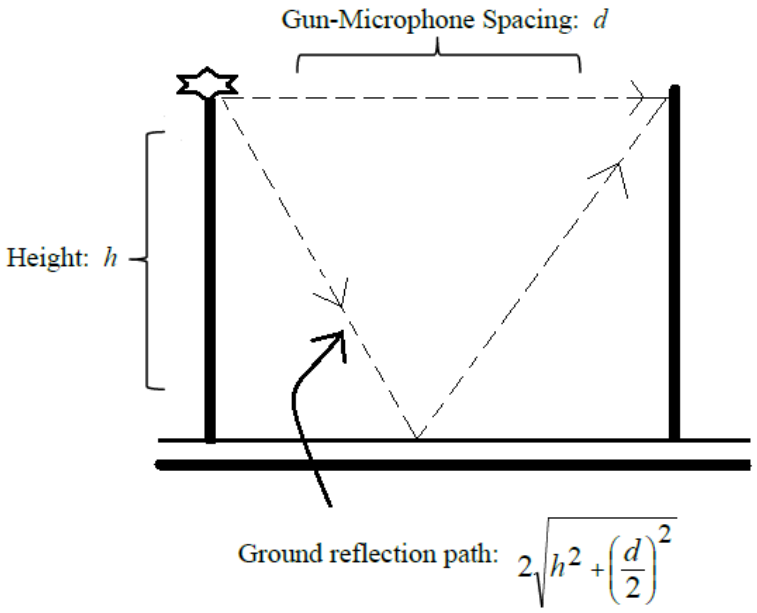

Figure 2.2.2: Quasi-anechoic Gunshot Capturing Model

If the velocity of sound is c, then the time difference between direct and indirect wave was simplified as,

$$T_{diff} = \left(\frac{1}{c}\right)\left[2\sqrt{h^2+\left(\frac{d}{2}\right)^2} - d\right] \tag{2.4}$$

This method held some limitations. Because gunshot signals may vary considerably for successive shots and there is no way to synchronize the waveforms, recording a succession of shots at different azimuths could be misleading. Moreover, the set up was inconvenient for efficient recording of multiple shots by multiple firearms.

For the current work, a new quasi-anechoic recording system was devised using multiple microphones that can record a single gunshot sound at multiple azimuths simultaneously.

2.3 Defining Muzzle Blast Wave

In 1939, Weber developed a primary model which worked fine for describing power emanating from a small pistol shot (Hirsch & Bertels 2013). In his model, the wave generated from a gunshot was considered as an acoustic noise source. He compared gunshot signals to the acoustic disturbance generated from an electronic discharge in between electrodes in a spark gap. The intensity of this wave was thought to be the same in all directions (omnidirectional).

If we consider, d= Distance, ζ = Frequency, θ= Direction, then energy output, *E*, from such a blast can be written as,

$$E\ (d, \zeta, \theta)\ =\ S\ (d, \zeta).D\ (\theta, \zeta) \qquad (2.5)$$

S is referred to as the Source Strength, and *D* is the Directionality factor (K.-W. Hirsch,1998).

The original Weber model does not deal with any directionality, so D (θ, ζ) can be considered 1. (K. Hirsch & Bertels, 2013)

Baker proposed a similar theory in slightly different manner (Baker, 1973). He modeled an ideal blast wave as shown in figure 2.4.1. He considered both positive and negative pressure durations of the blast wave.

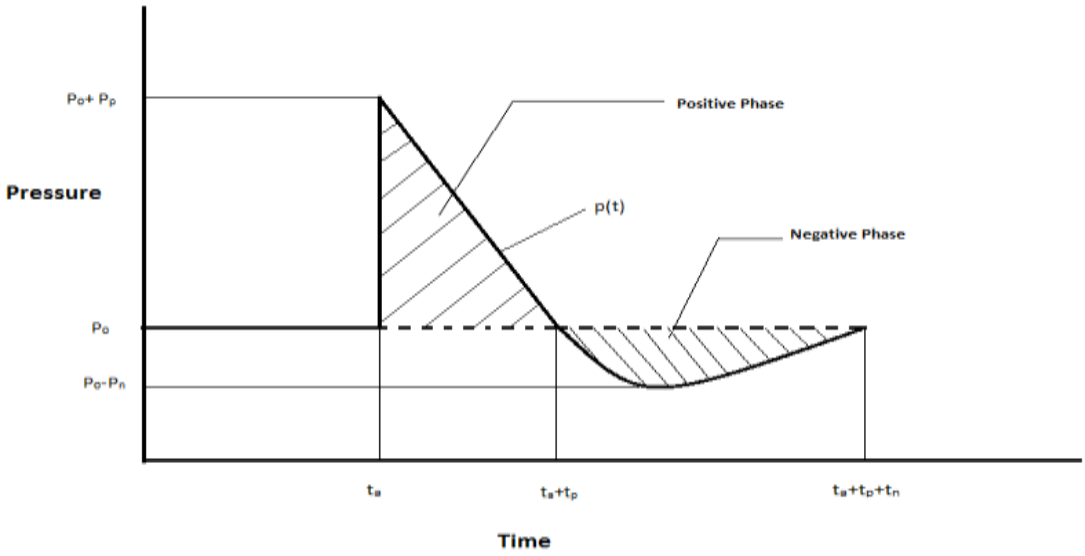

Figure 2.3.1: Ideal blast wave proposed by Baker (Baker 1973)

Thus the positive and negative impulses were defined as

$$I_{positive} = \int_{ta}^{ta+tp} [p(t) - po]dt \tag{2.6}$$

and

$$I_{negative} = \int_{ta+tp}^{ta+tp+tn} [po - p(t)]dt \tag{2.7}$$

2.4 Calculating Total Energy from a Blast Wave

The total acoustic energy for each signal can be calculated based on the framework provided by Deželak, Čurović, & Čudina (2016). Their assumption is that the gun muzzle can be considered as a point acoustic sound source and the muzzle blast can be considered the predominant portion of the total wave energy.

The total acoustic energy from a single shot was considered to be the area enclosed by the sound power as a function of t, *W(t)* as shown in figure 2.4.1. If the sound intensity in free field method is applied, sound intensity, *I(t)*, which is a function of time, is provided by,

$$I(t) = p(t)\boldsymbol{u}(\boldsymbol{t}) \tag{2.8}$$

Where, *p(t)*= sound pressure; ***u(t)*** = atmospheric particle velocity

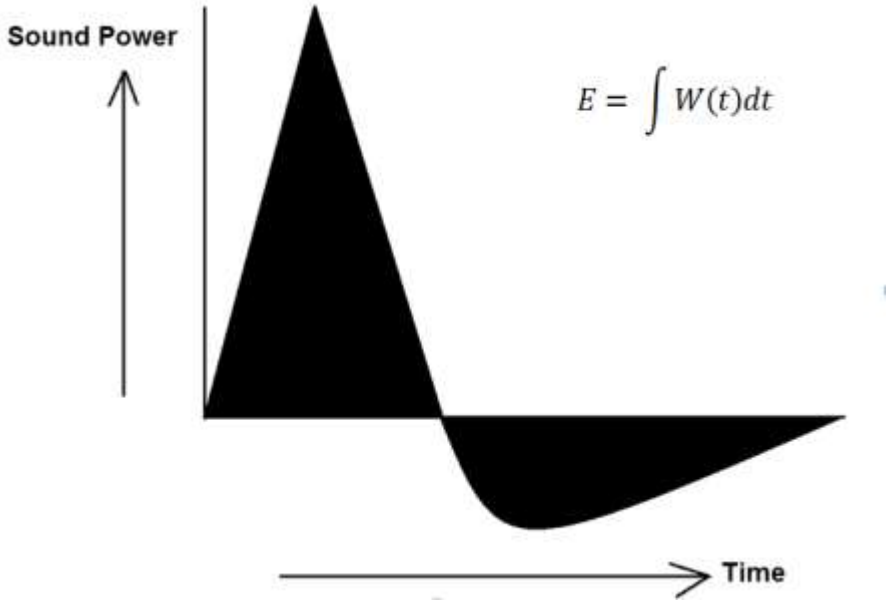

Figure 2.4.1: Total energy calculation of a transient sound energy source

In far field region, ***u(t)*** can be expressed as

$$\boldsymbol{u}(\boldsymbol{t}) = \frac{p(t)}{\rho c} \tag{2.9}$$

Where ρ_0 = equilibrium density of the medium; c = speed of the sound in that medium

Then *I(t)* [watts/m^2] can be expressed,

$$I(t) = \frac{p^2(t)}{\rho c} \tag{2.10}$$

The time integrated value is then written as *e* [joules/m^2],

$$e = \int_0^\infty I(t)dt \tag{2.11}$$

The total energy for a single transient event is then (Tachibana et al. 1987),

$$E = \frac{S}{\rho c}\int_0^\infty p^2(t)dt \tag{2.12}$$

where *S*= Total area of the measurement surface surrounding the source.

2.5 Significance of Anechoic Recording with High Sampling Rate

As mentioned earlier, the typical mixture of direct and reflected waves results in a complicated recording that can be very difficult to translate.

It is crucial to have a finite muzzle blast portion for analysis. Figure 2.5.1 shows a gunshot record from a Glock 19 pistol recorded in a reverberant environment that causes tens of milliseconds of decaying echoes. The position of the microphone was 90° off-axis; so the peak pressure level was low. As can be seen, it is difficult to point out the beginning and finishing mark of the muzzle blast duration from the reverberant recording (Maher and Shaw, 2014).

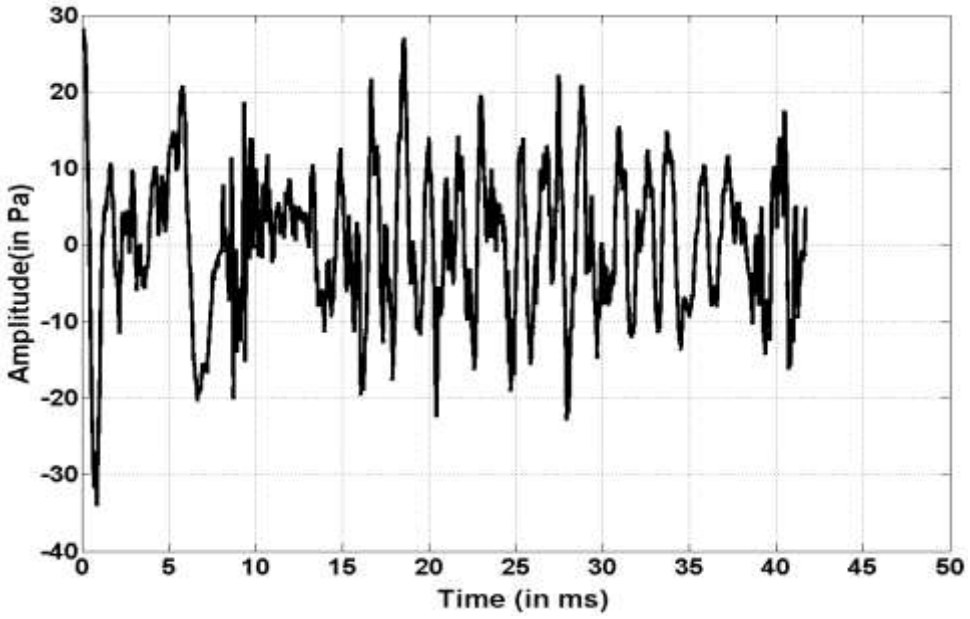

Figure 2.5.1: Reverberant gunshot signal with numerous surrounding reflections. Glock 19 with 9 mm ammunition, recorded 24-bit, 48 kHz PCM, with microphone distance 8 m, 90° off-axis, Peak Pressure 123 dB SPL re 20μPa ref.

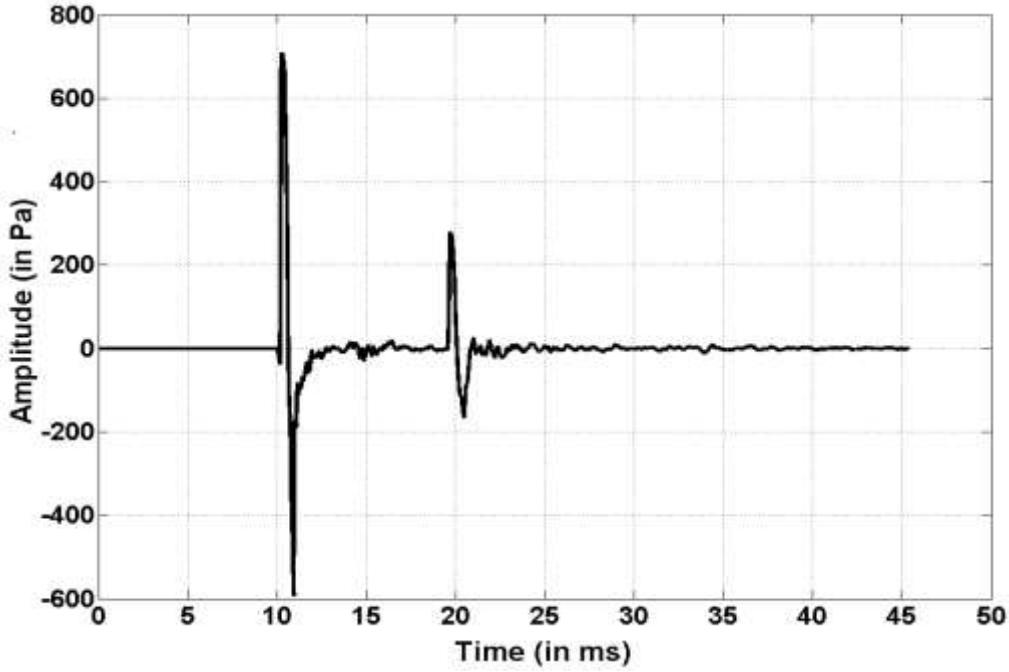

Figure 2.5.2: Anechoic recording of a single gunshot, Glock 19 with 9 mm ammunition, 24 bit, 44.1 kHz PCM, Microphone standing at a distance 8 m, 90◦ off axis, Peak Pressure 123 dB SPL re 20μPa ref.

Figure 2.5.2 shows a recorded gunshot from the same firearm, but in a quasi-anechoic environment. Although the muzzle blast portion is more obvious than in the reverberant version, the details of the muzzle blast signal seem indistinct, probably due to the relatively low bandwidth and sampling rate of the recording system. Muzzle blast signals exhibit a sharp rise time of only a few microseconds, so recording systems having a low sample rate and limited audio bandwidth may not include the extremely brief peak pressure spike and other waveform details.

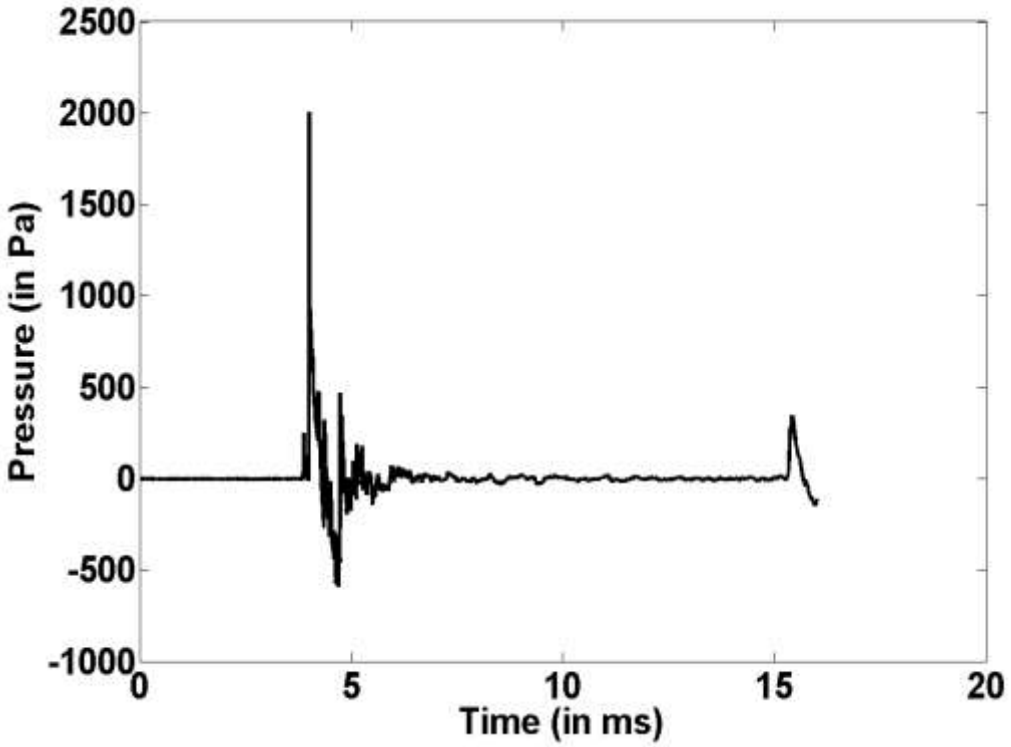

Figure 2.5.3: Anechoic recording of a single gunshot, Glock 19 with 9 mm ammunition, 16-bit, 500 kHz PCM. Microphone distance 3 m, 98° off axis, Peak pressure 158 dB SPL re 20μPa ref

Figure 2.5.3 shows the recorded muzzle blast from a Glock 19 pistol, but with a 500 kHz sampling rate and a microphone and amplifier with 200 kHz bandwidth (Frequency response ±1.0 dB @ gain ≤40 dB).

Here, the signal shows detail due to the wider frequency range of the recording. The elevated shooting platform ensured sufficient time difference between direct and reflected wave. Therefore, the gunshot recordings used in this investigation are captured with a 500 kHz sampling rate.

2.6 Calculating Muzzle Blast Duration

A typical gunshot record can be considered as a *Friedlander wave*, consisting of an interval of positive over-pressure (the portion of the blast that stays higher than the signal mean level) accompanied by an interval of negative down-pressure (sound pressure stays below the mean value). The positive pressure interval can also be divided into two parts, the ascending portion and the descending portion (Hamernik & Hsueh 1991) .

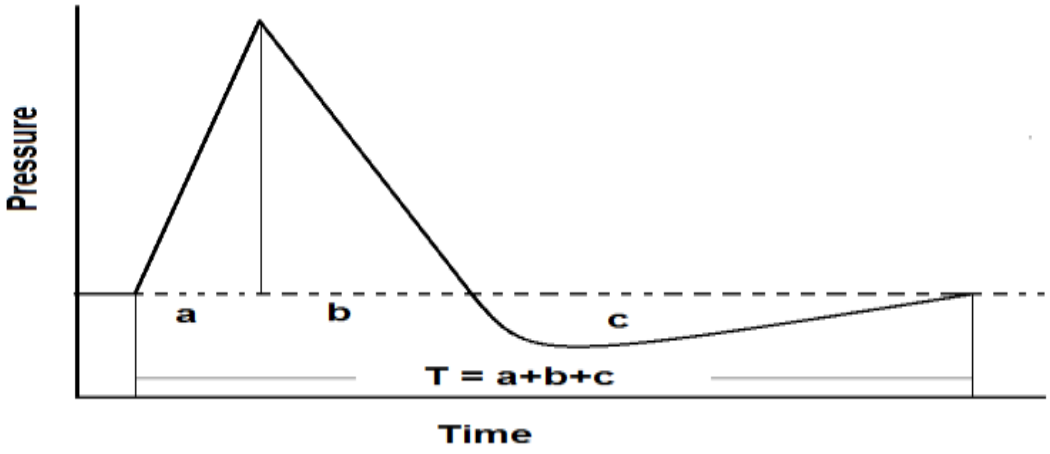

Figure 2.6.1: Friedlander assumption for describing muzzle blast shock wave characteristics (Hamernik & Hsueh 1991)

As depicted, the total duration for the muzzle blast can be written as

$$T = a + b + c \tag{2.13}$$

We use two different ideas to determine the muzzle blast time intervals from gunshot audio recordings. The first one is a simple waveform observation approach, and the other is an energy accumulation approach.

The waveform observation approach uses the average pressure over the interval prior to the gunshot as the baseline and then detects the points in the recorded waveform that cross the baseline. The duration is estimated to be the time in between those points. The limitation with this method is that the low-level waveform details vary sufficiently from shot to shot that even successive recordings of shots by the same firearm may give very different results. It is hard to conclude from the calculated duration whether the variance is due to some internal or external noise or due to inherent nature of gunshots.

The energy accumulation approach is based on determining the time required for the accumulated acoustic energy to reach a certain percentage of the total muzzle blast energy calculated for the entire blast duration. As the muzzle blast is the major contributor of the total blast energy, this technique is based on the hypothesis that the integral of the squared pressure (proportional to signal energy) will be a monotonically increasing function starting at zero, displaying a sharp rise during the muzzle blast, and then levelling off as the muzzle blast dies away.

In both techniques, the long-term mean value is initially calculated and subtracted from the signal to get rid of any DC offset. The peak value of the muzzle blast is calculated for each recording. The portion of each recording examined for the muzzle

blast parameters starts from 4 ms before the peak to 12 ms following the peak. It is confirmed that none of the muzzle blast intervals contained any reflections or ballistic shockwaves.

3. METHODOLOGIES

The experiment for gunshot data collection was executed at a ranch near Bozeman, Montana on October 14, 2015. Our target was to observe gunshot signal variation as a function of azimuth. A total number of twelve microphones were placed near the shot to form an array.

3.1 Test Rig

The previous test arrangements held some limitations. Because gunshot signals vary considerably for successive shots and according to the angles in between the line of fire and the microphone, recording different shots at different times could be misleading. Moreover, the set up should be flexible enough to change in between the experimentation. So it was really important to increase the number of microphones to capture the whole azimuthal variation of a single shot with a smart rig design.

In this study, a newly designed test rig is used. The features of this rig are:

- The platform is set at 3-meter height and the distance between the shooting ground and the microphone stands are also kept at 3 meters. If h=d=3 and if c= 343 m/sec, T_{diff} is near about 10.8 millisecond. As a result, muzzle blast portion from the direct shockwave can easily be separated from the reflected version.
- An array of twelve microphones is used to cover the azimuthal variation of nearly 180 degrees. That means the arrangement made it possible to go for time synchronous recording of gunshots from the line of fire to the angle just behind the shooter.

- The rig is oriented in a semicircular fashion. The location of the shooter was approximately at the center of that circle.
- The rig arms are adjustable. Made of aluminum, the arms can be replaced. That enables setting the whole structure at a different distance from the shooting position, in other words, the radius of the semi-circle can be varied by changing arm length.
- Separation between the shooter and the microphones are necessary to be constant, as signal strength differs according to distance. Adjustable length holders are used for microphones.
- The designed rig is also capable of capturing particular firearm characteristics exhibits asymmetric behavior. In other words, the rig supported firearms to be rotated along its firing axis (figure 3.1.1).

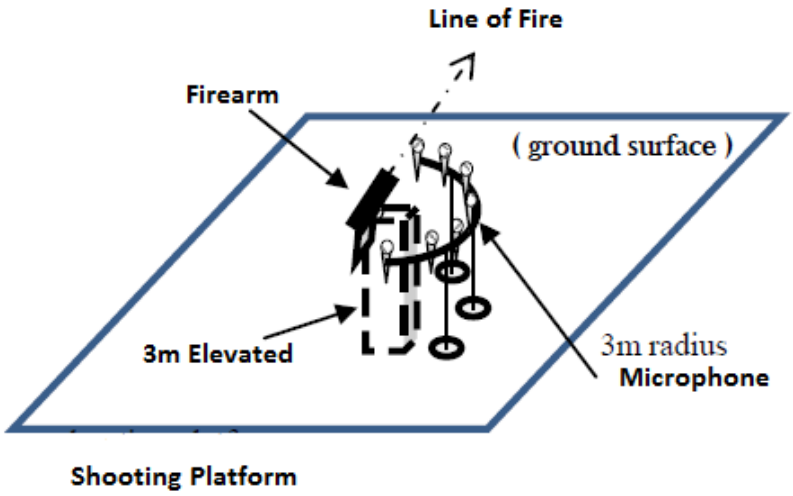

Figure 3.1.1: Experimental Setup for Gunshot Recording with newly designed rig (Maher, Robert C. & Routh 2015)

The aluminum rig was built using 80/20 band material aluminum struts. The shape of the frame was like half of an octagon, where adjustable metallic arms had been welded at the corners (shown in Figure 3.1.2).The planar view of microphones (GRAS 40DP) can be considered located on the circumference of the semi-circle as depicted in figure 3.1.4. Precise angular location of twelve microphones is given in the following table 1. Figure 3.1.4 portrays approximate angular positioning of microphones relative to the line of fire.

Table 1: Microphone angular position relative to the line of fire

Microphone No.	Angular Position (in degree)	Microphone No.	Angular Position (in degree)
1	0	7	98.2
2	16.4	8	114.5
3	32.7	9	130.9
4	49.1	10	147.3
5	65.5	11	163.6
6	81.1	12	180

Figure 3.1.2: 3 meter elevated aluminum frame with expandable arms

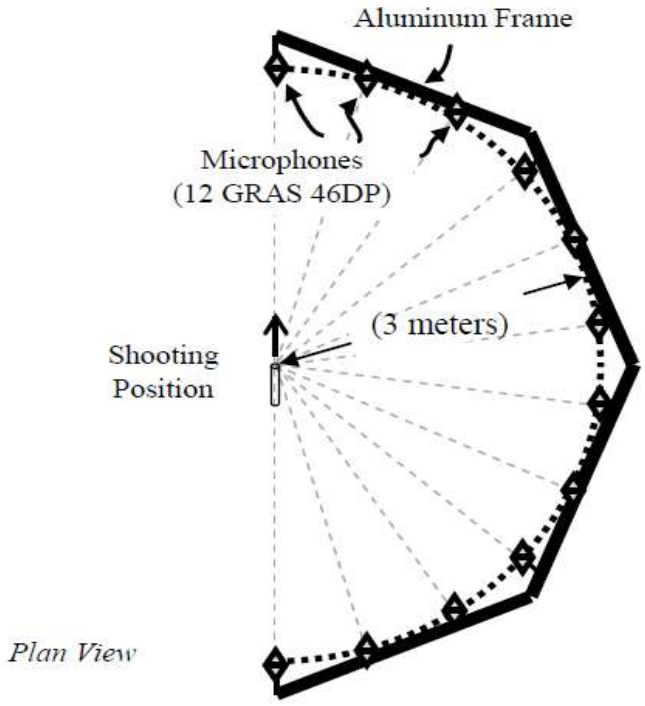

Figure 3.1.3: Planar view of twelve microphone array (Maher, Robert C. & Routh 2015)

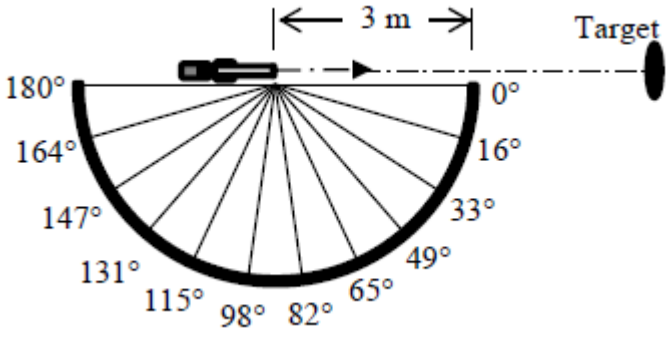

Figure 3.1.4: Approximate angular position of Microphone Array (Routh & Maher, 2016)

3.2 Recording System

As microphones with smaller diameters are well suited for measuring signals that have a higher frequency with high amplitudes like gunshot blasts, G.R.A.S. 40DP (a diameter of one-eighth of an inch) microphones were chosen for this experiment. These condenser microphones are externally polarized with rear venting features. Its low sensitivity (from highest 0.9 mV/Pa to lowest 0.68 mV/Pa for this experiment), wide frequency response (flat response from 6.5 KHz to nearly 70 KHz) in addition to a wide dynamic range (from 40dB to 175 dB) makes them very suitable for conducting this sort of analysis. Microphones were calibrated using 42AB type G.R.A.S. calibrator which generates a pressure equivalent to 10 Pa at 250 Hz (Calibration level is 114 dB with reference to 20μPa).

Among twelve microphones, the first eight were connected to G.R.A.S. 12AG 8-Channel Power Module. They provide the flexibility to carry out experiment either from a mains/line supply or from an external DC supply (12 V – 18 V). To capture the whole range of amplitude, 20dB attenuators were connected on the output side of each channel. The rest of the four microphones were connected to two G.R.A.S. 12AA 2-Channel power modules with inbuilt attenuation ranges from -20dB to +40dB.

(a)

(b)

(c)

Figure 3.2.1: (a) 40DP (1/8 inch) Condenser Microphone (b) G.R.A.S. 12AG Amplifier (c) 12AA Amplifier

To record 12 channels simultaneously at high sampling rate, amplifiers output was then connected to Multichannel Data Acquisition System developed by National Instruments. NI PXIe-1071 PXI express chassis was used along with NI PXIe-6358 data acquisition device (DAQ). This multifunction system supports 16 simultaneous analog

inputs at 1.25 MS/s/channel with 16-bit resolution. For our analysis, we used eight channels on one slot and four on the other.

Signals were then gathered using a program developed with LABVIEW. Twelve separate channels were recorded simultaneously at a sampling rate of 500 kilohertz. It is expected that this high sampling rate would enable sensors to capture high-pressure peaks of very brief duration. The acquisition mode was set differential and the voltage range was specified in between +5V to -5V. Each sample was stored in a 16-bit integer using MATLAB.

3.2.1 Microphone Sensitivity

In this study, microphones with different sensibilities were arranged to cover half of a circle (angular range). The first one was nearly set on the line of fire and the last one was kept approximately behind the shooter. Calibrated sensitivity values for different microphones are shown in the table 2.

Table 2: Measured sensitivities of twelve G.R.A.S. 40DP microphones

Microphone	Sensitivity (in mV/Pa)	Microphone	Sensitivity (in mV/Pa)
01	0.90	07	0.90
02	0.68	08	0.84
03	0.85	09	0.91
04	0.88	10	0.75
05	0.84	11	0.84
06	0.69	12	0.82

3.3 Selection of Firearms

To cover a wide range of commonly used firearms, our experiment was conducted by ten different types of firearm including shotguns, pistols, revolver, and rifle. Table 3 exhibit the list of the firearms and ammunition used in this experiment. Our goal was to:

- Observe the dissimilarities in gunshot acoustic signals from one shot to another within the same firearm and same sort of bullet.
- Observe the deviation of acoustic characteristics within similar type of firearm. Like in the pistol category, we observed signals from Colt 1911A1 (45 ACP), Glock 19/135 JHP, Glock 23 and Sig 239.
- Examine variation of waves within the same firearm but with different sort of bullets. For example, we observed gunshots from Ruger revolver with two different types of bullets: bullets with 0.38 caliber and with 0. 357 caliber.

Table 3: Firearm and ammunition list for this study

Firearm	Ammunition	Type	No. of shots observed
Remington 870	00 buckshot	Shotgun	3
CZ 452	22LR	Winchester Rifle	10
Custom	308 Win	Winchester Rifle	10
Stag AR15	5.56×45 NATO	Rifle	10
Colt 1911A1	45ACP	Pistol	10
Glock 19	9×19	Pistol/Handgun	10
Glock 23	40 S &W	Pistol	10
Ruger SP 101	357 Magnum	Revolver	10
Ruger SP_101	38 Special	Revolver	9
Sig Sauer 239	357 Sig	Semi-Automatic Pistol	10

3.4 Determining the Muzzle Blast Duration

The details of the waveform observation and energy accumulation methods for calculating the Muzzle blast durations are discussed below.

3.4.1 Muzzle Blast Duration by Waveform Observation

- After selecting the portion of interest as described earlier, identify the first sample, p_0 that crosses above the mean value (zero) prior to reaching the peak of the signal.
- Identify the first sample, p_1 that crosses below the mean value (zero) after the signal has reached its peak.
- Determine the time interval between sample p_0 and p_1. This is the positive pressure interval ($a + b$).
- Identify p_2, the next sample in the waveform that crosses above the mean value following the negative peak of the waveform.
- Determine the time interval between sample p_1 and p_2. This is the negative pressure interval (c).
- These two durations are then summed up to get the calculated Muzzle blast duration, T.

3.4.2 Muzzle Blast Duration by Energy Accumulation

- Choose the signal portion of interest according to the previously described process.

- Beginning from the first crossing point before positive phase duration, calculate the square of each sample value in the muzzle blast interval (proportional to signal power) and accumulate the total energy over the entire interval.
- Calculate the time required for the accumulated energy to reach a certain percentage of its final total. From empirical examination, 93% showed the best consistency for successive shots, so that has been the accumulation total chosen to define the duration for all firearms.

3.5 Determining the Positioning of the Firearm for Each Shot

As multiple shots were taken in our experiment for each category firearm and ammunition, it was important to fire all the shots at the same target and position of the firearm should not be disturbed from shot to shot. Figure 3.5.1 shows the arrangement for firing from an elevated platform to avoid ground reflections.

Figure 3.5.1: Shooting in open target from elevated platform

During the shot, there might have been some movement of the shooter which could result in gunshot waveform variation at the receivers. Keeping that in mind, it was tried to figure out what could be the possible displacement for consecutive shots.

Time difference of arrival algorithm was used to localize source, which was described by Derek, Matthew, Ahmed & Tim termed *Spherical Localization* method in 2008 (Thai, Hashemi-sakhtsari, & Pattison, n.d) . The source was supposed to generate a spherical wave and captured using more than three sensors. This method was actually a least square estimate method which makes use of source coordinates and radial distance in between source and sensors.

Suppose,

Position of Sensors= (x_i, y_i); Position of any source = (x, y) ;

Distance = r_i;

Then in geometric form,

$$(x_i - x)^2 + (y_i - y)^2 = {r_i}^2 \tag{3.1}$$

A matrix was formed for all the cases

$$\boldsymbol{X} = \begin{bmatrix} (x - x_1) & (y - y_1) \\ (x - x_2) & (y - y_2) \\ (x - x_i) & (y - y_i) \end{bmatrix}, K_i = {x_i}^2 + {y_i}^2; \tag{3.2}$$

N= Number of sensors

Mathematical operation of these two equation resulted (for *i* =2 to N),

$$\begin{bmatrix} x \\ y \end{bmatrix} = \boldsymbol{C} r_1 + \boldsymbol{D}; \tag{3.3}$$

$$\boldsymbol{C} = (\boldsymbol{X}^T \boldsymbol{X})^{-1} \boldsymbol{X}^T \begin{bmatrix} -r_{2,1} \\ -r_{3,1} \\ -r_{N,1} \end{bmatrix} \tag{3.4}$$

$$\boldsymbol{D} = (\boldsymbol{X}^T \boldsymbol{X})^{-1} X^T \left(\frac{1}{2}\right) \begin{bmatrix} -{r^2}_{2,1} + K_2 - K_1 \\ -{r^2}_{3,1} + K_3 - K_1 \\ -{r^2}_{N,1} + K_N - K_1 \end{bmatrix} \tag{3.5}$$

where, $r_{i,j}$ is the time difference of various signals arriving at the receivers at different times.

$\boldsymbol{X}$ was substituted in the above equation to get an equation in a quadratic form,

$$\alpha {r_1}^2 + \beta r_1 + \gamma = 0 \tag{3.6}$$

Solving the above equation produced two solutions for r_1; values of r_1 was put pack to get the values *(x,y).* These values had several possible outcomes.

Research carried out by resulted in following outcomes

Table 4: Different solutions based on TDOA for variation of parameters (Thai et al)

Case	Solution
Both of them are positive	Smaller number should be chosen
One of positive and other one is negative	Positive number should be chosen
Both of them are negative or either one is complex	No Solution

In our experiment, we assumed that the location of the shooter was exactly at the center of the semi-circle and its coordinate was *(x,y)= (0,0).* The location of the first microphone was considered to be *(0, 3).* According to the microphone orientation, the distance from the source to center was approximately equal for all, which results in K_i to be zero (discussed in firearm positioning section). The orientation and the consideration for our analysis are shown in the following figure.

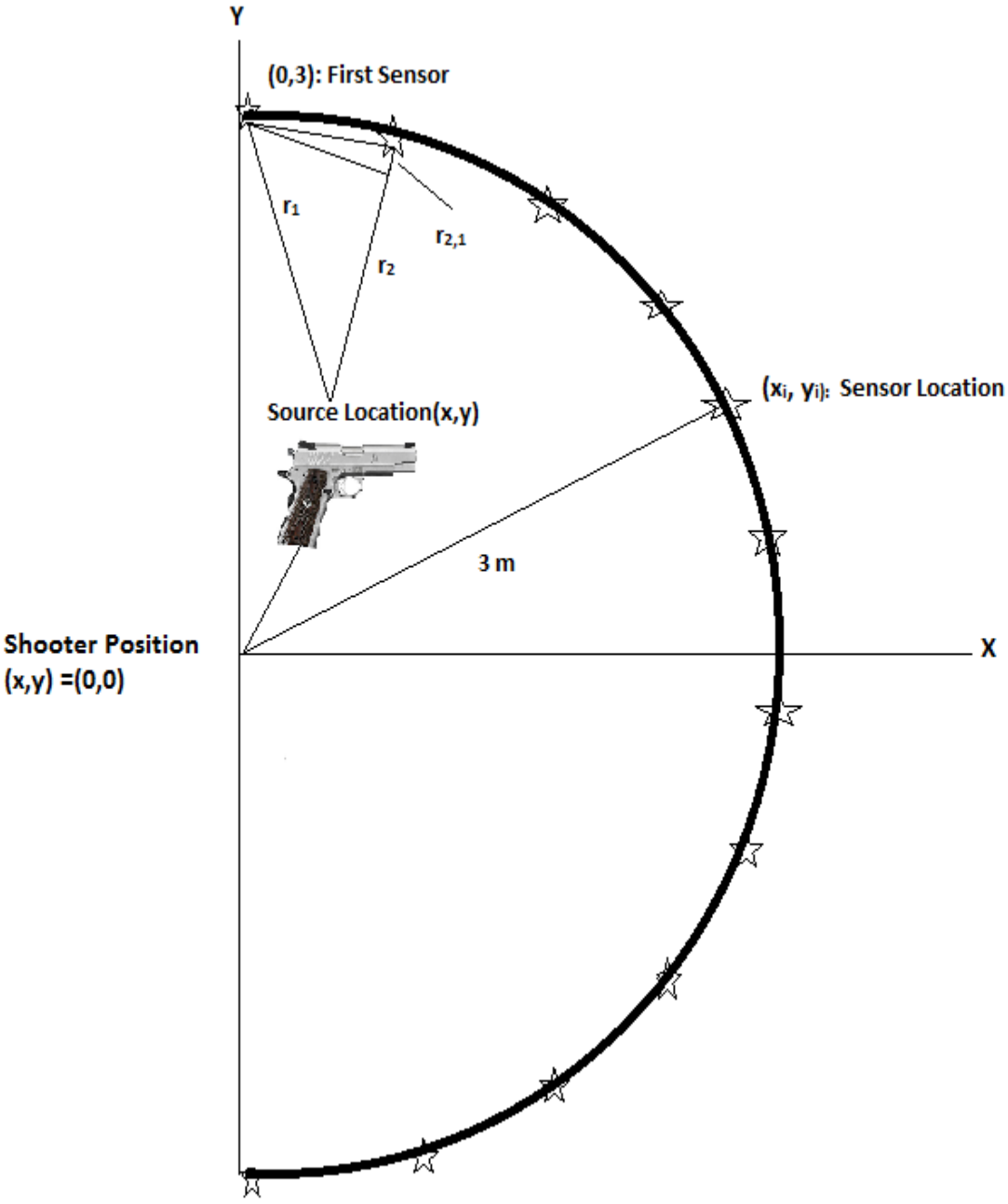

Figure 3.5.2: Finding the position of firearm at every shot

3.6 Methodology Used for Calculating Acoustical Power from a Single Shot

Total acoustic energy propagating from each shot is calculated in the following way:

- Select the portion of interest through the same process as earlier (subtracting mean from the long haul signal and choosing 8001 points). The waveform is then converted into pressure waveform.
- Identifying point *p0* as described in the section of determining waveform based Muzzle blast duration.
- From *p0*, a total no of 4500 points were chosen. It was ensured that the portion does not contain any reflection.
- As muzzle blast is the major contributor of the total blast energy of the signal, we have calculated the square of pressures of each sample value of the portion of interest.
- In our experiment, we set up twelve microphones to cover an azimuth of 180. We have assumed that the total energy can be measured by calculating the total energy of 0°-180° plane and then rotate the plane in 3D space. It was assumed that the pressure values are symmetrical values over 0° to 180° line.
- To calculate total energy of that plane, it was necessary to interpolate the pressure values of intermediate azimuths. Total energy was calculated as a function of r, which is the distance from the firearm to the microphone. It will then be a multiplication of distance and intensity of the acoustic pressure wave.
- The intensity at any particular azimuth over the blast period is calculated by

$$Intensity, I = \frac{1}{\rho c}\int_0^t p^2(t)dt \tag{3.7}$$

Where ρc = specific acoustic impedance, which has a value 415 under standard atmospheric condition (20°C and 1.013 bars) and has a unit of rayl (kg/m^{2}s).

- The intensities at the other azimuths were then estimated by a standard interpolation method. As pressure values are not purely spherical, taken that variation into consideration, the intermediate pressure values were calculated (from 0° to 180°) using mathematical interpolation technique. MATLAB was used to do the calculation. Three interpolation techniques were used: linear, cubic spline and Piecewise Cubic Hermite Interpolating Polynomial. The last one was chosen for the continuity of the pressure values and providing smoother outputs.

If we consider energy from a blast supposed to be spill over in a spherical manner as shown in figure 3.6.1, the total energy calculation would be three dimensional.

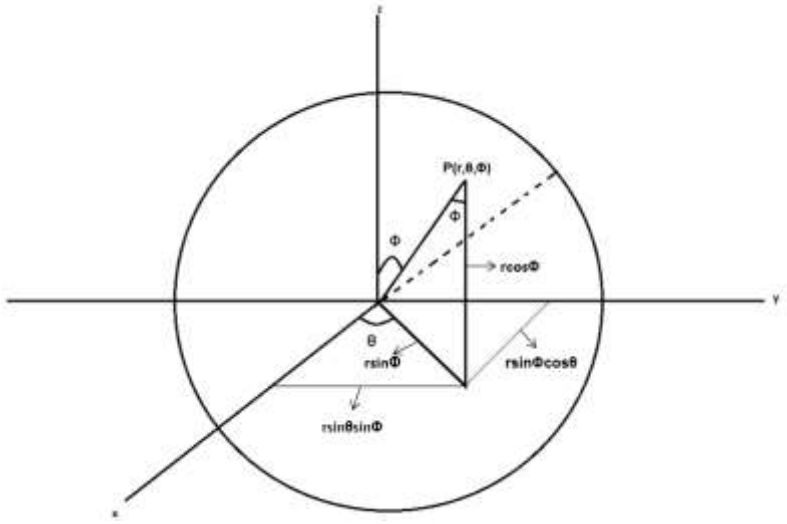

Figure 3.6.1: Spherical spill-over of gun blast energy

The total energy would be

$$E_{total} = \int_{\theta=0}^{\theta=2\pi} \int_{\emptyset=0}^{\emptyset=\pi} \int_{r=0}^{r=R} r^2 \, I(\theta) \, dr d\emptyset d\theta \tag{3.8}$$

In our case, all our microphones were set at a fixed distance r=R=3 meter. As our observation suggests, the energy spill over is not purely spherical, it varies at different azimuths. So our limit for θ stays within θ= θ_1 to θ= θ_2. Because we have a discrete data of azimuths, our energy equation will become

$$E_{total} = 2\pi R^2 \sum sin\theta I(\theta) d\theta \tag{3.9}$$

3.7 Correlation between Signals

In this experiment, all the weapons are fired a number of times. To find out the variability, we have compared each of the captured signals with one reference signal. We evaluated the cross-correlation coefficient to figure out the similarity. Because we have two independent time series data, the normalized correlation coefficient was used which is defined as

$$r = \frac{\sum_{i=1}^{N}(x_i - \overline{x})\,(y_i - \overline{y})}{(\sqrt{\sum_{i=1}^{N}(x_i - \overline{x})^2})(\sqrt{\sum_{i=1}^{N}(y_i - \overline{y})^2})} \tag{3.10}$$

Where there are N pairs of values (x_i, y_i) and there means are $\overline{x}$ and $\overline{y}$ respectively (University of Iowa 2004).

The range of values for r is, $-1 \leq r \leq 1$.

Depending on the value of r, we can draw the following conclusion

Table 5: Conclusions based on the value of r

Value of r	Conclusion
1	A perfect correlation with the same phase
-1	A perfect correlation with opposite phase
0	Does not ensure that they have no correlation but implies that they lack linear correlation

3.8 Comparing Experimental Recording with Real Life Gunshot Recordings

In this study, one of our goals was to compare our high sampled recorded signal with real life signals. We were lacking any real life recording. So to emulate real life recording and to compare them with our recorded signals, the following process was followed:

- All the signals were down sampled from previous sampling frequency to two different frequencies: 15 KHz and 20 KHz.
- In conventional recorders, the signals then go through some kind of filtration. For these two different sample rates, two different filters were designed using MATLAB fdatool. The parameters were given in the following Table 8.
- The down sampled signal is then passed through these filters.
- The filtered signals were then up sampled to a sampling rate equal to the original recorded signal.

- Correlation between them was then calculated using the procedure described earlier.

The following table shows the parameters set for the fdatool. Figure 3.8.1 and figure 3.8.2 depicts the magnitude response of those filters.

Table 6: fdatool parameters for two different type of sampling rate signals

Sampling Frequency of 15000 Hz		Sampling Frequency of 20000 Hz	
FPASS	7000	FPASS	9300
FSTOP	7490	FSTOP	9990
APASS	1 (in dB)	APASS	1 (in dB)
ASTOP	80 (in dB)	ASTOP	80 (in dB)
Filter Order	78	Filter Order	73

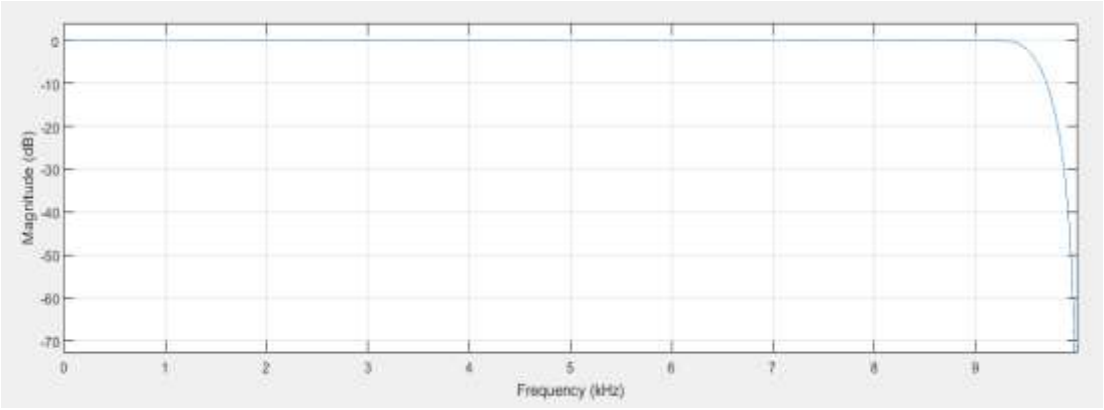

Figure 3.8.1: Magnitude response of filter having a cutoff nearly at 7.5 KHz

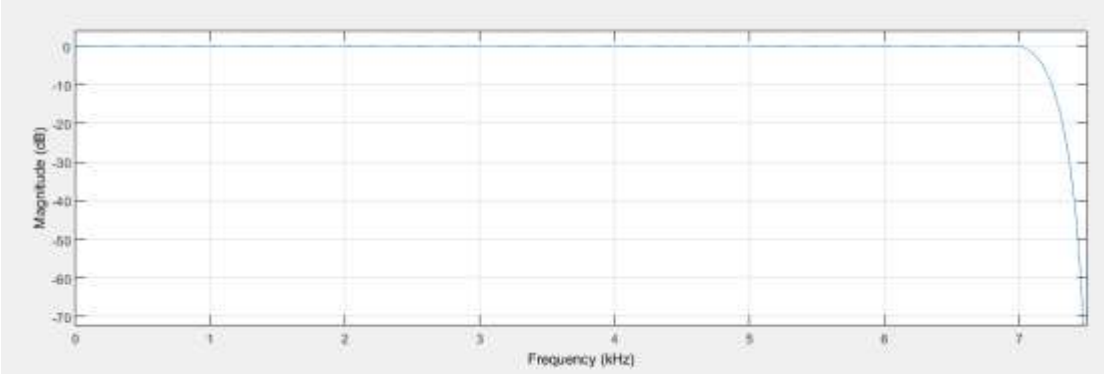

Figure 3.8.2: Magnitude response of filter having a cutoff nearly at 10 KHz

3.9 Prediction of Gunshot Signal at a Particular Direction

One of the major questions of interest is determining the position of the shots. Based on the available recordings, it is of great importance that whether we can predict the directionality of a shot. In this experiment, it has been tried to predict the peak pressure of a gunshot fired at a particular azimuth.

The process followed was:

- A particular azimuth was picked up for prediction (in this paper, the prediction azimuth was chosen at 49°, the position of the fourth microphone).
- Based on the data available for other azimuths, peak pressure level at that particular angle was estimated using mathematical interpolation.
- Three kinds of mathematical interpolation techniques were used: linear, Cubic Spline and Piecewise Cubic Hermite Interpolating Polynomial. Linear interpolation was picked up for its better accuracy. These results were then compared with the recorded peak pressure at that particular angle and the angle of nearby two microphones.

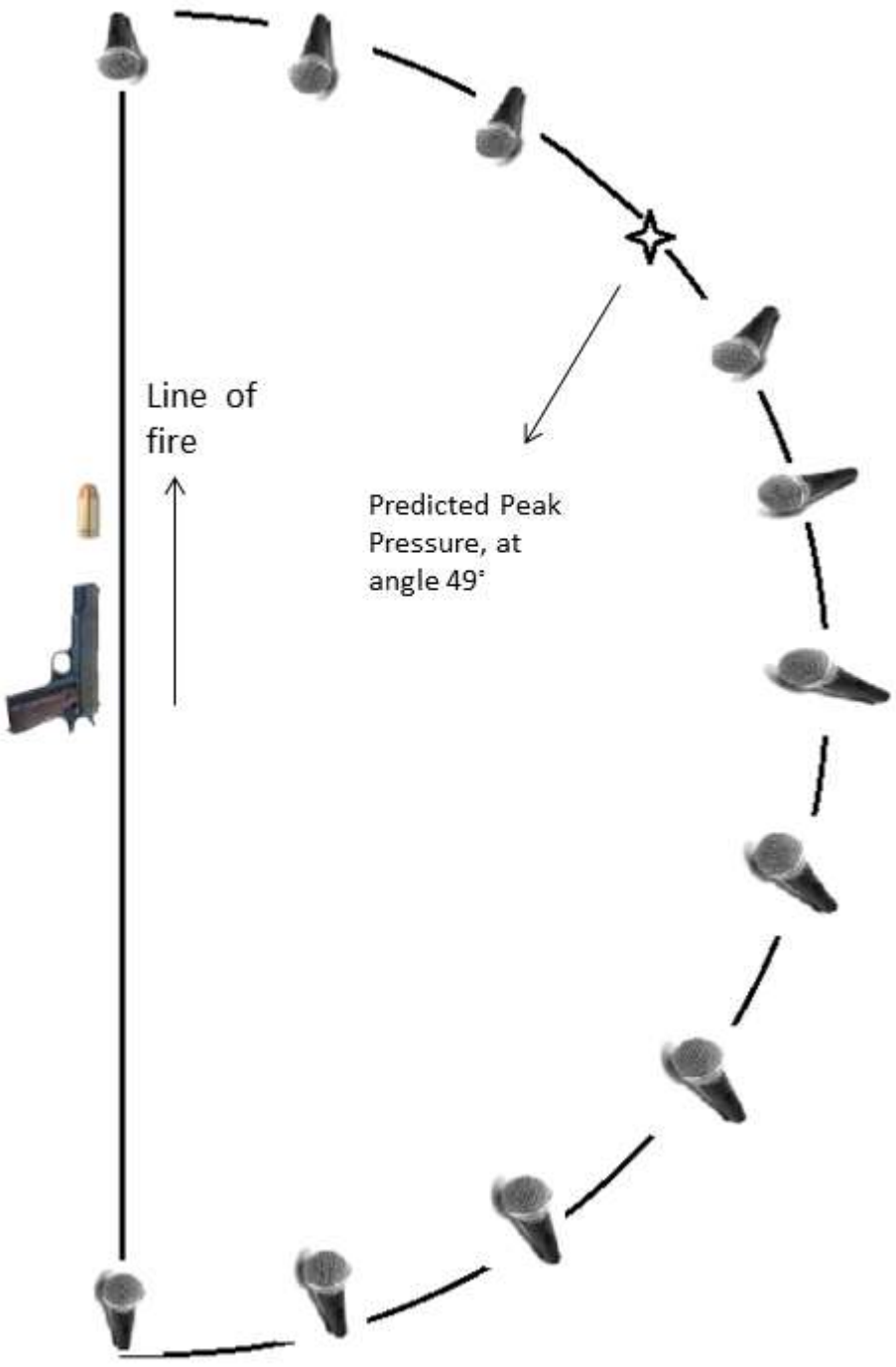

Figure 3.9.1: Prediction of muzzle blast peak pressure by interpolation method

4. RESULTS

For all the shots, M8 was recording unexpectedly high pressure values. The reason could not be found. We have made corrections for the recorded signal for M8 in the following manner:

- First of all, the peak pressure values at M8 were calculated using linear interpolation method using pressure values from other microphones.
- The overpressure factors were calculated by dividing experimental data with interpolated data. The mean values were taken for each type of gunshot.
- Then the average value was calculated for the 10 different types of gunshots. The factor was found to be 1.98.
- Then the experimental pressure values from M8 were divided by this factor to estimate the pressure values.

For 8 channel 12AG amplifier, we used 20dB attenuation with external attenuators. The attenuations were found not exactly to be 20dB. In this analysis, we have ignored this variation; considered all the attenuators have the same attenuation and equal to 20dB. The acoustical characteristics of the gunshots observed in this study are discussed below, with a separate section for each firearm.

4.1 Colt 1911A1 (45ACP)

The M1911A1 70 made by Colt 45 is a semi-automatic single action pistol based on a design by John Browning from the early 20th century. In this experiment, the pistol was chambered in 45 ACP.

Figure 4.1.1: 1911 Colt 45 (Wikipedia)

45 ACP 230 gr Remington Golden Sabre High-Performance Jacket HPJ (hand loaded) cartridges with hollow point bullets.

Figure 4.1.2: 230gr Remington Golden Sabre HPJ
(https://www.youtube.com/watch?v=unNZaB0pL4Q)

Table 7: Features of 230 gr Golden Saber bullets

Feature	Description
Bullet type	Jacketed Hollow Point
Bullet weight (in grain)	230
Bullet Diameter (in inch)	0.45
Muzzle Energy (in foot pounds)	391
Muzzle Velocity (based on bullet kinetic energy) (in fps)	900
Cartridge Casing	Nickel Plated Brass
Special Features	Boxer-primed, non-corrosive, and reloadable

4.1.1 Muzzle Blast Pressure Variation for Colt 1911A1 (45 ACP)

10 shots were fired in succession from the Colt 1911A1 (45 ACP) and recorded by the twelve microphone system. Each recording was analyzed to identify the peak pressure observed during the muzzle blast. From figure 4.1.3, we observe that there are variations in the muzzle blast peak pressure for consecutive shots.

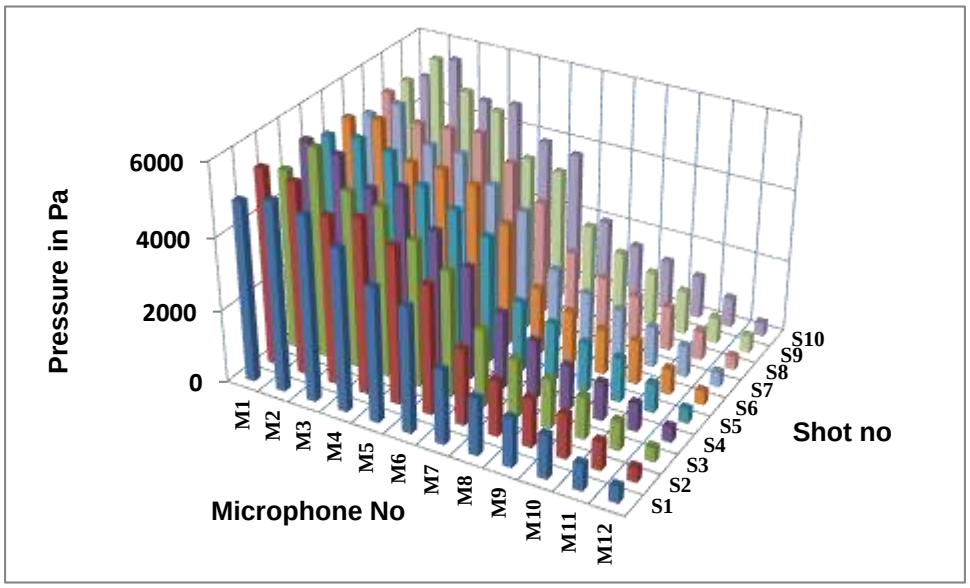

Figure 4.1.3: Peak pressure at 3 meters for the Colt 1911A1 (45 ACP) muzzle blast as a function of azimuth (10 shots)

4.1.2 Position of the Firearm
during 10 Shots of Colt 1911A1 (45 ACP)

Using time difference of arrival (TDOA), positioning of the firearm during 10 shots for Colt 1911A1 (45 ACP) is shown in figure 4.1.4.

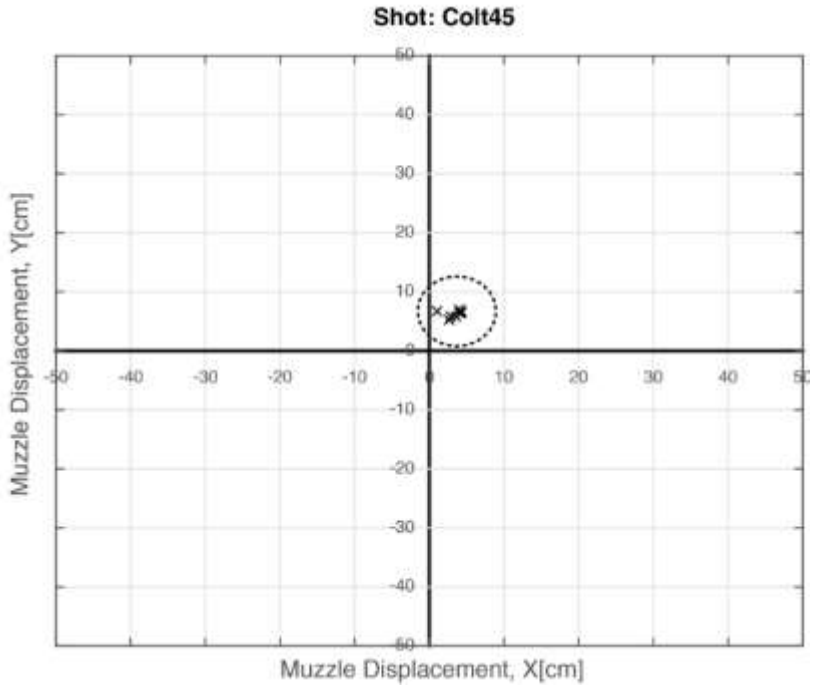

Figure 4.1.4: TDOA based position of the muzzle for ten successive shots from Colt 1911A1 (45 ACP) pistol

4.1.3 Muzzle Blast Duration of Colt 1911A1 (45 ACP)

Figure 4.1.5 shows the muzzle blast duration variation for different shots. Both waveform observation and energy accumulation methods were used.

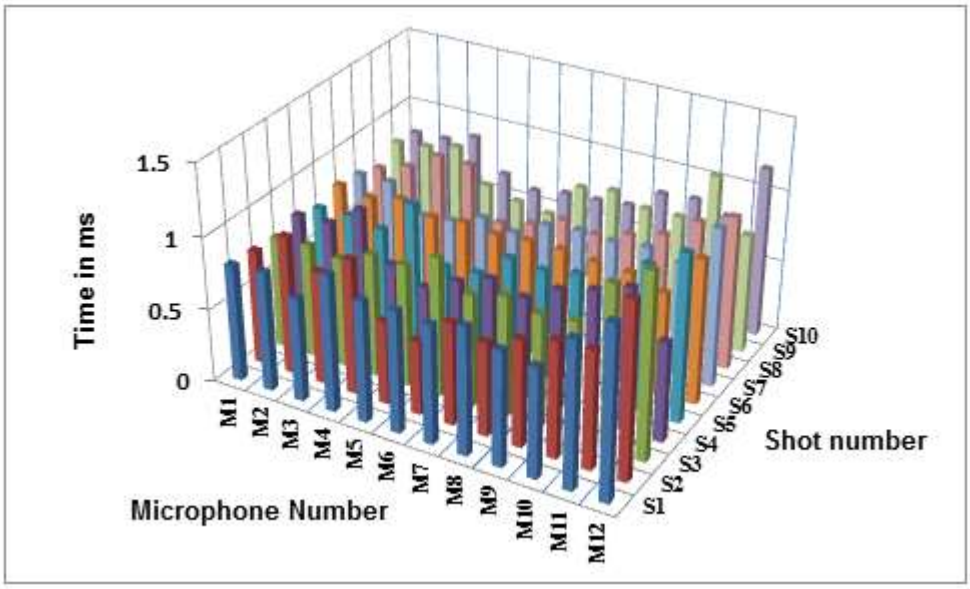

Figure 4.1.5: Waveform observation based analysis of the muzzle blast durations for Colt 1911A1 (45 ACP) (for 10 shots)

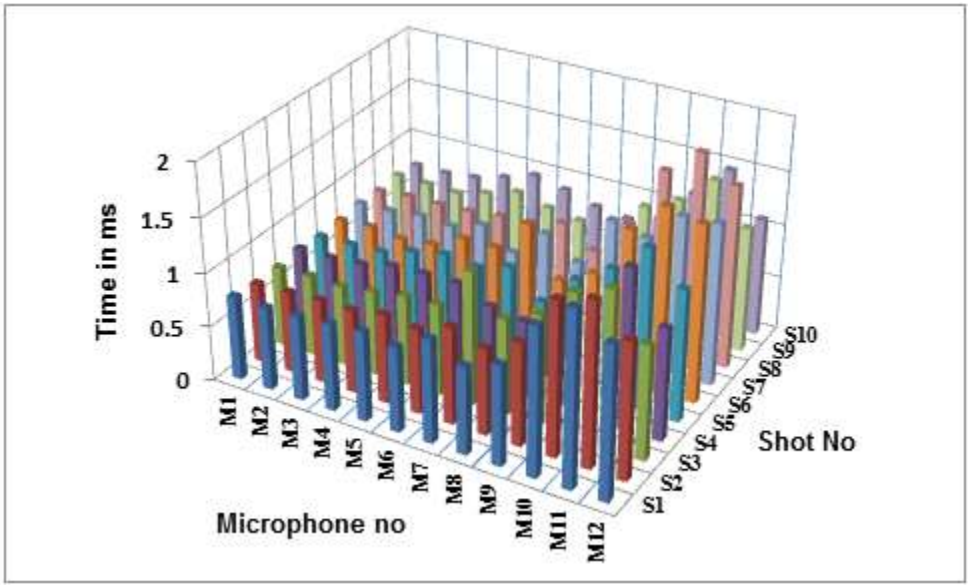

Figure 4.1.6: Muzzle blast duration variation based on energy accumulation for Colt 1911A1 (45 ACP) (for 10 shots)

4.1.4 Total Acoustic Energy Variation for Successive Shots of Colt 1911A1 (45 ACP)

As seen from the peak pressure graph, the maximum pressure values are observed at S9. As our total energy is based on pressure values at different azimuths, the peak energy is also observed at S9 (shown in figure 4.1.7). Colt 1911A1 (45 ACP) exhibit total energy variation for successive shots.

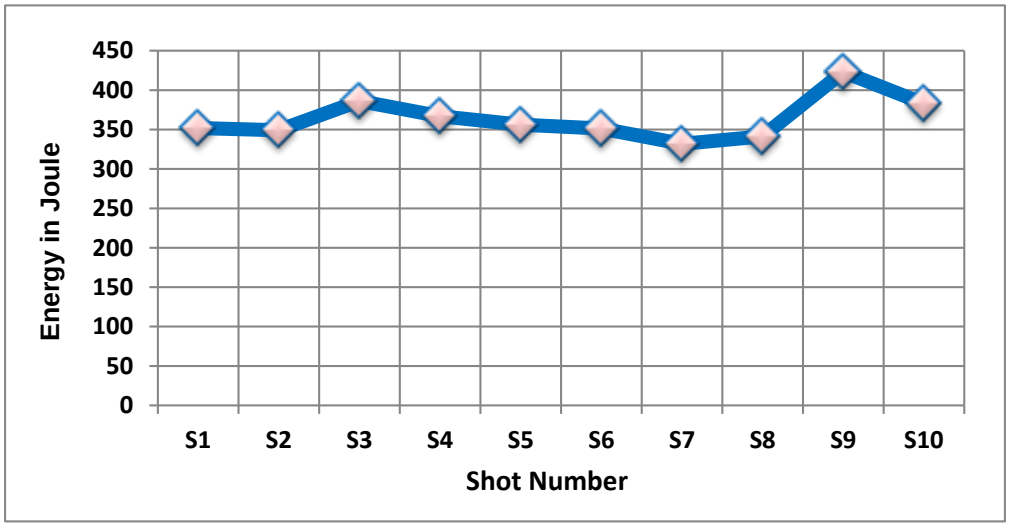

Figure 4.1.7: Shot to shot total energy variation for Colt 1911A1 (45 ACP)

4.2 Glock 19

Introduced in 1988, Glock 19 is a semi-automatic pistol tested with 357 Sig ammunition.

Figure 4.2.1: Glock 19 pistol (www.bayoushooter.com)

In this experiment, we have used Glock 19 pistol with Hornady 9 mm, 135 gr FlexLock® bullets.

Figure 4.2.2: 135gr Hornady 9 mm critical duty FlexLock® bullets (www.luckygunners.com)

Table 8: Features of 135 gr Hornady FlexLock® bullets

Feature	Description
Bullet type	Jacketed Hollow Point
Bullet weight (in grain)	135
Bullet Diameter	0.354 inch or 9 mm
Muzzle Energy (in foot pounds)	369
Muzzle Velocity (based on bullet kinetic energy) (in fps)	110
Cartridge Casing	Nickel Plated Brass
Special Features	Penetration with moderate speed

4.2.1Muzzle Blast Peak Pressure

10 shots were fired in succession from the Glock 19/ 135 JHP. From figure 4.2.3, we observe that there are variations in the muzzle blast peak pressure for consecutive shots at different azimuths.

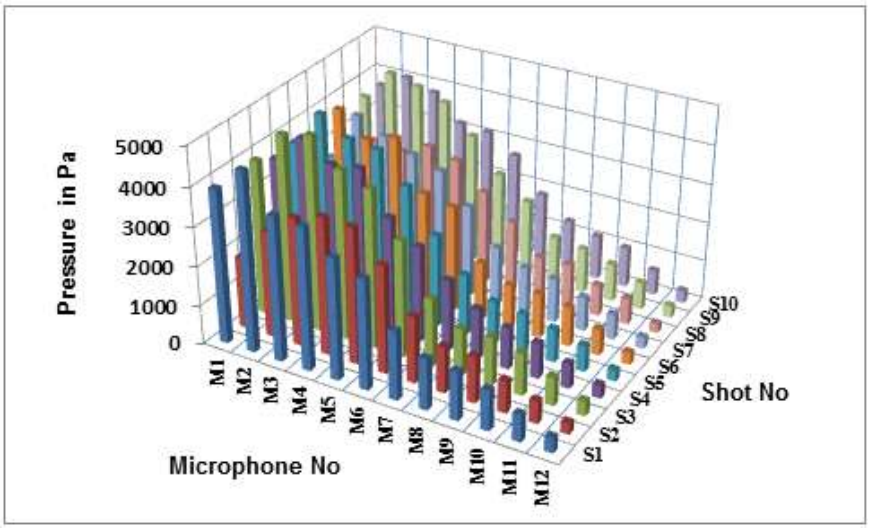

Figure 4.2.3: Peak pressure at 3 meters for the Glock 19/135 JHP muzzle blast as a function of azimuth (10 shots)

4.2.2 Position of the Firearm
during 10 Shots of Glock 19/135 JHP

Position of the firearm during 10 shots of Glock 19/135 JHP is shown in figure 4.2.4.

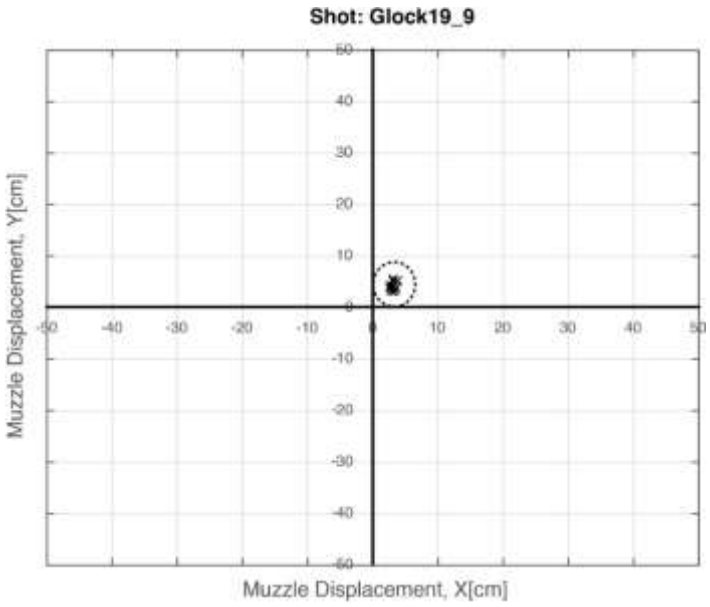

Figure 4.2.4: TDOA based position of the muzzle for ten successive shots from Glock 19/135 JHP

4.2.3 Muzzle Blast Duration

Figure 4.2.5 and figure 4.2.6 shows the muzzle blast duration variation for different Glock 19/135 JHP shots (waveform observation and energy accumulation based methods were used).

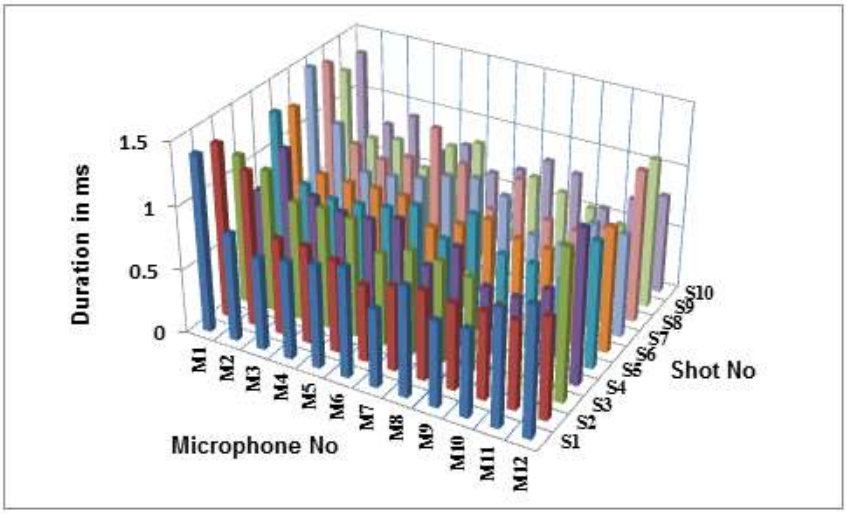

Figure 4.2.5: Waveform observation based muzzle blast duration variations for Glock 19/135 JHP (for 10 shots)

Energy accumulation based approach was also tried (as seen from figure 4.2.4).

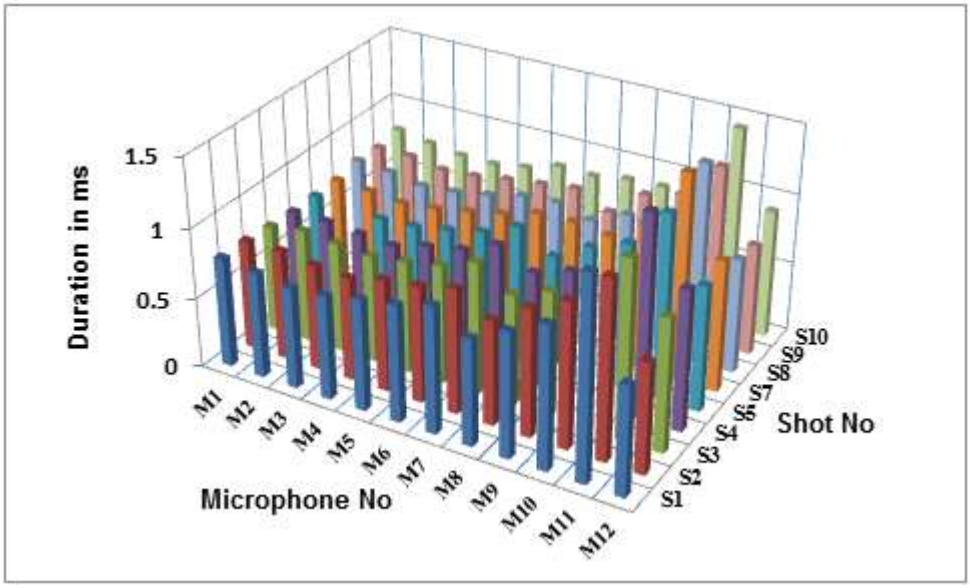

Figure 4.2.6: Energy accumulation based muzzle blast duration variations for Glock 19/135 JHP (for 10 shots)

4.2.4 Total Energy
Variation from One Shot to Other

From one shot to another, the acoustical energy emission from a single shot varies for Glock 19/135 JHP. S3 records the highest peak pressure values. Total energy for this shot was 343 Joule whereas lowest was for S8 (which was 224 Joule). The variation is shown in figure 4.2.7.

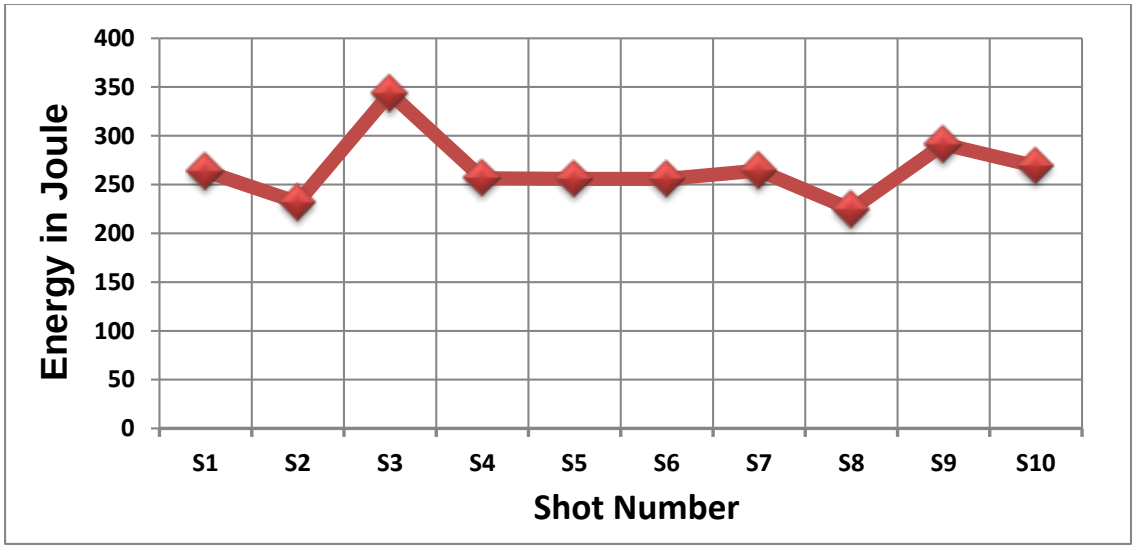

Figure 4.2.7: Shot to shot total energy variation for Glock 19/135 JHP

4.3 Glock 23

The Glock 23 is identical to the Glock 19, except for the fact that it accommodates the 40S&W cartridge with a different magazine, barrel, slide, and ejector.

Figure 4.3.1: Glock 23 (Bob Campbell)

In this experiment, Glock 23 was fired with 165 gr Remington golden saber bullets.

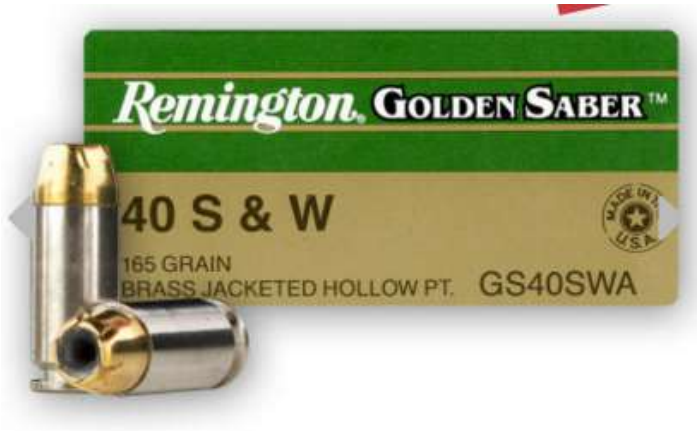

Figure 4.3.2: 0.40 caliber (Smith & Wesson) bullets for Glock 23 pistol (165 gr Golden Saber JHP)

Table 9: Features of 165 gr Golden Saber JHP Bullets

Feature	Description
Bullet type	Jacketed Hollow Point
Bullet weight (in grain)	165
Bullet diameter(in inch)	0.40
Muzzle Energy (in foot pounds)	485
Muzzle Velocity (based on bullet kinetic energy) (in fps)	1150
Cartridge Casing	Nickel Plated Brass
Special Features	Boxer-primed, non-corrosive, and reloadable

4.3.1Muzzle Blast Peak Pressure

10 shots were fired one after the other from the Glock 23. From figure 4.3.3, the variations in muzzle peak pressure is observed for consecutive shots.

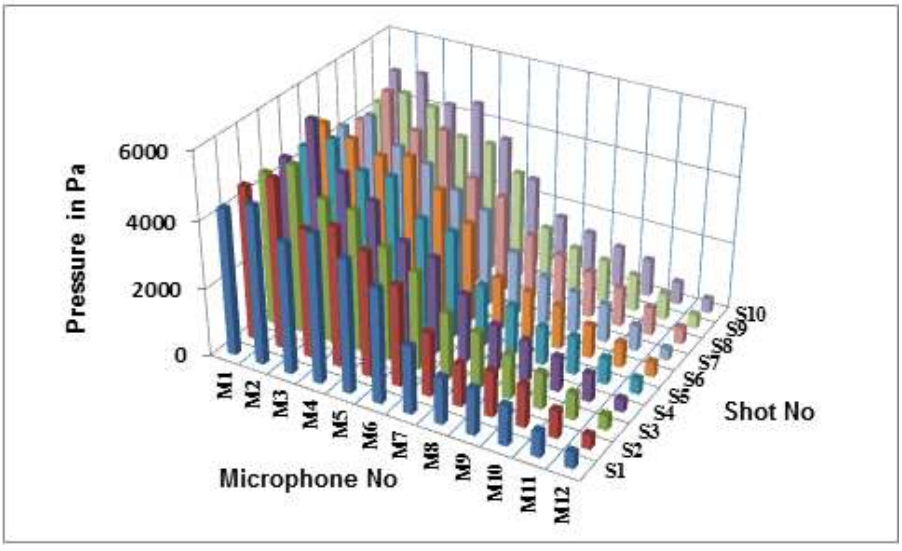

Figure 4.3.3: Muzzle blast peak pressures at 3 meters as a function of azimuth (10 shots)

4.3.1 Position of the Firearm
during 10 Shots of Glock 23

Position of the firearm during 10 shots of Glock 23 is shown in figure 4.3.4.

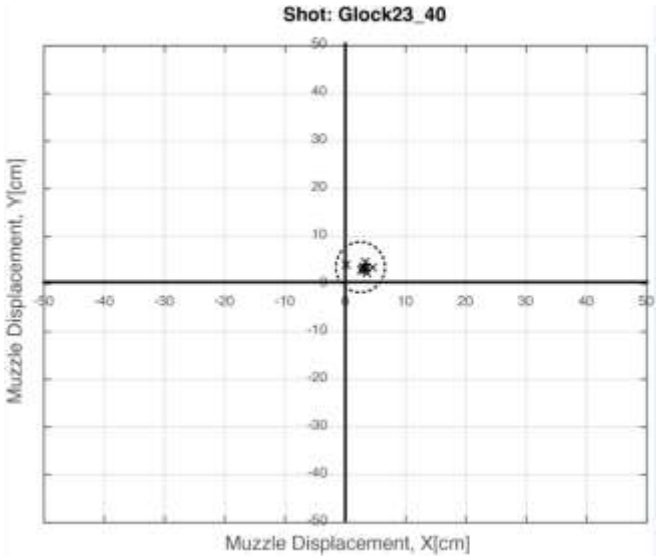

Figure 4.3.4: TDOA based position of the muzzle for ten successive shots from Glock 23 pistol

4.3.2Muzzle Blast Duration

Figure 4.3.5 shows the Muzzle blast duration variation for different Glock 23 shots

(using both waveform observation and energy accumulation method).

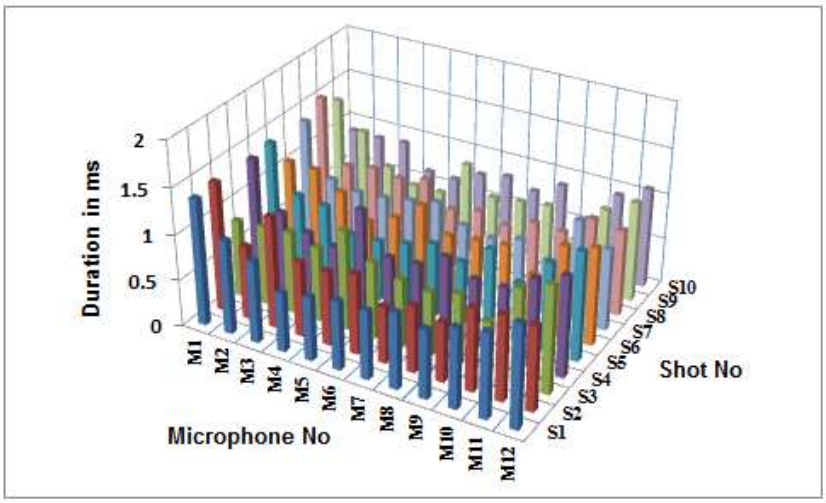

Figure 4.3.5: Azimuthal variation of the Muzzle blast durations for Glock 23 for 10 shots (waveform observation)

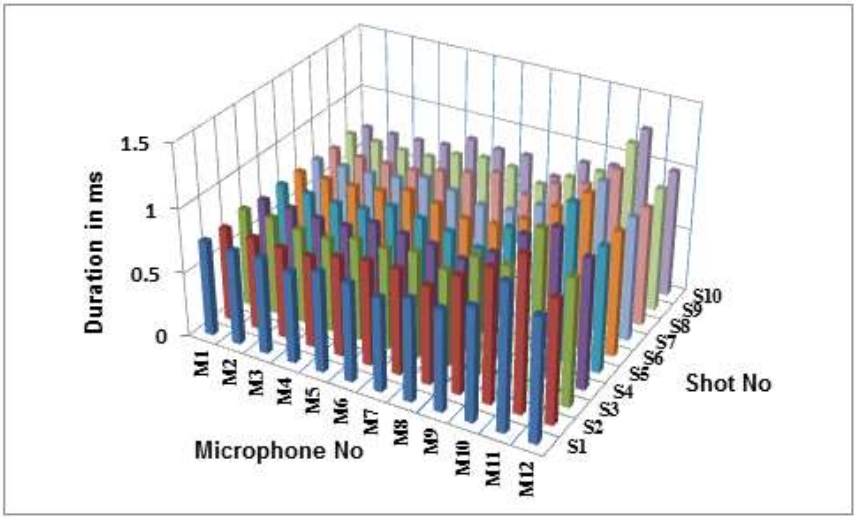

Figure 4.3.6: Azimuthal variation of the Muzzle blast durations for Glock 23 for 10 shots (energy accumulation)

4.3.4 Total Energy Variation
from One Shot to Another for Glock 23

Total energy was uniform from one shot to the other for Glock 23 as seen from the figure 4.3.7. The mean energy level is higher than Glock 19/135 JHP. This may not

be the case for Glock 23 in general because Glock 19 and Glock 23 used different type of ammunitions.

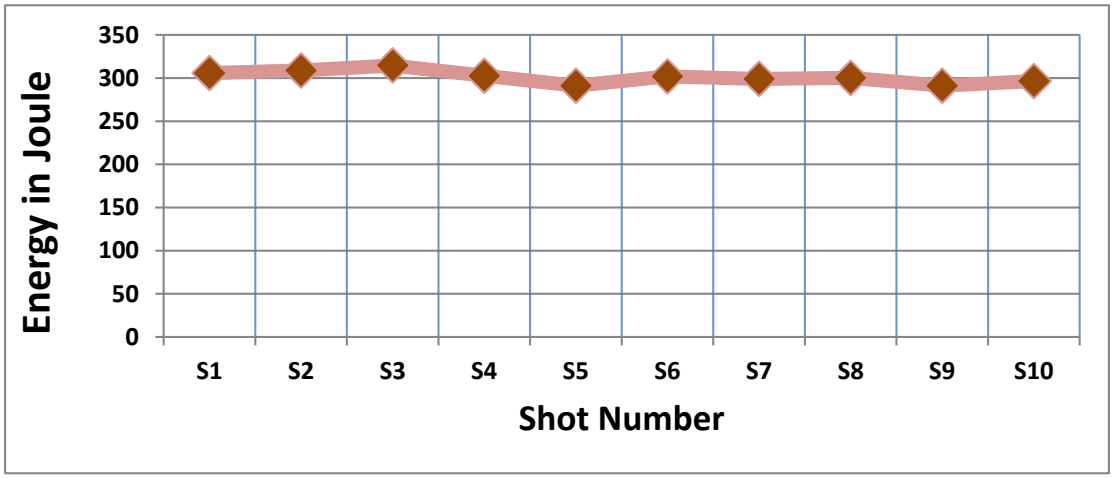

Figure 4.3.7: Shot to shot total energy variation for Glock 23

4.4 Sig 239

It is a semi-automatic pistol tested with 357 Sig ammunition.

Figure 4.4.1: Sig 239 pistol outlook (Sigsauer.com)

Figure 4.4.2: 125 gr Jacketed hollow point Winchester bullets (www.luckygunners.com)

Table 10: Features of 125 gr Winchester bullets

Feature	Description
Bullet type	Jacketed Hollow Point
Bullet weight (in grain)	125
Bullet diameter (in inch)	0.357
Muzzle Energy (in foot pounds)	506
Muzzle Velocity (based on bullet kinetic energy) (in fps)	1350
Cartridge Casing	Nickel Plated Brass
Special Features	Boxer-primed, non-corrosive, and reloadable

4.4.1Muzzle Blast Peak Pressure of
Sig 239 with 125 gr Winchester Bullets

10 shots were fired in succession from the Sig 239. From figure 4.4.3 we observe that for consecutive shots, there are variations in the muzzle blast peak pressure.

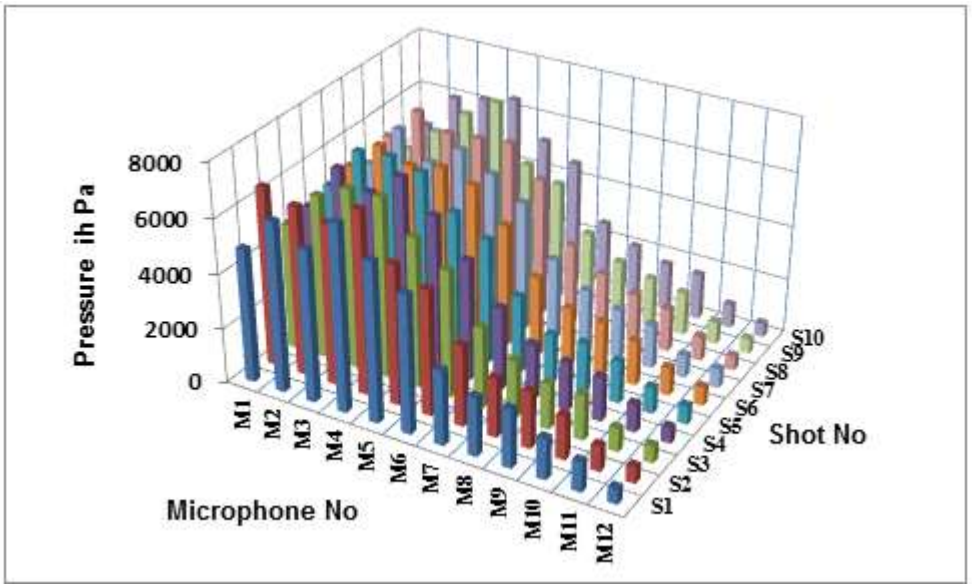

Figure 4.4.3: Muzzle blast peak pressures at 3 meters for the Sig 239 as a function of azimuth (10 shots)

4.4.2 Position of the
Firearm during 10 Shots of Sig 239

Position of the firearm during 10 shots of Sig 239 is shown in figure 4.4.4.

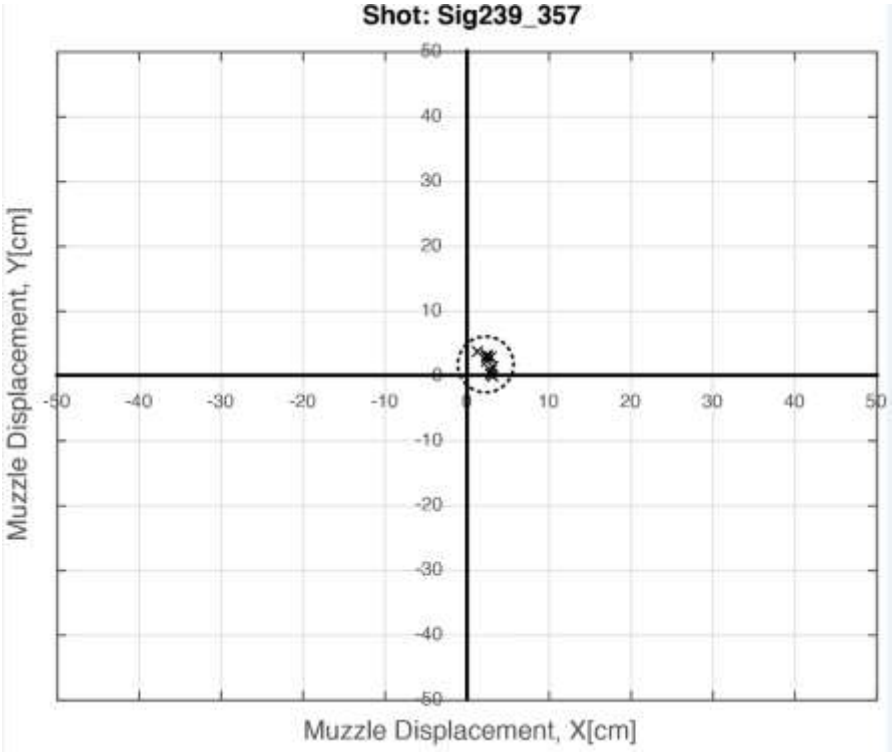

Figure 4.4.4: TDOA based position of the muzzle for ten successive shots from Sig 239 pistol

4.4.3 Muzzle Blast Duration

Figure 4.4.5 shows the Muzzle blast duration variation for different Sig 239 shots (using both waveform observation and energy accumulation method).

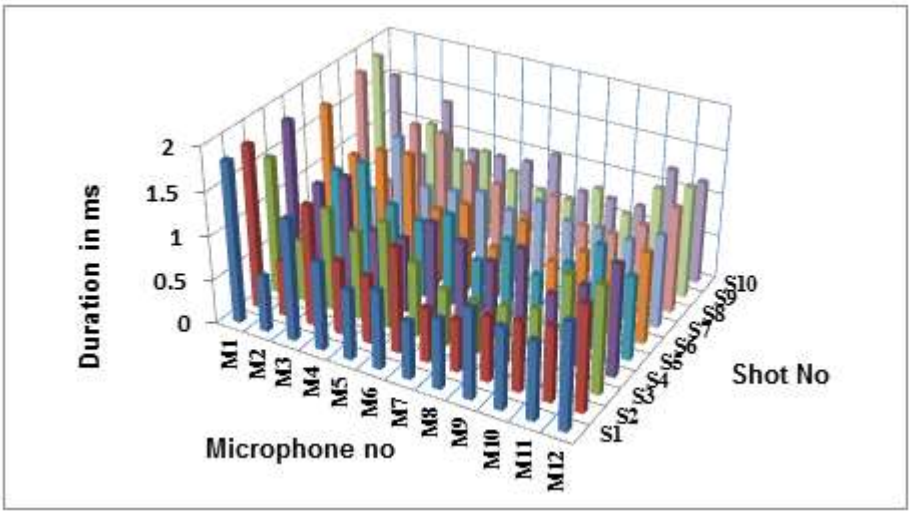

Figure 4.4.5: Azimuthal variation of the muzzle blast durations for 10 shots of Sig 239 (waveform observation approach)

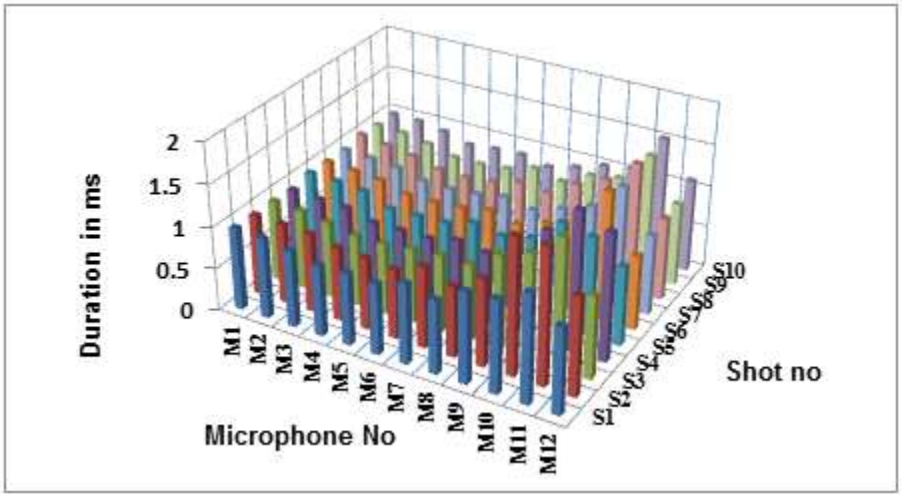

Figure 4.4.6: Azimuthal variation of the Muzzle blast durations for 10 shots of Sig 239 (energy accumulation approach)

\

4.4.4 Total Energy Variation from One Shot to Another

The total energy for successive shots roams around of 700 Joule. This is the highest among the pistol category chosen for this study. Sig 239 exhibits good shot to shot consistency in terms of total acoustic energy emission (figure 4.4.7).

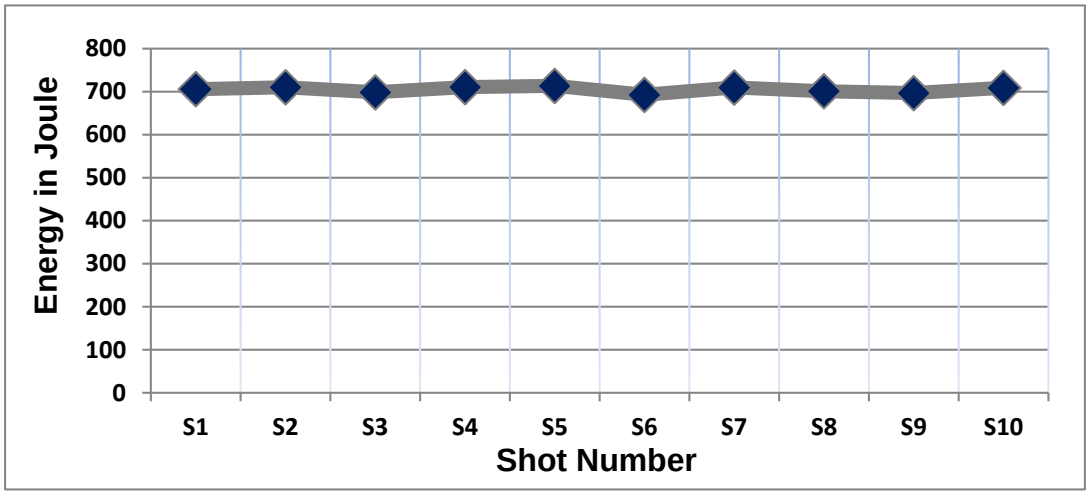

Figure 4.4.7: Shot to shot total energy variation for Sig 239

4.5 Surgeon/AI

This firearm has an AI AICS stock; similar to the L96A1 and made in England, a Surgeon receiver (made in OK USA, surgeonrifles.com), and a 24” Krieger MTU contour barrel (made in WI). It’s capable of hitting 18” targets at 1200 m, although the maximum effective range given by the Army for 308 matches is 800m (figure 4.5.1).

Figure 4.5.1: Surgeon CSR .308 Winchester rifle (Surgeon rifles)

Figure 4.5.2: 175 gr Sierra MATCHKING® 0.308 caliber bullet (www.luckygunners.com)

Table 11: Features of 175 gr Sierra MATCHKING® bullets

Feature	Description
Bullet type	Match king
Bullet weight (in grain)	175
Bullet Diameter (in inch)	0.308
Muzzle Energy (in foot pounds)	2627
Muzzle Velocity (in fps)	2650
Ballistic Coefficient	0.496
Special Features	Federal 210 match primer

4.5.1 Muzzle Blast Peak Pressure
of Surgeon Rifle with 175 gr Sierra MATCHKING®

10 shots were fired one after the other from the Surgeon rifle. From 4.5.3 we observe that there are variations in the muzzle blast peak pressure for consecutive shots.

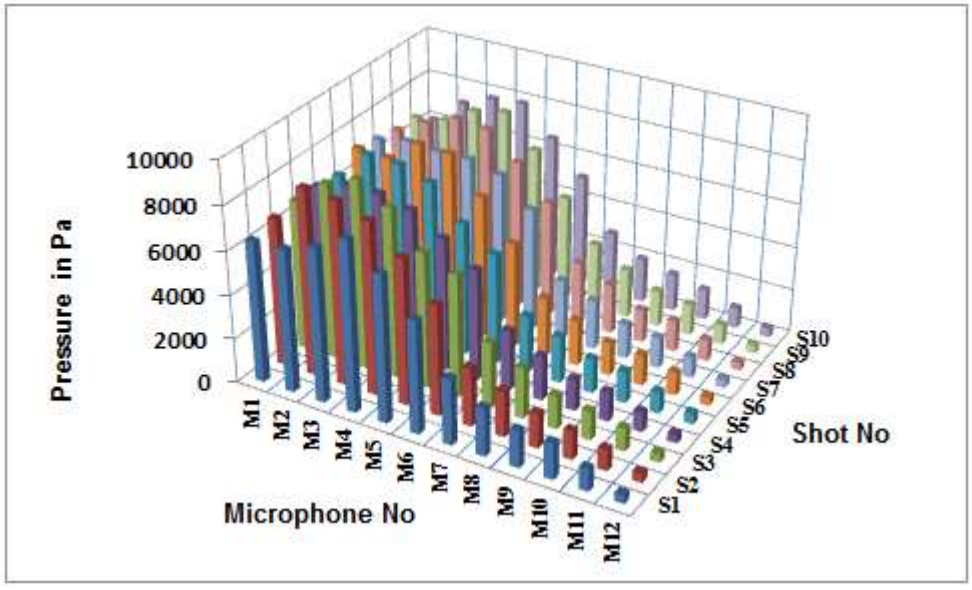

Figure 4.5.3: Peak pressure at 3 meters for the Winchester 0.308 caliber bullets muzzle blast as a function of azimuth (10 shots)

4.5.2 Position of the Firearm
during 10 Shots of Surgeon Rifle

Position of the firearm during 10 shots of Surgeon rifle is shown in figure 4.5.4.

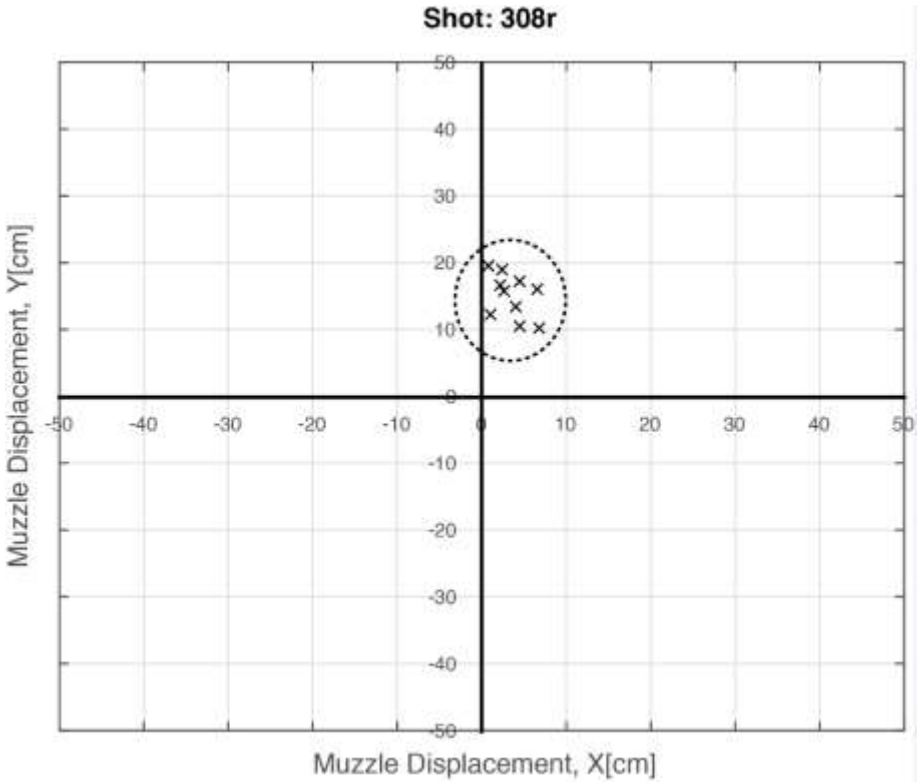

Figure 4.5.4: TDOA based position of the muzzle for ten successive shots from Surgeon rifle

4.5.3 Muzzle Blast Duration

Figure 4.5.5 and 4.5.6 show the muzzle blast duration variation for different shots (using both waveform observation and energy accumulation method).

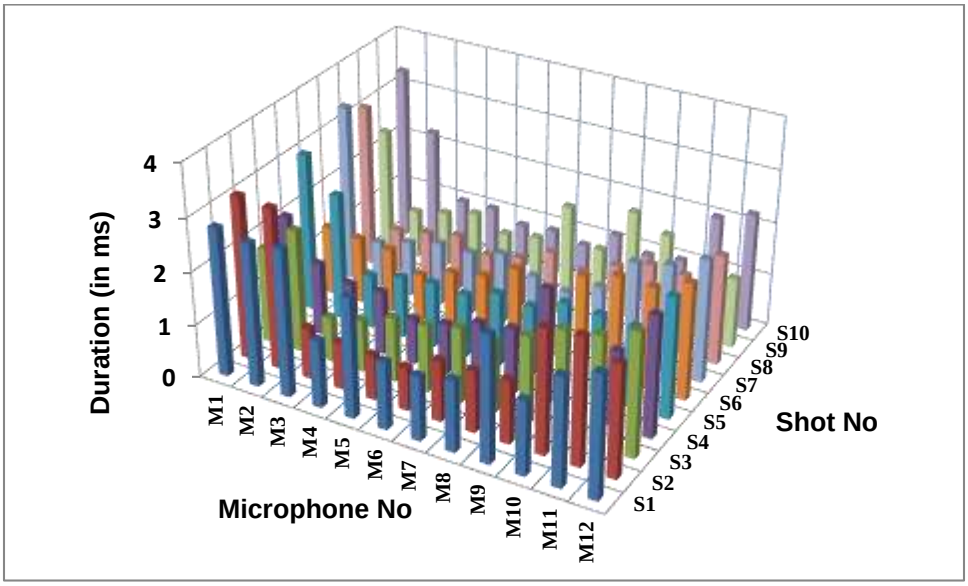

Figure 4.5.5: Azimuthal variation of the muzzle blast durations for 10 shots with Winchester 0.308 caliber bullets (waveform analysis approach)

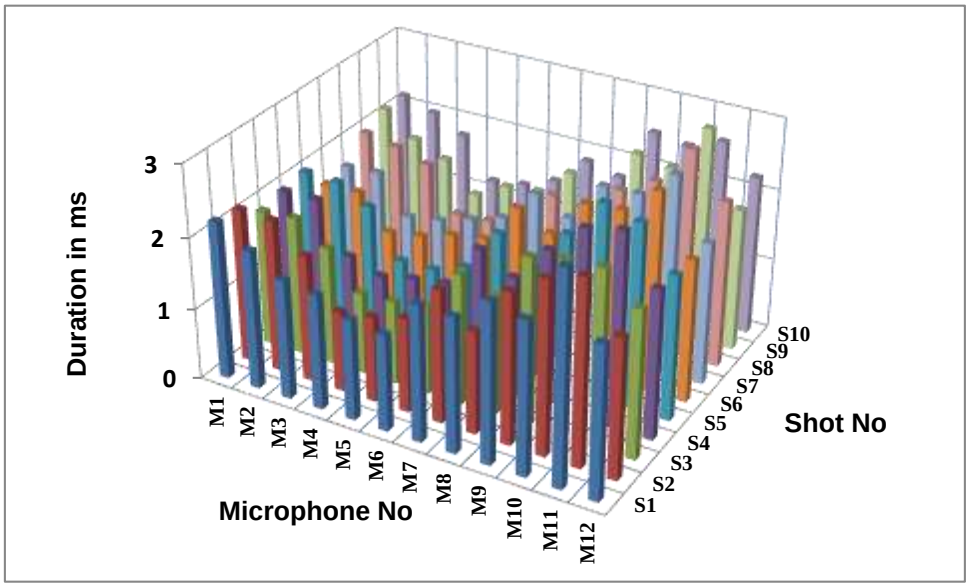

Figure 4.5.6: Azimuthal variation of the muzzle blast durations for 10 shots with Winchester 0.308 caliber bullets (energy accumulation approach)

4.5.4 Total Energy Variation from One Shot to Another

The total energy variation has been seen for 308 Winchester for consecutive shots (shown in figure 4.5.7). For successive shots, the energy value varies from 1212 Joule to 1108 Joule.

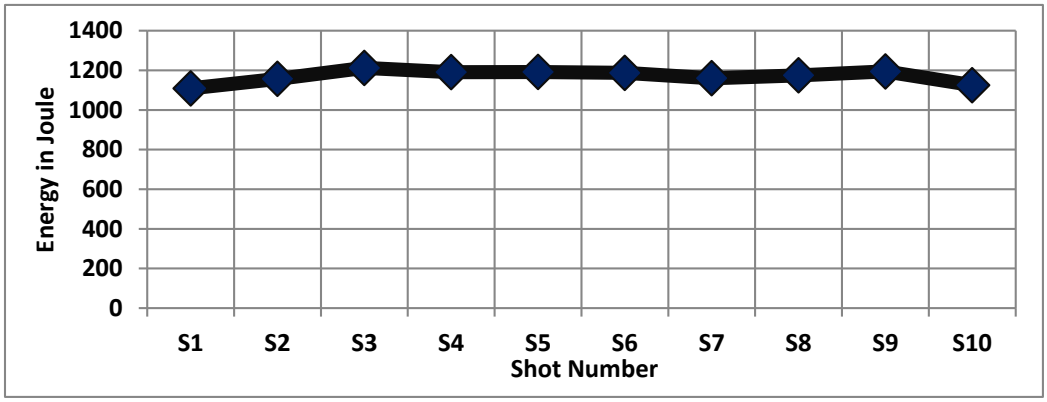

Figure 4.5.7: Shot to shot total energy variation for Winchester 0.308 caliber bullets

4.6 Stag Arms AR15

The AR-15 was a lightweight design that preceded and eventually led to the military M16. AR-15 is a trademark registered to Colt for civilian sales that refers to a broad class of firearms made by numerous manufacturers, hence the designation. This particular model is a Stag Arms model 2. It has an A2 flash hider, and a 16-inch barrel with the AP4 contour.

Figure 4.6.1: Stag Arms AR 15 (model 2) (Stag Arms)

In this experiment, Stag Arms AR15 is loaded with 5.56 NATO bullets.

Figure 4.6.2: 62 grain 5.56 NATO Lake City 2014 bullets (www.luckygunners.com)

Table 12: Features of 62 Grain NATO Lake City Bullets

Feature	Description
Bullet type	Full metal jacket
Bullet weight (in grain)	62
Bullet Caliber	5.56x45mm
Muzzle Energy (in foot pounds)	1256
Muzzle Velocity (based on bullet kinetic energy) (in fps)	3000
Cartridge Casing	Brass
Special Features	Boxer-primed, non-corrosive, and reloadable

4.6.1 Muzzle Blast Peak
Pressure of AR15 with 62 gr Lake City

10 shots were fired in succession from the AR15. Azimuthal muzzle blast peak pressure variation is plotted in figure 4.6.3.

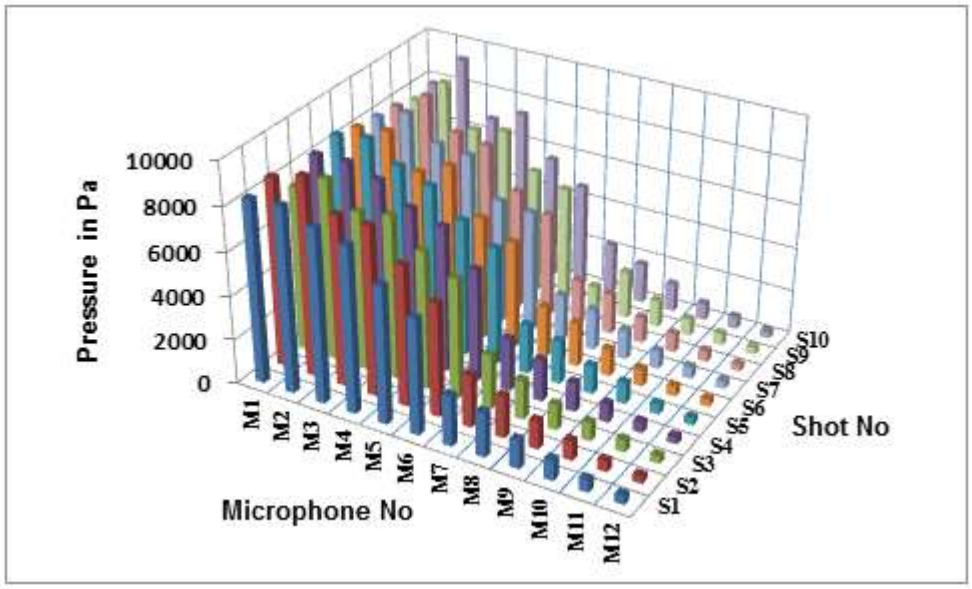

Figure 4.6.3: Peak pressure at 3 meters for the AR15 muzzle blast as a function of azimuth (10 shots)

4.6.2 Position of the Firearm
during 10 Shots of AR 15 Rifle

Position of the firearm during 10 shots of Winchester 308 rifle is shown in figure 4.6.4.

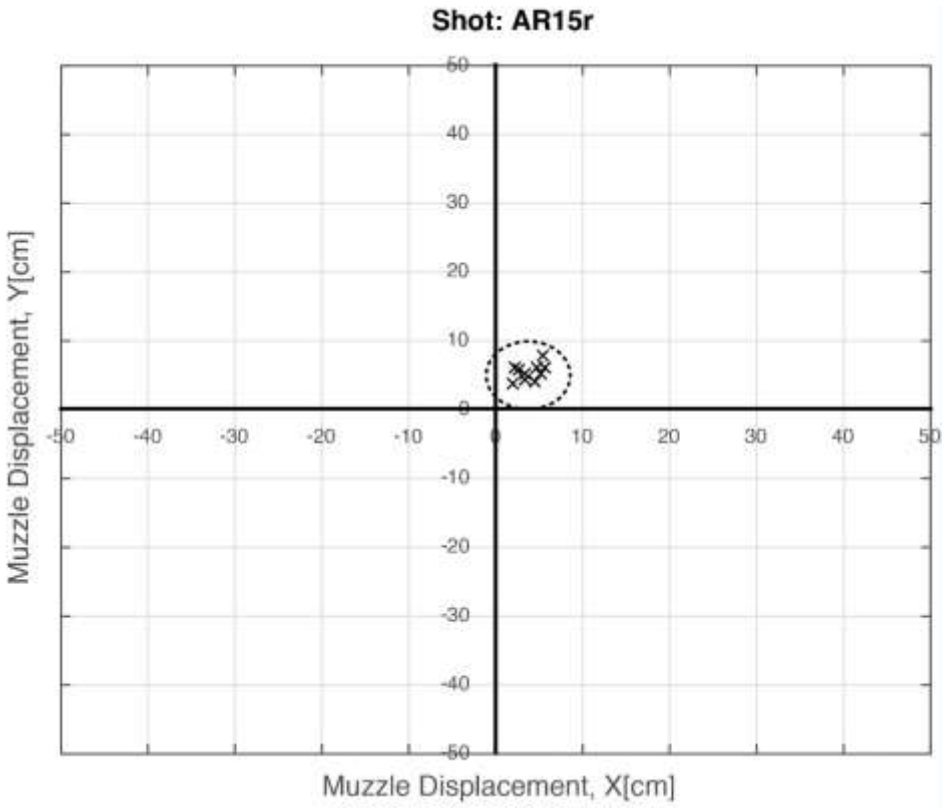

Figure 4.6.4: TDOA based position of the muzzle for ten successive shots from AR15 rifle

4.6.3 Muzzle Blast Duration

Figure 4.6.5 and 4.6.6 show the muzzle blast duration variation for different AR15 shots (using both waveform observation and energy accumulation method).

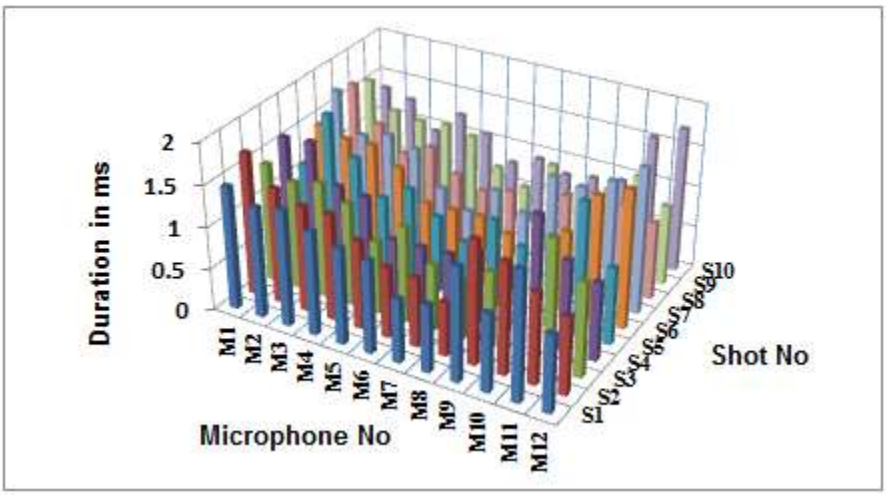

Figure 4.6.5: Azimuthal variation of the Muzzle blast durations for AR15 for 10 shots (waveform observation approach)

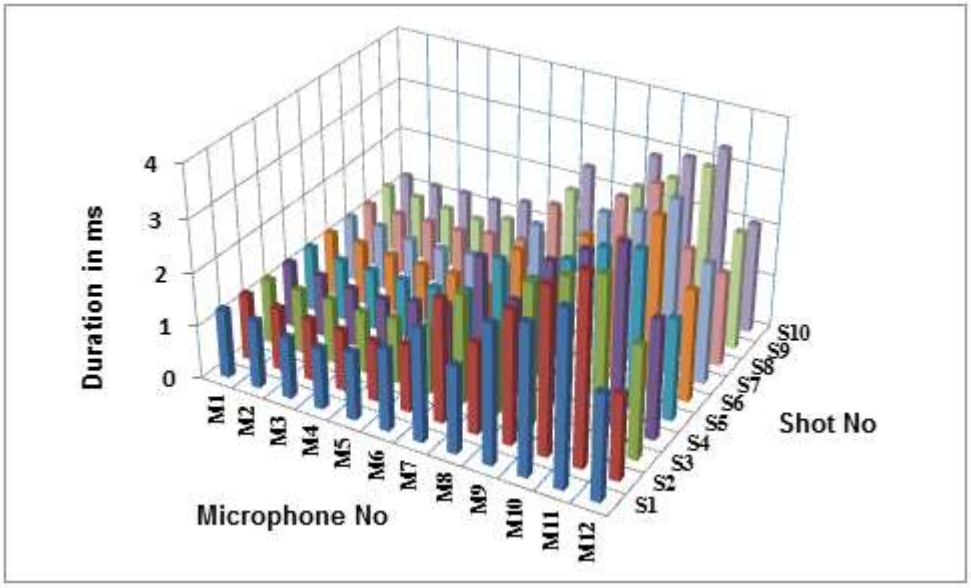

Figure 4.6.6: Azimuthal variation of the Muzzle blast durations for AR15 for 10 shots (energy accumulation method)

4.6.4 Total Energy Variation from One Shot to Another

To ensure enough speed of these bullets, these bullets contain a considerable amount of gunpowder. The lowest energy observed was from S8 (1127 Joule) and the highest was for S8 (1224 joule), as seen from figure 4.6.7.

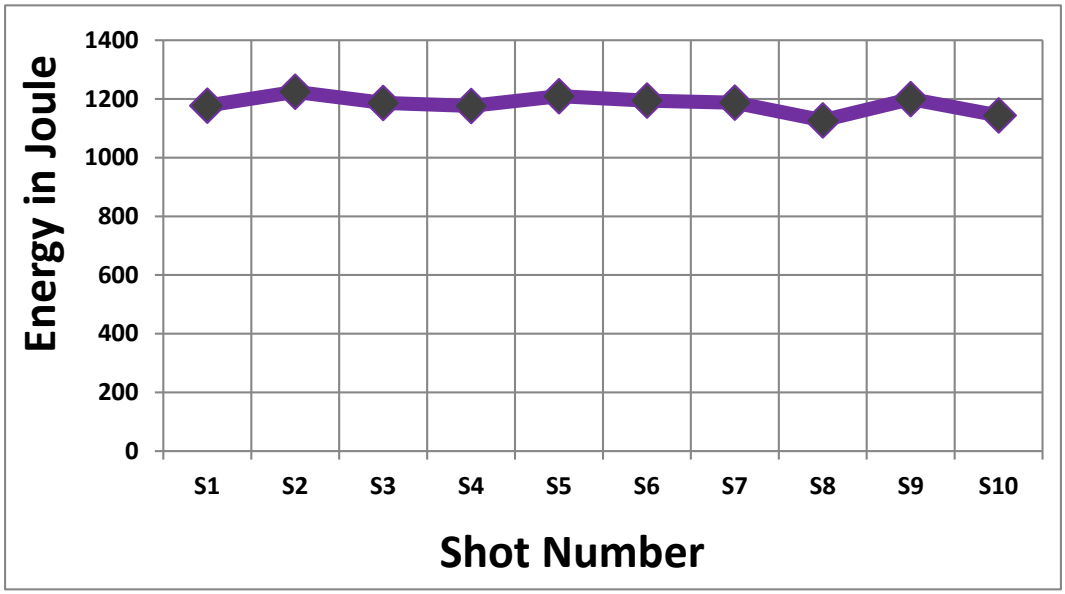

Figure 4.6.7: Shot to shot total energy variation for AR15

4.7 CZ 452 (Ceska Zbrojovka) (.22 cCliber)

Made in the Czech Republic, model 452 offers several variations and can be chambered with different types of cartridges. In our experiment, this firearm was equipped with 0.22 inches caliber bullet (figure 4.7.1).

Figure 4.7.1: CZ 452 (CZ-USA)

For our analysis, we have used a CZ 452 with 40 gr Fiocchi ammunition that has a flat head round nose (FLRN) configuration (figure 4.7.2).

Figure 4.7.2 : Fiocchi Ammunition 22 Long Rifle 40 Grain FLRN(www.midwayusa.com)

Table 13: Features of 40 gr 0.22 caliber long rifle

Feature	Description
Bullet type	0.22 Long rifle ammunition
Bullet weight (in grain)	40
Bullet Caliber	0.22
Muzzle Energy Total(in foot pounds)	102
Muzzle Velocity (based on bullet kinetic energy) (in fps)	1070
Special Features	Rim fire, Brass Casing, Flat lead round nose & Non corrosive

4.7.1Muzzle Blast Peak Pressure

The muzzle blast peak pressure for consecutive shots was observed as shown in figure 4.7.3.

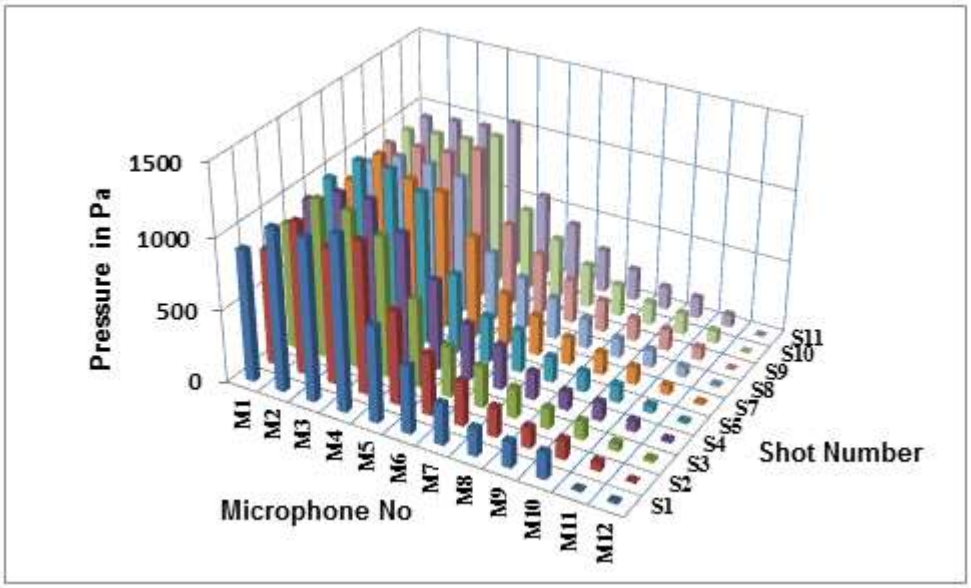

Figure 4.7.3: Muzzle blast peak pressure at 3 meters for the 0.22 caliber long rifle muzzle blast as a function of azimuth (10 shots)

4.7.2 Position of the Firearm
during 10 Shots of 0.22 Caliber Long Rifle

Position of the firearm during 10 shots of Winchester 0.22 caliber long rifle is shown in figure 4.7.4.

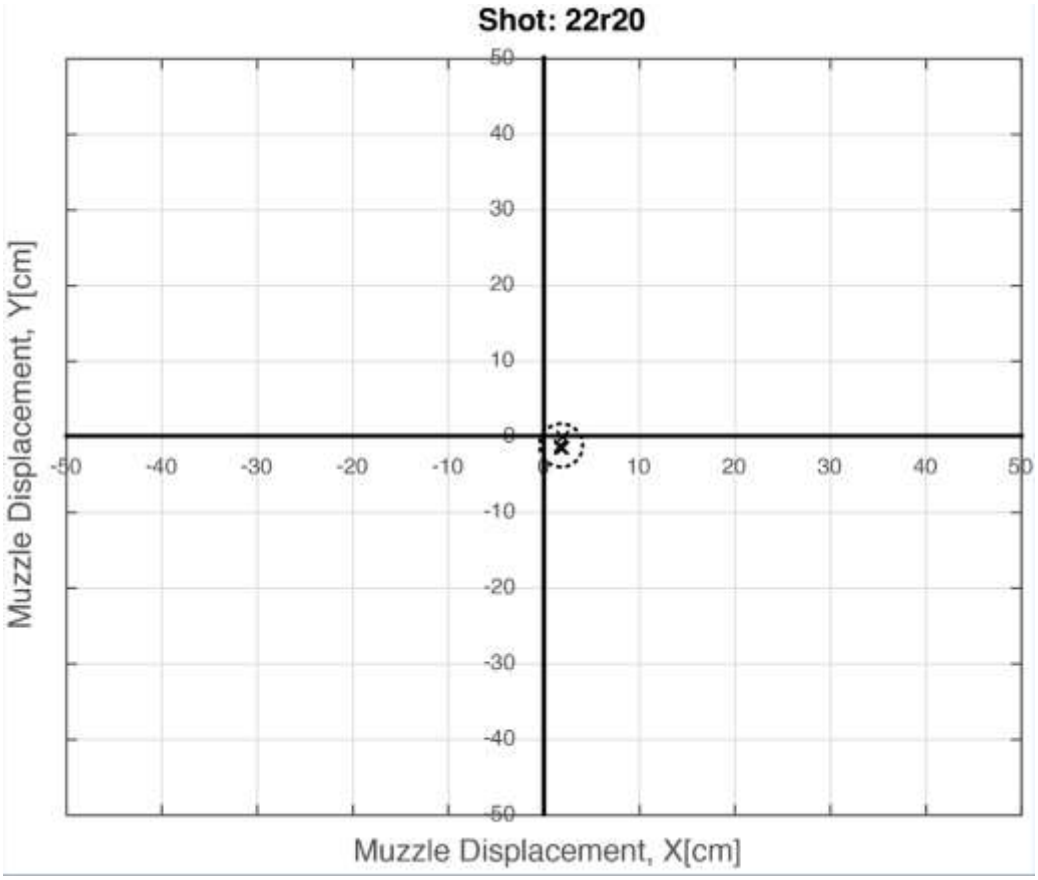

Figure 4.7.4: TDOA based position of the muzzle for ten successive shots from CZ 452 Rifle

4.7.3 Muzzle Blast Duration

Due to unusual behavior of these shots, waveform observation based muzzle blast duration (adding the positive and negative phase duration) was not included in this analysis. We have calculated the duration based on energy accumulation (figure 4.7.5).

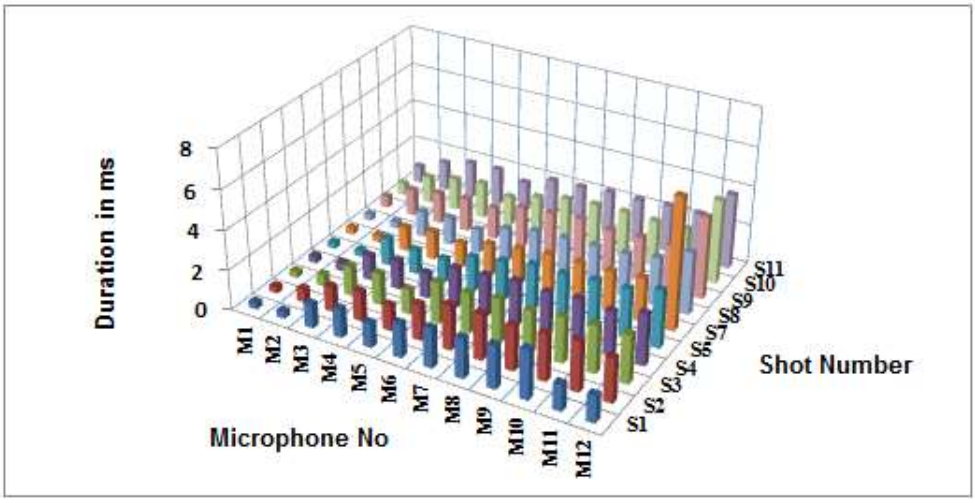

Figure 4.7.5: Shot to shot Muzzle blast duration variation for 0.22 LR (unfiltered)

4.7.4 Total Energy Emission from 0.22LR

The firing of rim fire bullets are as follows: as the trigger is pulled, the primer ignites the gunpowder. As it is ignited, the thin rim gets crushed before starting detonation. A major portion of the total energy gets lost during this destruction, so the total energy emanating from a single is much less than other bullets (Heard 2008). Shot to shot variation is shown in figure 4.7.6.

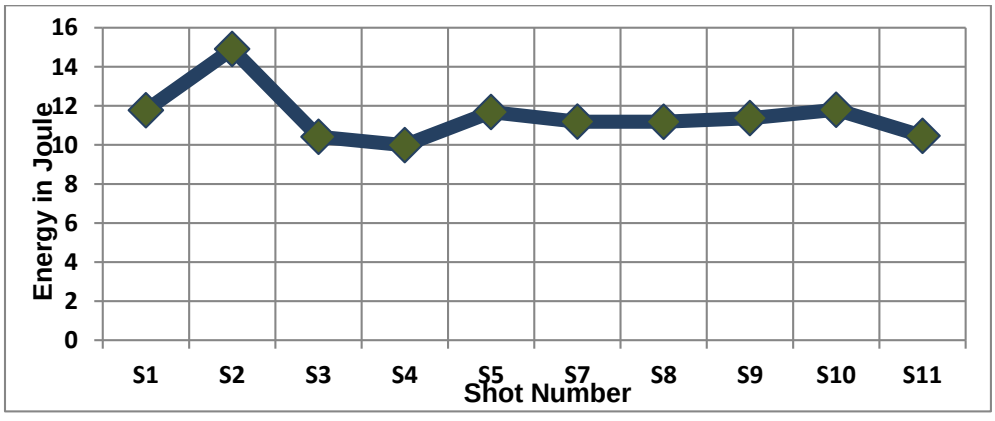

Figure 4.7.6: Shot to shot energy variation for 0.22 long rifles

4.8 Ruger SP 101

The SP101 is a modern double action revolver. Ruger SP 101 is used with two different type of ammunition: 0.357 inch caliber magnum and 0.38 inch special. All 357 magnum revolvers can be used with 38 special ammunitions. The difference is length, and allowable pressure. 38 special ammunition features less recoil. Both types of ammunition can be very accurate. Some shooters prefer 357 over 38 for better precision (Home Defense Gun).

Figure 4.8.1: Ruger SP 101 with 0.38 special (www.ruger.com)

Figure 4.8.2: 125 gr Winchester silvertip bullet (0.38 caliber)(http://www.ammunitiontogo.com)

Table 14: Features of 125 gr Silvertip bullets

Feature	Description
Bullet type	Silvertip Hollow Point
Bullet weight (in grain)	125
Bullet Caliber	0.38
Muzzle Energy (in foot pounds)	248
Muzzle Velocity (based on bullet kinetic energy) (in fps)	945
Cartridge Casing	Brass
Special Features	non-corrosive primer, low recoil

4.8.1 Muzzle Blast Peak Pressure of Ruger SP 101 with 0.38mm Caliber Ammunition

9 shots were fired in succession from the Ruger SP 101 with 0.38mm caliber ammunition. From figure 4.8.3, we observe that there are variations in the muzzle blast peak pressure for consecutive shots.

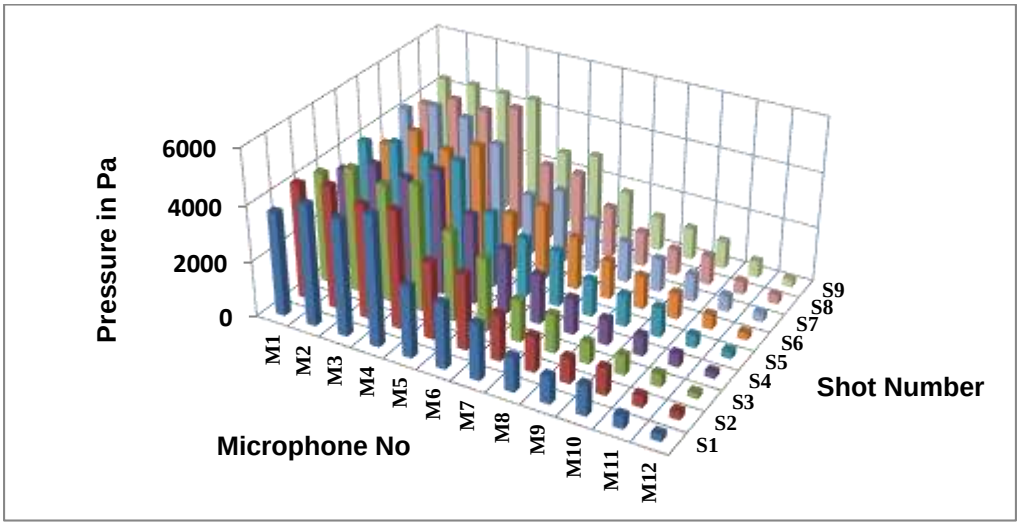

Figure 4.8.3: Peak pressure at 3 meters for Ruger sp101 with 0.38 caliber muzzle blast as a function of azimuth (9 shots)

4.8.2 Position of the Firearm during
10 Shots of Ruger SP101 with 0.38 Caliber

Position of the firearm during 10 shots of Winchester 0.22 caliber long rifle is shown in

figure 4.8.4.

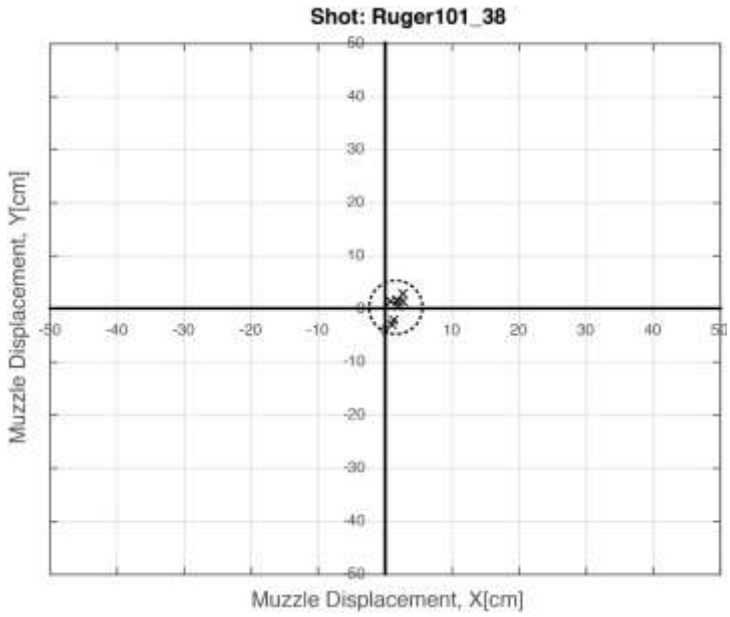

Figure 4.8.4: TDOA based position of the muzzle for ten successive shots from Ruger sp101 revolver with 0.38 caliber

4.8.3 Muzzle Blast Duration

Figure 4.3.5 shows the muzzle blast duration variation for different shots (using both waveform observation and energy accumulation method).

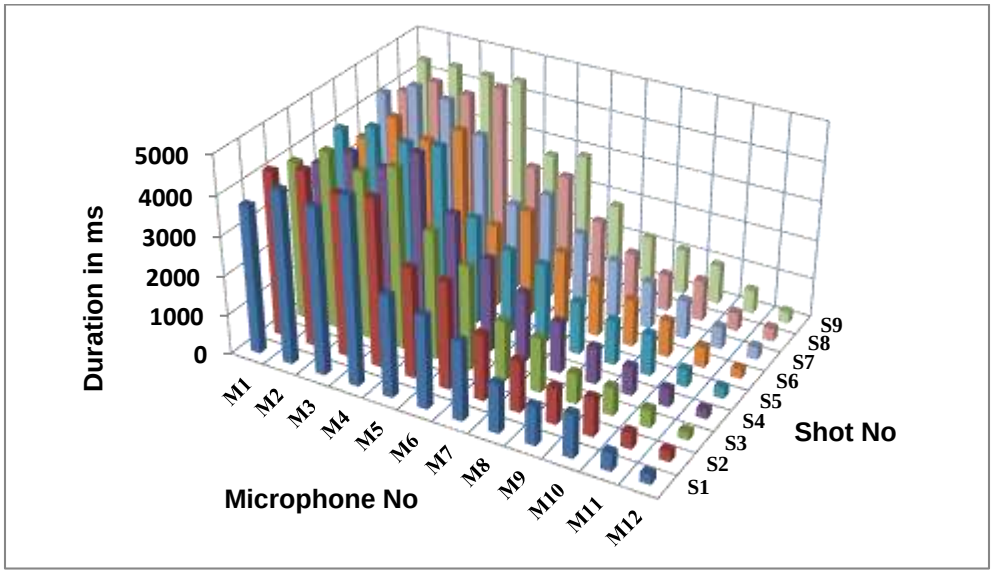

Figure 4.8.5: Azimuthal variation of the muzzle blast durations for Ruger SP101 with 0.38 caliber for 9 shots (waveform observation method)

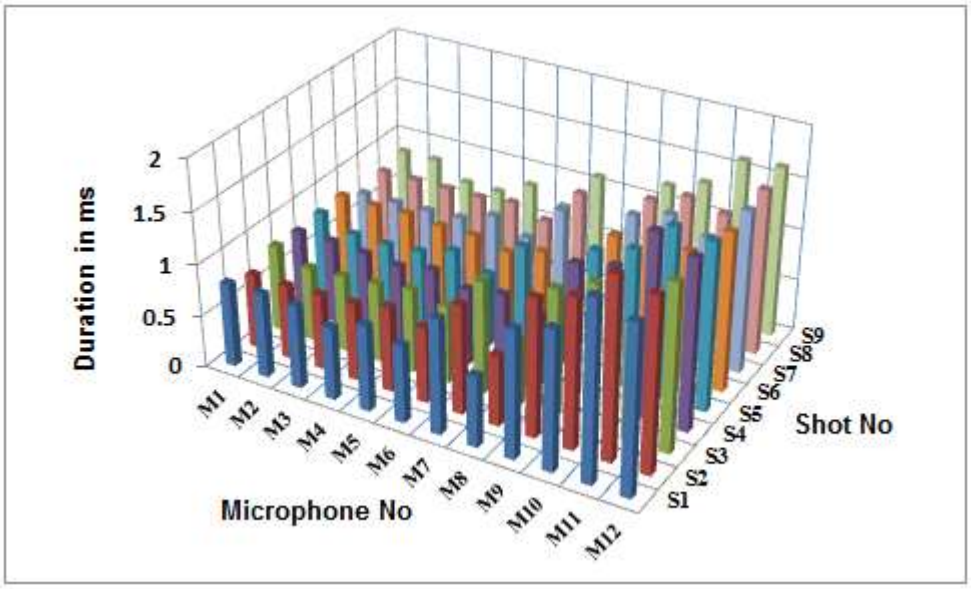

Figure 4.8.6: Azimuthal variation of the muzzle blast durations for Ruger SP101 with 0.38 caliber for 9 shots (energy accumulation method)

4.8.4 Total Energy Variation for Different Shots

Figure 4.8.7 shows total energy variation for consecutive shots. The energy varies from 291 joules (for S9) to 259 joules (for S2).

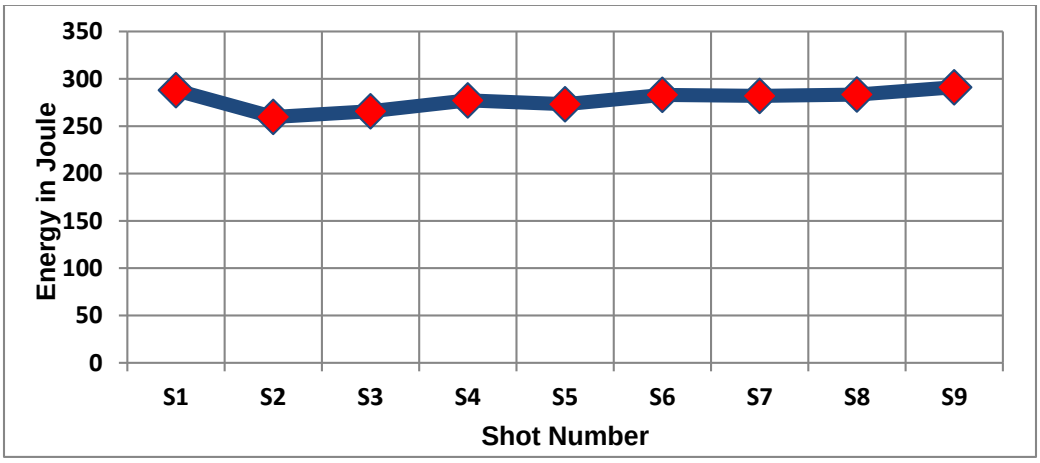

Figure 4.8.7: Shot to shot total energy variation for Ruger SP101 with 0.38 caliber ammunition

4.9 Ruger sp101 with 357 Magnums Ammunition

The acoustical characteristics of Ruger SP101, fired with 357 magnums are discussed below.

.

Figure 4.9.1: Ruger SP 101 with .357 Magnum (Chris Baker)

Figure 4.9.2: 0.357 inch jacketed flat/soft point bullet (www.luckygunners.com)

Figure 4.9.3: Outlook difference between 38 special and 357 magnums (www.usacarry.com)

Table 15: Features of 158 grain JSP bullets

Feature	Description
Bullet type	Jacketed Flat point/ soft point
Bullet weight (in grain)	158
Bullet Diameter (in mm)	0.357
Muzzle Energy (in foot pounds)	539
Muzzle Velocity (based on bullet kinetic energy) (in fps)	1240
Cartridge Casing	Brass
Special Features	boxer-primed, non-corrosive, and reloadable

4.9.1 Muzzle Blast Peak Pressure of Ruger SP 101 with 0.357 Inch Caliber Ammunition

10 shots were fired in succession from the Ruger SP 101 with 0.38mm caliber ammunition. From figure 4.9.4 we observe that there are variations in the muzzle blast peak pressure for consecutive shots.

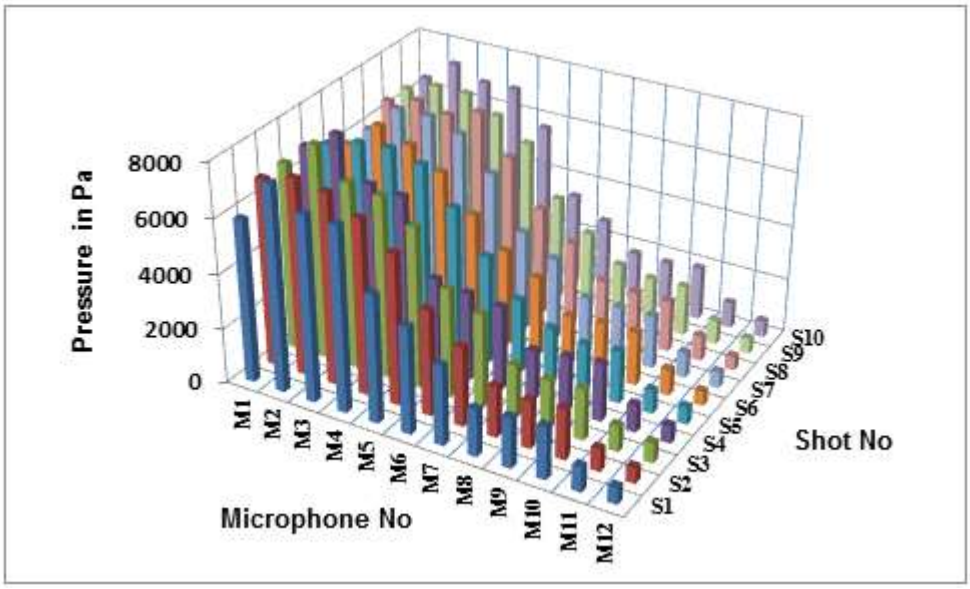

Figure 4.9.4: Peak pressure at 3 meters for Ruger sp101 with 0.357 caliber muzzle blast as a function of azimuth (10 shots)

4.9.2 Position of the Firearm during
10 Shots of Ruger SP101 with 0.38 Caliber

Position of the firearm during 10 shots of Winchester 0.22 caliber long rifle is shown in

figure 4.9.5.

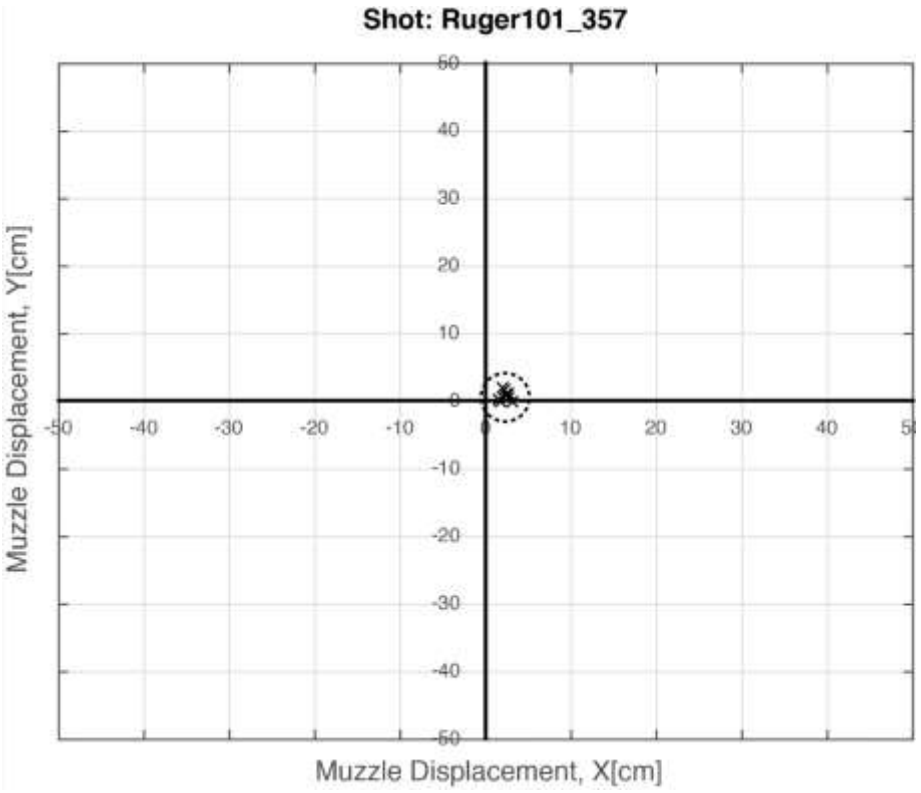

Figure 4.9.5: TDOA based position of the muzzle for ten successive shots from Ruger SP101 revolver with 0.38 caliber

4.9.3 Muzzle Blast Duration

Figure 4.9.6 and 4.9.7 show the muzzle blast duration variation for different Ruger SP101 shots with 0.357 caliber (waveform observation method was used). The duration is much higher than 0.38 caliber for lower azimuths.

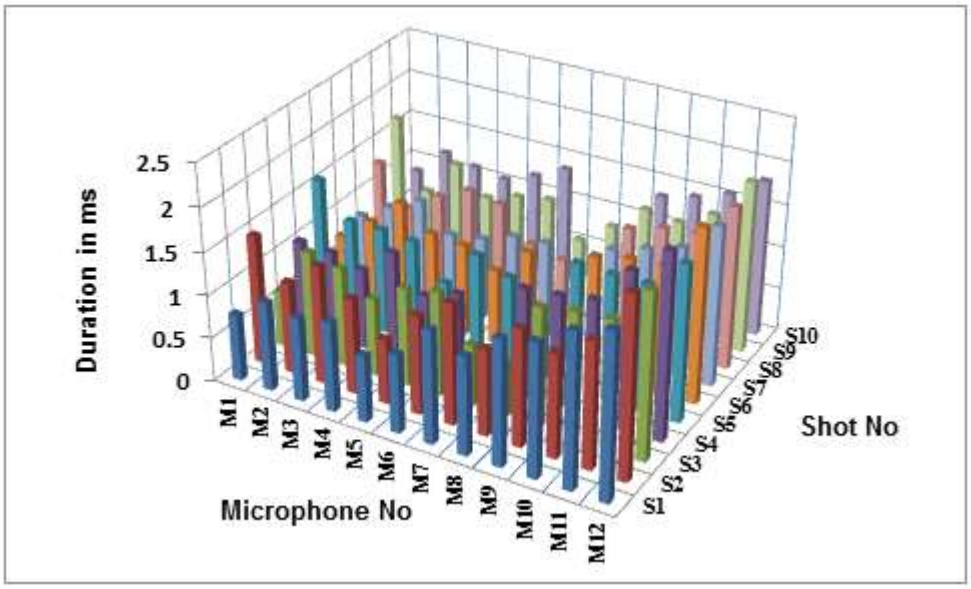

Figure 4.9.6: Azimuthal variation of the Muzzle blast durations for Ruger SP101 with 0.357 caliber for 10 shots (waveform analysis)

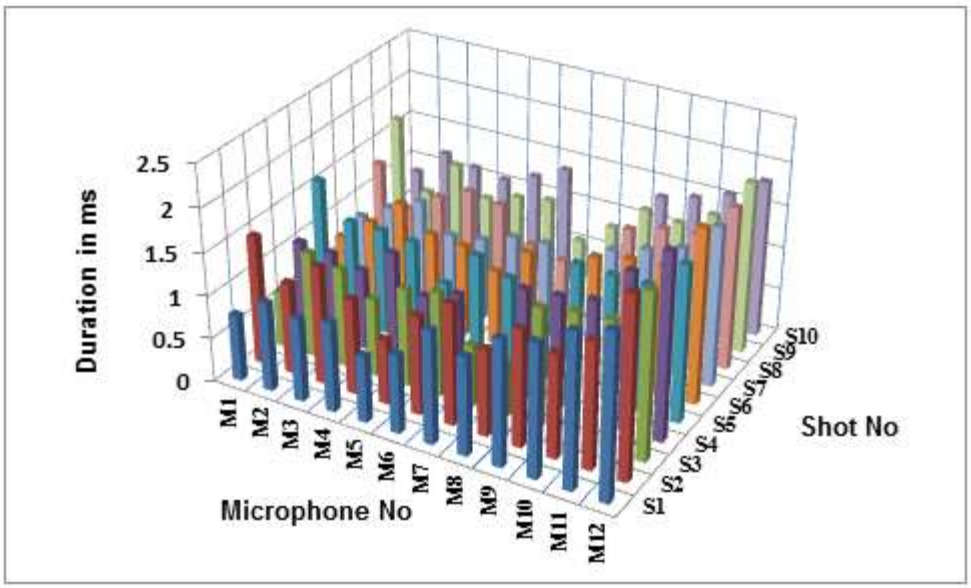

Figure 4.9.7: Azimuthal variation of the Muzzle blast durations for Ruger SP101 with 0.357 caliber for 10 shots (energy accumulation)

4.9.4 Total Energy Variation from One Shot to Another

Figure 4.9.8 portrays the total acoustic energy variation for Ruger SP101 for different shots with 0.357 ammunitions. The energy level was higher than 0.38 caliber bullets. The energy varies from 934 joules (for S3) to 847 joules (for S4).

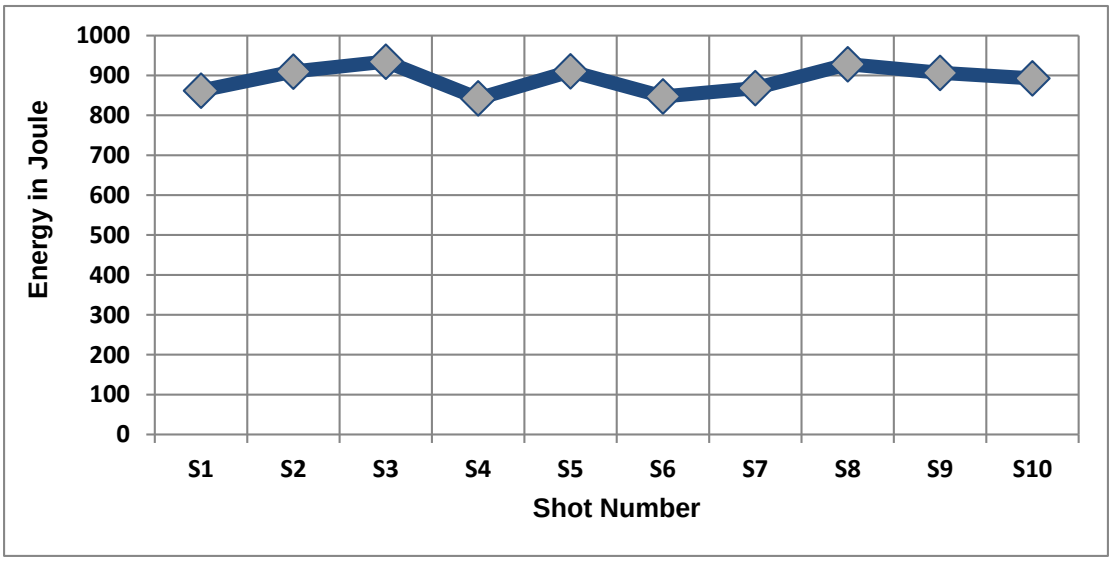

Figure 4.9.8: Shot to shot total energy variation for Ruger SP101 with 0.357 ammunitions

4.10 Shotgun

Shotguns are fired with cartridge with individual pellets rather than a single bullet.

In our experiment, Remington 870 was used with 00 buck shots.

Figure 4.10.1: Remington 870 (www.remington.com)

Figure 4.10.2: 12ga Remington 3" buckshot ammunition (Anon n.d.)

Table 16: Features of Remington 00 buck shots

Feature	Description
Bullet type	#00 Buckshot
Average pallet weight (in grain)	53
Pallet Diameter (in inch)	0.33
Muzzle Energy Total(in foot pounds)	1899
Muzzle Velocity (based on bullet kinetic energy) (in fps)	1100
Special Features	Copper plated, modified choke

4.10.1 Muzzle Blast Peak Pressure
Variation of 12ga with 00 Buckshot

3 shots were fired in succession from the Remington 870. Figure 4.10.3 describes the variations in the muzzle blast peak pressure for consecutive shots.

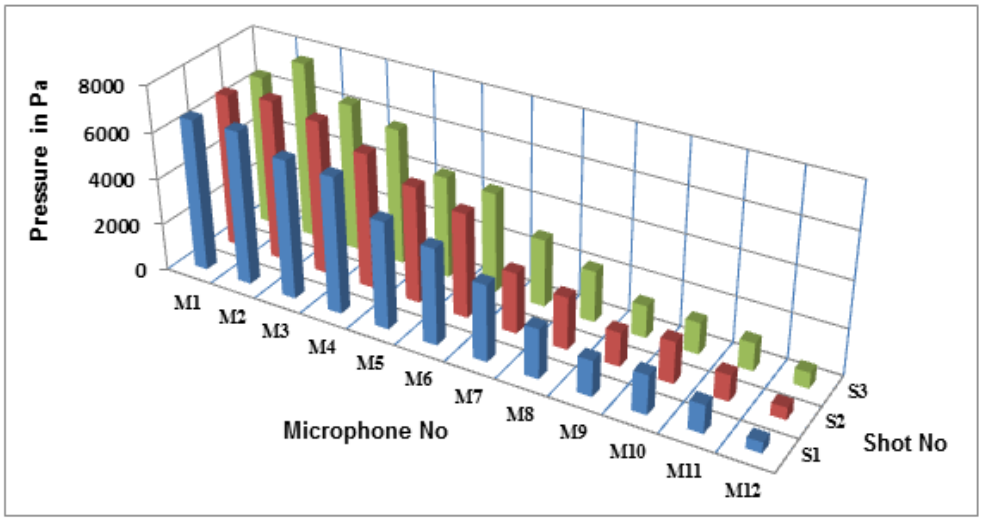

Figure 4.10.3: Peak pressure at 3 meters for 12ga shotgun muzzle blast as a function of azimuth (3 shots)

4.10.2 Position of the Firearm
during 10 Shots of 12ga with 00 Buckshots

Position of the firearm during 10 shots of Winchester 0.22 caliber long rifle is shown in figure 4.2.4.

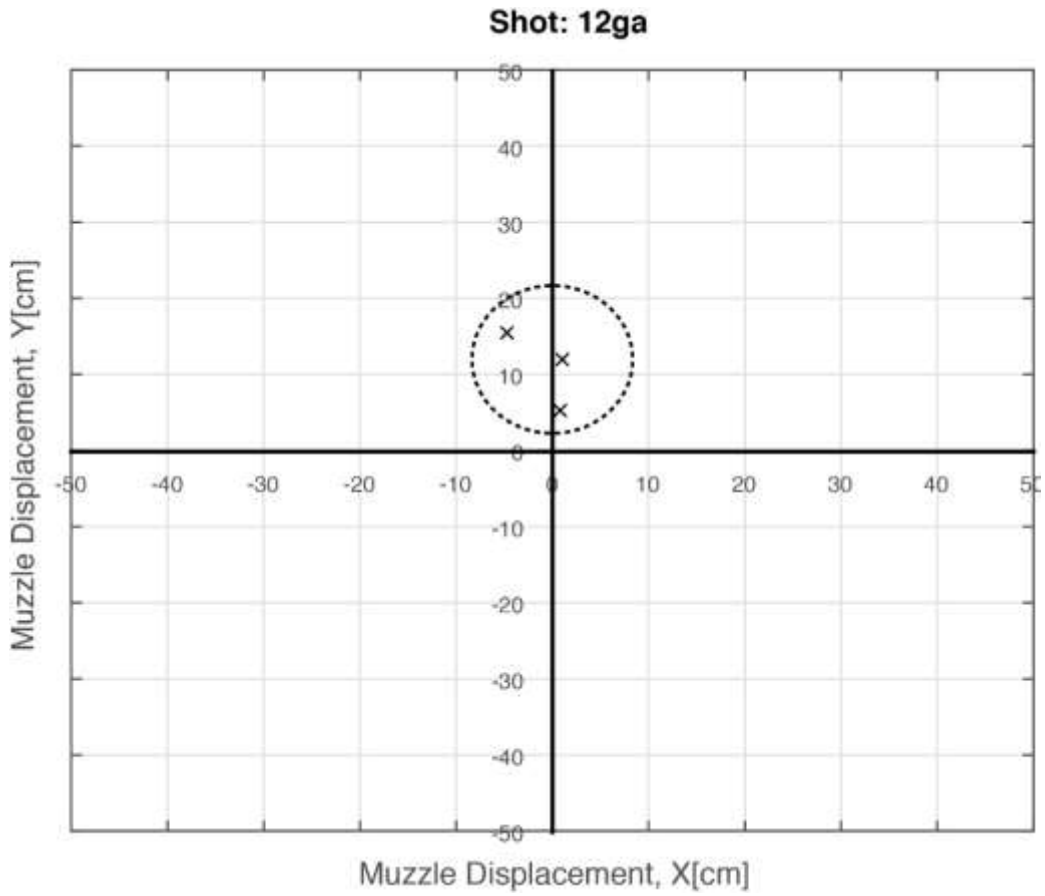

Figure 4.10.4: TDOA based position of the muzzle for ten successive shots from 12ga 00 buckshots

4.10.3 Muzzle Blast Duration Variation

Figure 4.10.5 and 4.10.6 show the muzzle blast duration variation for different shots from 12 ga 00 buck shots (waveform observation method was used).

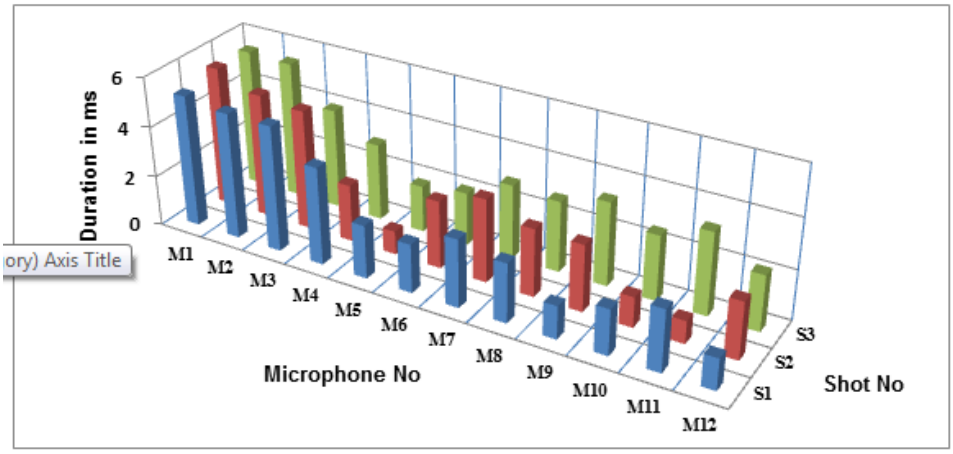

Figure 4.10.5: Shot to shot azimuthal variation of the muzzle blast duration for 12ga for 3 shots (waveform observation)

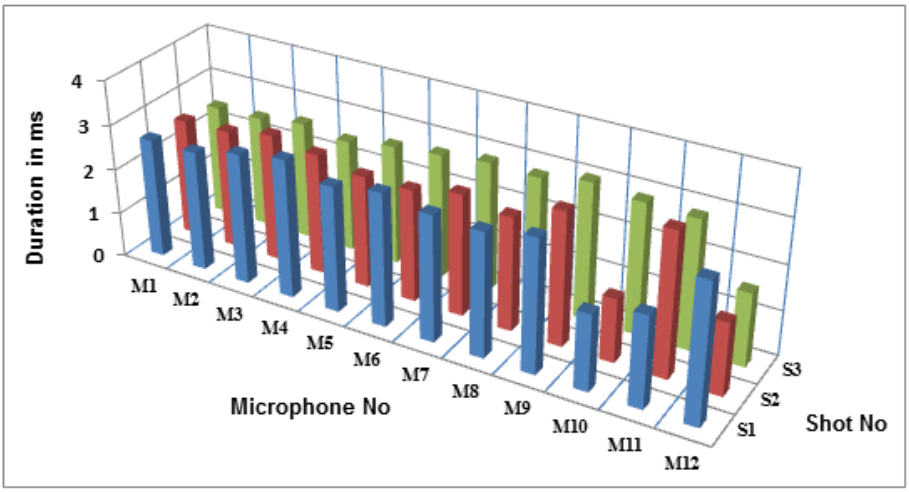

Figure 4.10.6: Energy accumulation based Muzzle blast duration (93%) for 12ga shotgun (3 shots)

4.10.4 Total Energy of Each Shot

The variation of total energy is observed from one shot to the other. Peak pressure values are slightly greater at S2 than other shots as shown in figure 4.10.7.

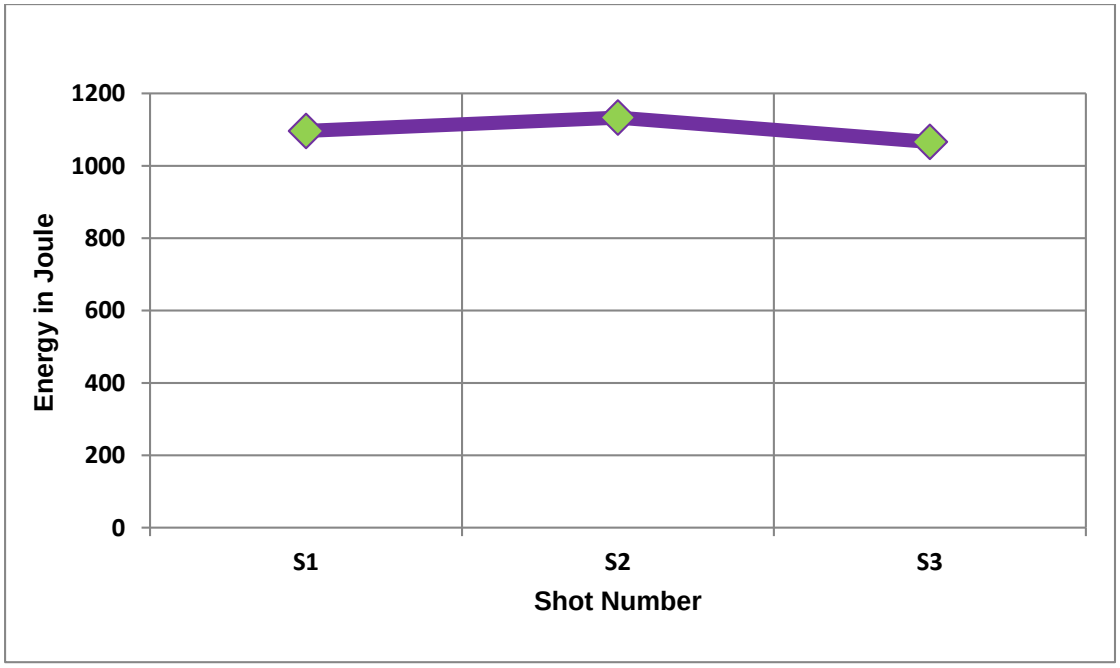

Figure 4.10.7: Total energy variation from one shot to another

4.11 Correlation of Gunshots with Colt 1911A1 (45 ACP)

Correlation factors were calculated of various gunshots with respect to the Colt 1911A1 45 ACP. To find out the correlation factor, the signal captured at M1 from the first shot was taken as the reference. The ideas behind this observation were:

1. How similar the firearm sound?
2. How they are correlated according to the azimuth?

Figure 4.11.1 shows the variation of the correlation factors compared with the reference signal with successive shots.

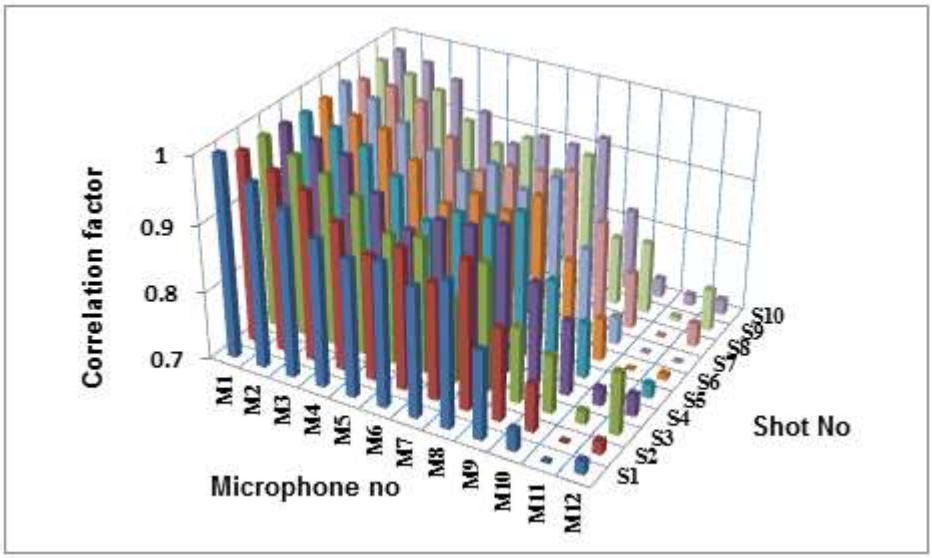

Figure 4.11.1: Azimuthal variation of correlation factor for 10 shots of Colt 1911A1 (45 ACP) (compare to S1, M1)

In figure 4.11.2, we have considered the azimuthal variation for the first shot of Colt 1911A1 (45 ACP). Starting from value 1 (exact match for the same signal), the correlation factor tends to decrease with increasing azimuth.

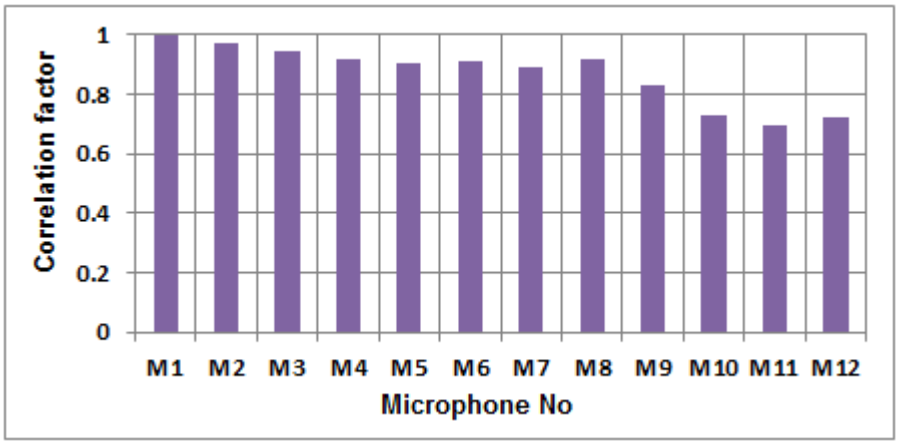

Figure 4.11.2: Azimuthal variation of correlation factor for the first shot of Colt 1911A1 (45 ACP)

If we look at the variation at the same azimuth (M1) for different shots, we also observe that there is variation from one shot to the other, as seen in figure 4.11.3. The lowest correlation was observed for S8.

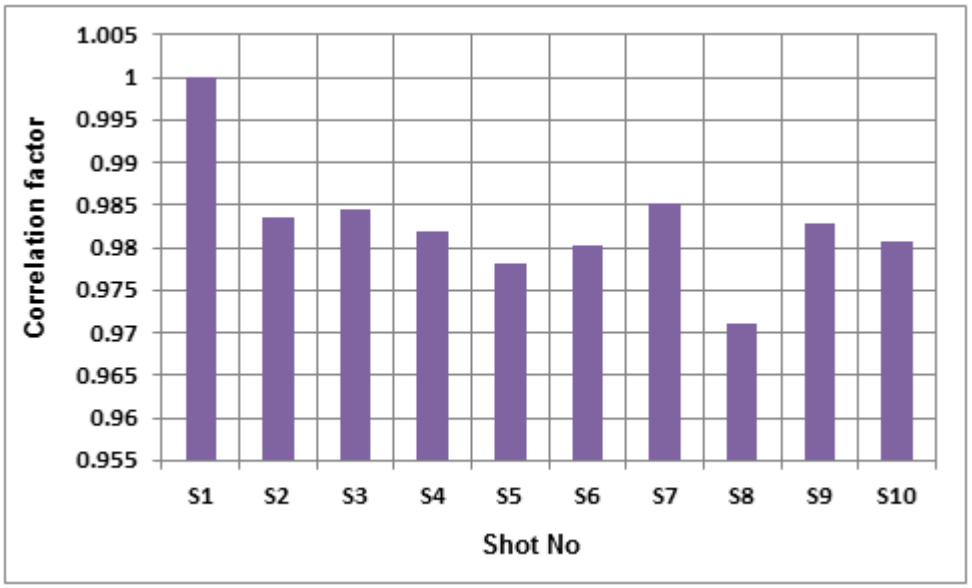

Figure 4.11.3: Successive shot variation of correlation factor at M1 of Colt 1911A1 (45 ACP)

As said before, to make a comparison between different firearms, the correlation was also tried in between Colt 1911A1 (45 ACP) and other firearms. Figure 4.11.4 shows the correlation coefficient variation between other pistol categories.

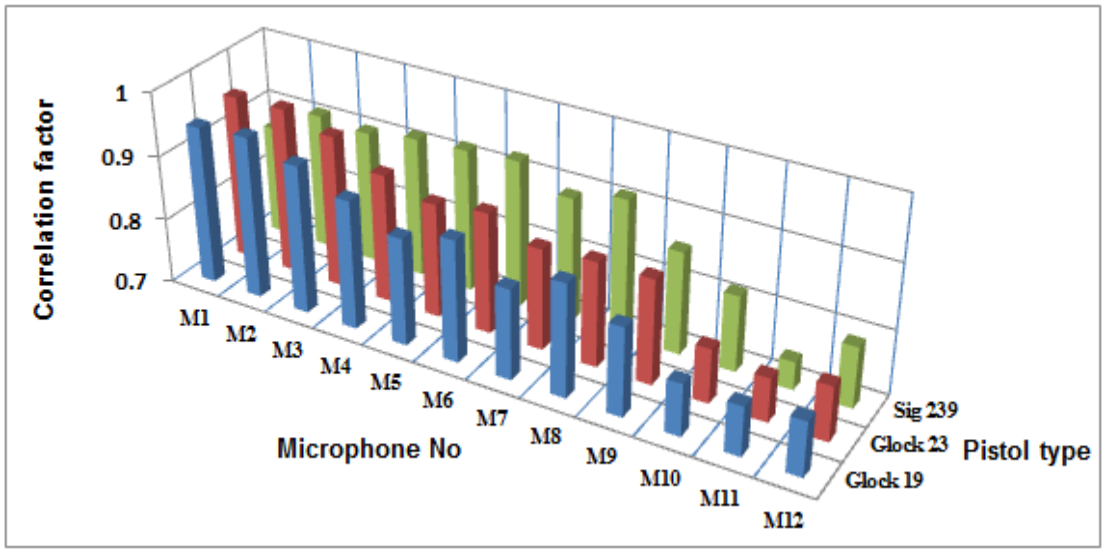

Figure 4.11.4: Variation of correlation factor of Colt 1911A1 (45 ACP) with other pistols

Each signal was taken from first shot of the firearm, the correlation of Colt 1911A1 (45 ACP) was found highest with Glock 19/ 135 JHP. With increasing azimuth, the correlation value decreases in all the cases. The lowest correlation values were observed for Sig 239.

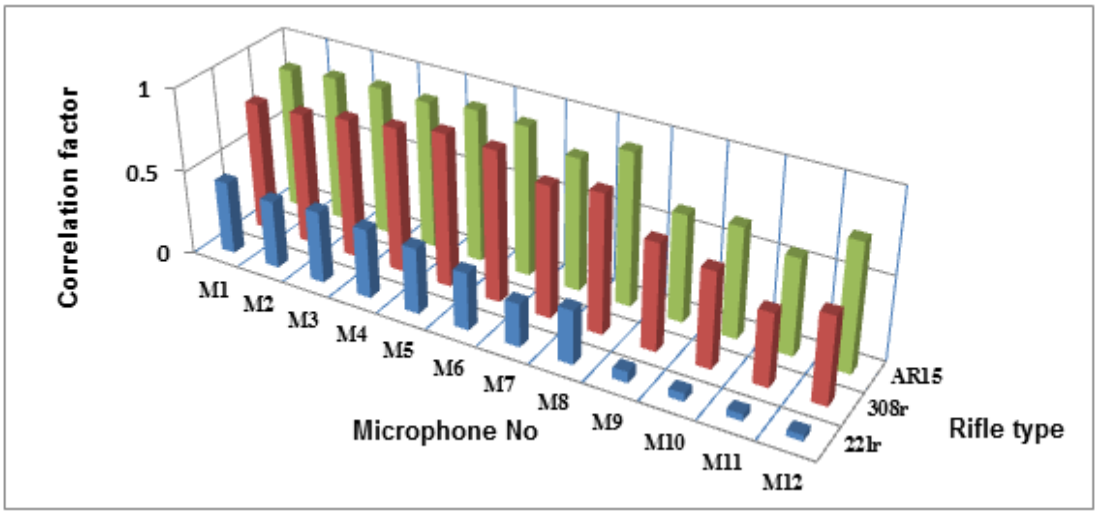

Figure 4.11.5: Variation of correlation factor of Colt 1911A1 (45 ACP) with rifles

Figure 4.11.5 compares Colt 1911A1 (45 ACP) with 3 different rifles types: 22r, 308r and AR15. 0.22 caliber long rifle shots were quiet, as seen from the peak pressure amplitude. The correlation was also the lowest for this rifle. Values were high at the line of fire (near about 0.8) for 308r and AR15 but tend to decrease rapidly after the azimuth of M8.

Colt 1911A1 (45 ACP) exhibits very high correlation with revolver category as found from the analysis (figure 4.11.6).

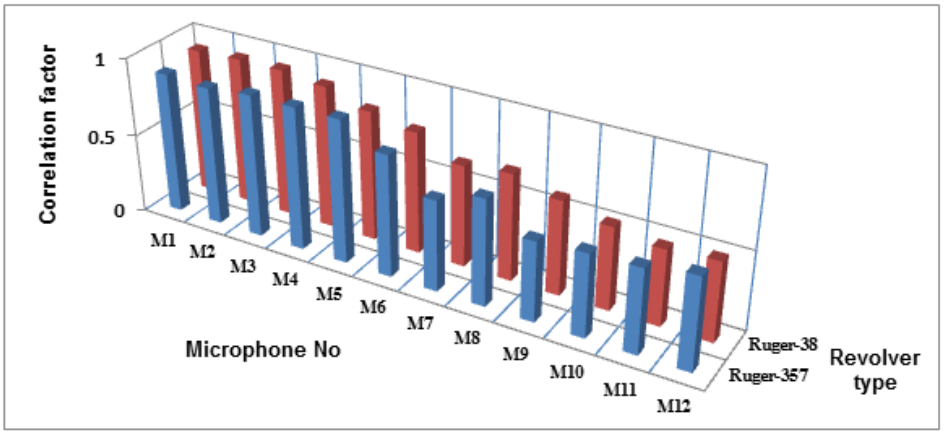

Figure 4.11.6: Variation of correlation factor of Colt 1911A1 (45 ACP) with revolvers

If Colt 1911A1 (45 ACP) gunshot signals are compared with the shotgun signal, we can see highest correlation factors are near about 0.68, less than both rifle or revolver category (figure 4.11.7).

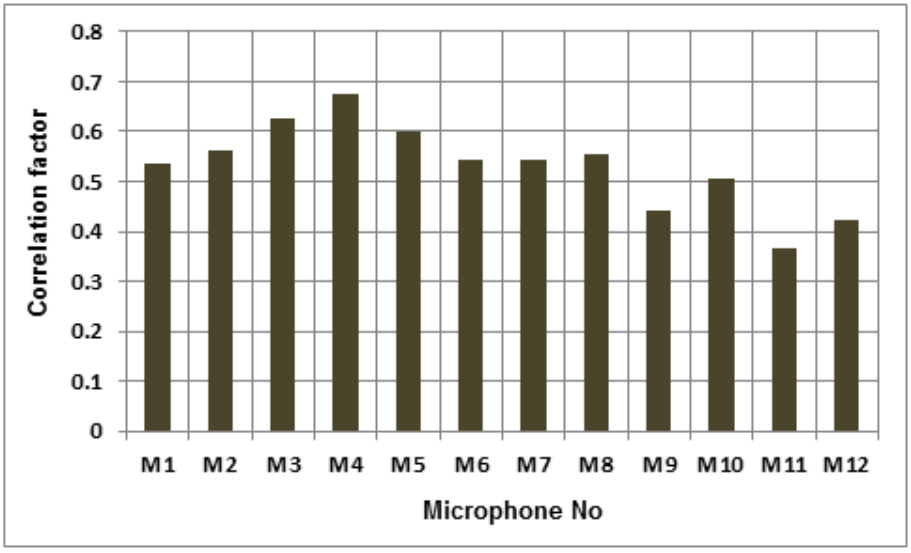

Figure 4.11.7: Variation of correlation factor of Colt 1911A1 (45 ACP) with 12ga Shotgun

4.12 Comparison between Experimental Recording and Real Life Recording

As described earlier, in real life, gunshots signals are captured using low sampling rate, limited bandwidth audio recorders. Due to the lack of any real life recording, we modified our recorded signal, through resampling and filtering and tried to simulate real world gunshot signals, as described earlier. We have selected a firearm from each category (pistol, rifle, revolver, and shotgun) and compared simulated signals (15 kHz resampled recording, lower cutoff at7.5 kHz and 20 kHz resampled recording, lower cutoff at 10 kHz) with 500 kHz recorded signal. The reference signals that were picked for comparisons were at the line of fire from the first shot. The correlation factors were calculated as stated earlier. The goal was to make a simple observation that if we compare the real life recorded data with gunshot data acquired in a controlled environment, what is the nature of linear correlation factors.

To see the variability, we have chosen S1, M1 signal of each type of firearm and compared 500 KHz signal with 15 KHz and 20 KHz sampling rate signals of different firearms at different azimuths for the first shot. Figure 4.12.1 shows the muzzle blast waveforms for Colt 1911A1 (45 ACP) signals, chosen from pistol category for comparison. With different sampling rates, these are not the same length signals, along with variation in signal amplitude. As seen from the figure 4.12.1, the lower sampled signals fail to follow the sudden rise and fall during the blasts. Higher linear correlation was observed for the 15 kHz than 20 KHz version for this category. The correlation was the highest at M5 for 20 KHz. At different azimuths, the correlation value seems to vary randomly (showed in figure 4.12.2 and figure 4.12.3).

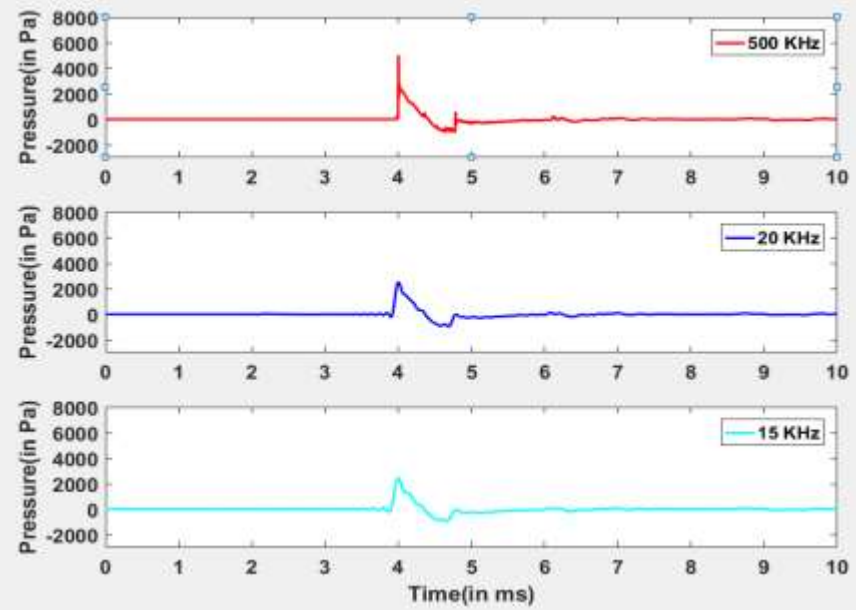

Figure 4.12.1: Muzzle blast portion of Colt 1911A1 (45 ACP): S1: M1 for different sampling rate

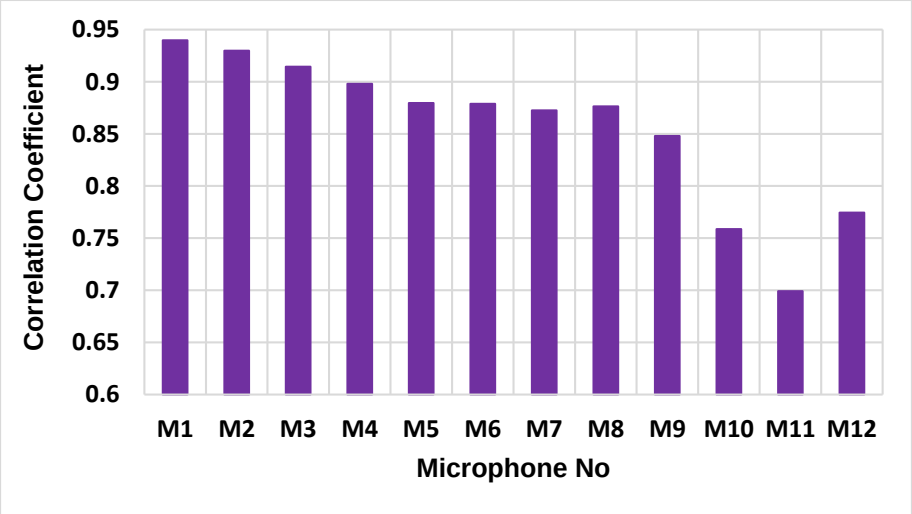

Figure 4.12.2: Correlation factors of 500 kHz Colt 1911A1 (45 ACP) (S1: M1) with 15 kHz Colt 1911A1 (45 ACP) (S1)

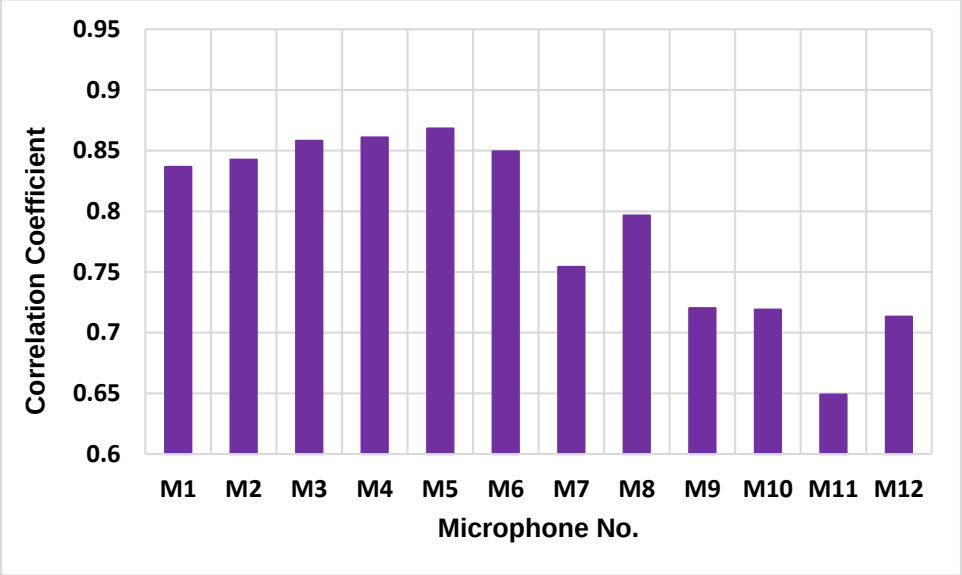

Figure 4.12.3: Correlation factors of 500 kHz Colt 1911A1 (45 ACP) (S1: M1) with 20 kHz Colt 1911A1 (45 ACP) (S1)

From rifle category, Winchester 0.308 caliber gunshot signals were picked for analysis. Again, the factors were higher for 15 kHz (figure 4.12.4 and fig 4.12.5). One of the interesting facts was that the correlation factor for M5 was the highest for 15 kHz, whereas M6 was found in the case of 20 KHz sampling rate. It means that, although this high correlation value indicates that the shot was probably taken from a rifle, it does not indicate the directionality of the recording medium in this case. Figure 4.12.6 showed the comparison of the muzzle blast portions of 3 signals having different sampling rate for Winchester 0.308 caliber.

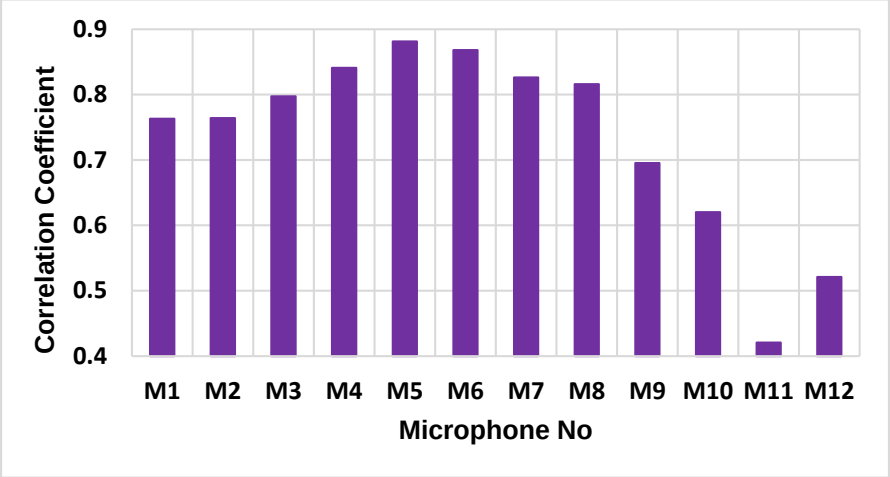

Figure 4.12.4: Correlation factors of 500 kHz with 308r signal (S1: M1) with 15 kHz 308r (S1) signal

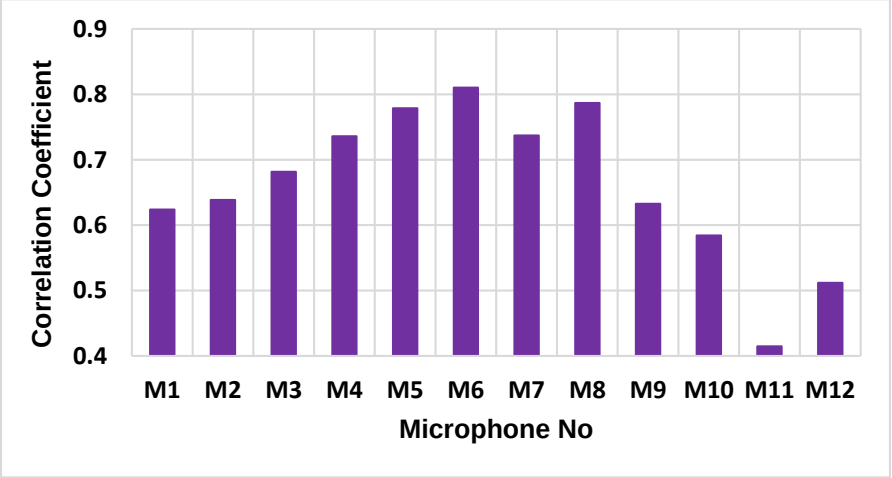

Figure 4.12.5: Correlation factors of 500 kHz with 308r signal (S1: M1) with 20 kHz 308r (S1) signal

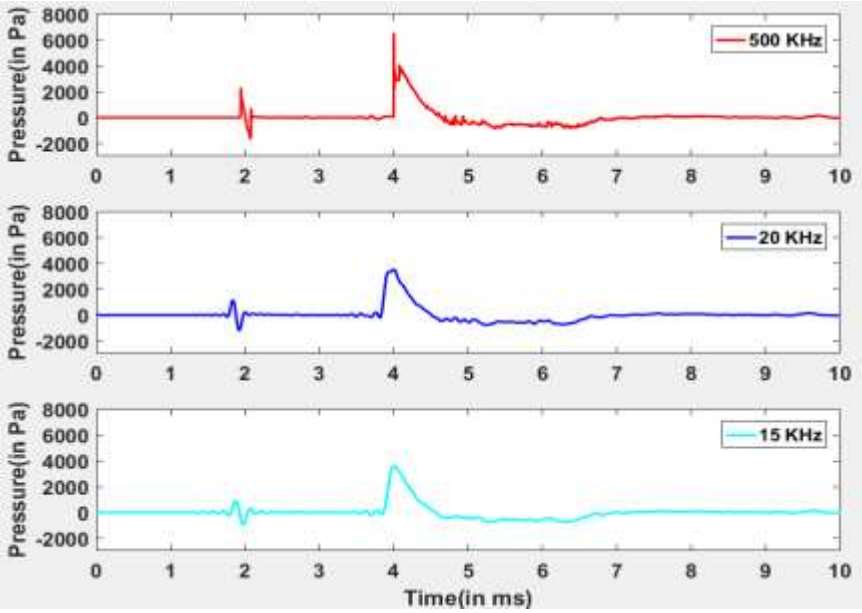

Figure 4.12.6: Muzzle blast portion of Winchester 0.308 caliber: S1: M1 for different sampling rates

Ruger SP 101 with 357 magnum bullets was picked up from revolver category. Again, the maximum linear correlation values for the 500 kHz, M1, S1 signal was observed at different azimuths other than M1 (M5 for both 15 kHz and20 kHz) as seen from figures 4.12.7 and figure 4.12.8.

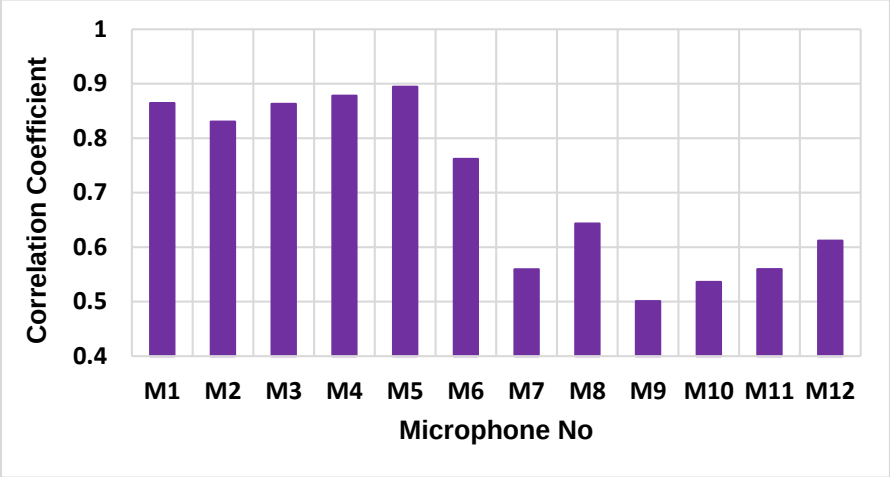

Figure 4.12.7: Correlation factors of 500 kHz Ruger SP 101 with 357 magnums (S1: M1) with 15 kHz Ruger SP 101 with 357 magnums (S1)

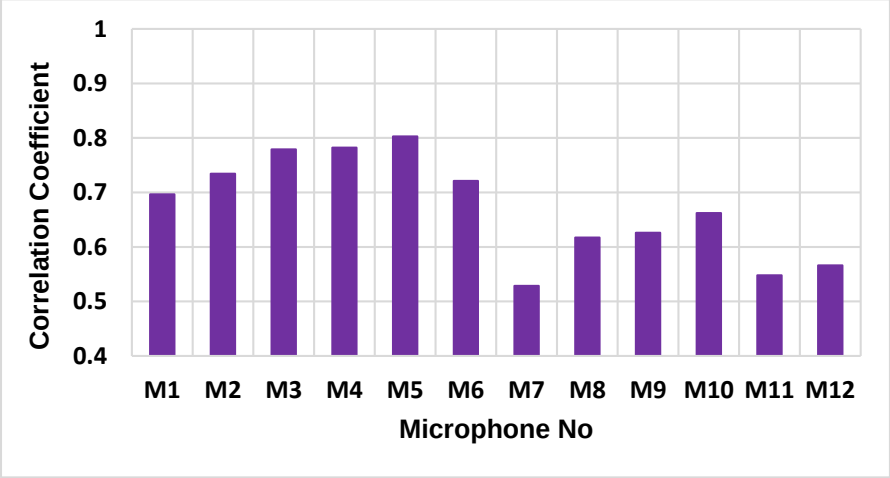

Figure 4.12.8: Correlation factors of 500 kHz Ruger SP 101 with 357 magnum (S1: M1) with 20 kHz Ruger SP 101 with 357 magnums signal (S1)

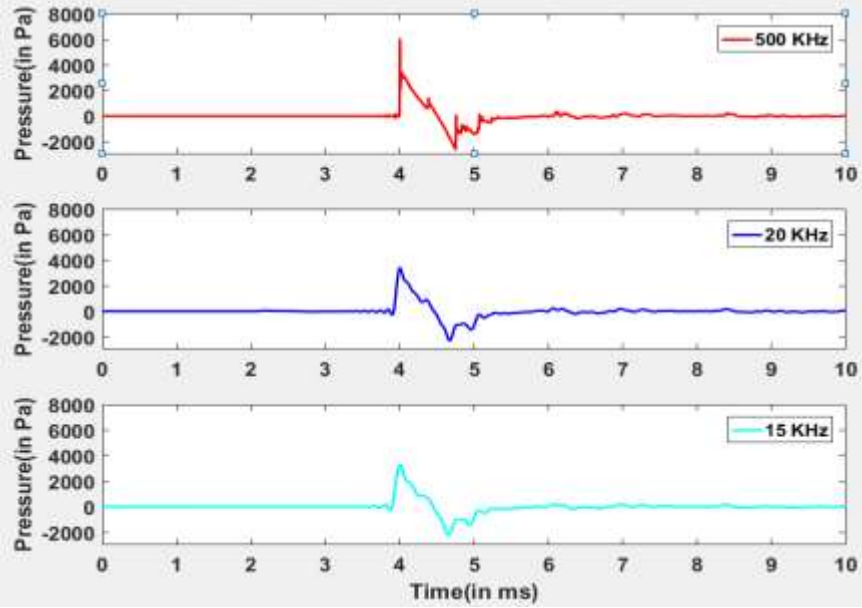

Figure 4.12.9: Muzzle blast portion of Ruger SP 101: S1: M1 for different sampling rates

For shotgun signals (12ga: 00 buck shot), it was found that there is azimuthal variation in linear correlation values among signals having different sampling rates. Again, highest correlation value occurs at a different azimuth than M1 (M4 in both the cases). Therefore, for shotgun signals, the correlation factors cannot reveal the firearm type and the azimuthal information of the recorder.

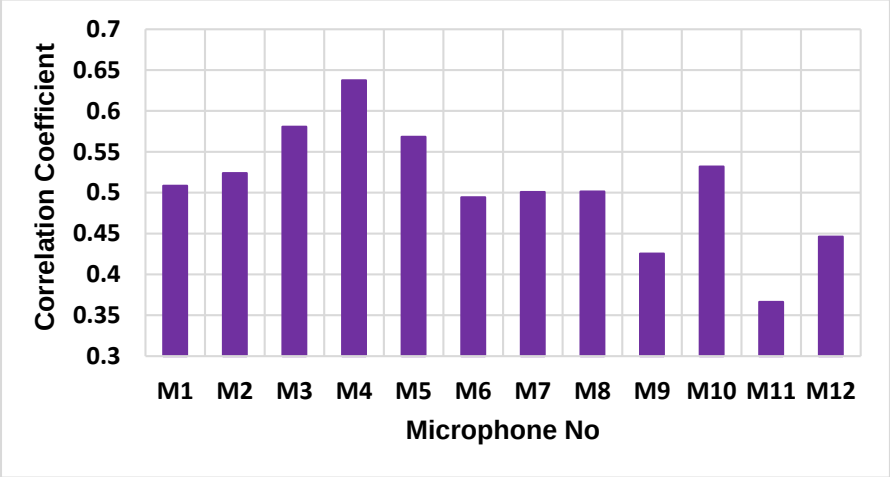

Figure 4.12.10: Correlation of 500 kHz 12ga shotgun (S1: M1) with 15 kHz 12ga shotgun signal (S1)

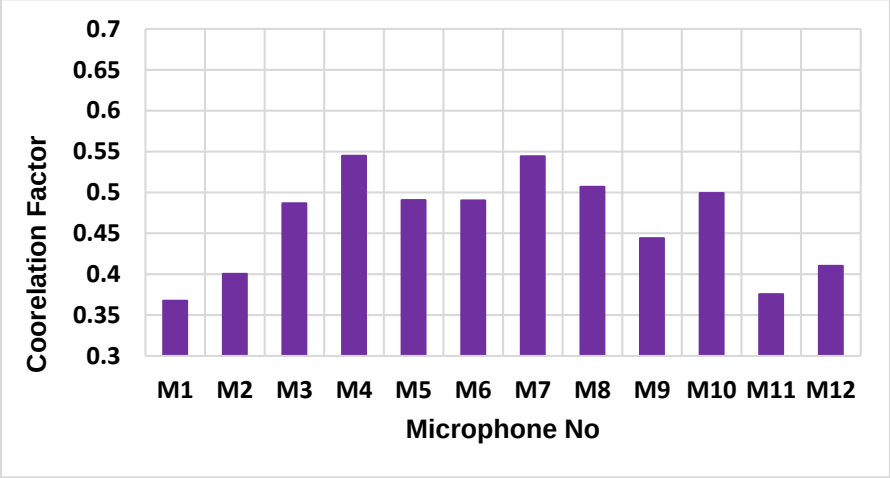

Figure 4.12.11: Correlation factors of 500 kHz 12ga shotgun (S1: M1) with 20 kHz 12ga shotgun signal (S1)

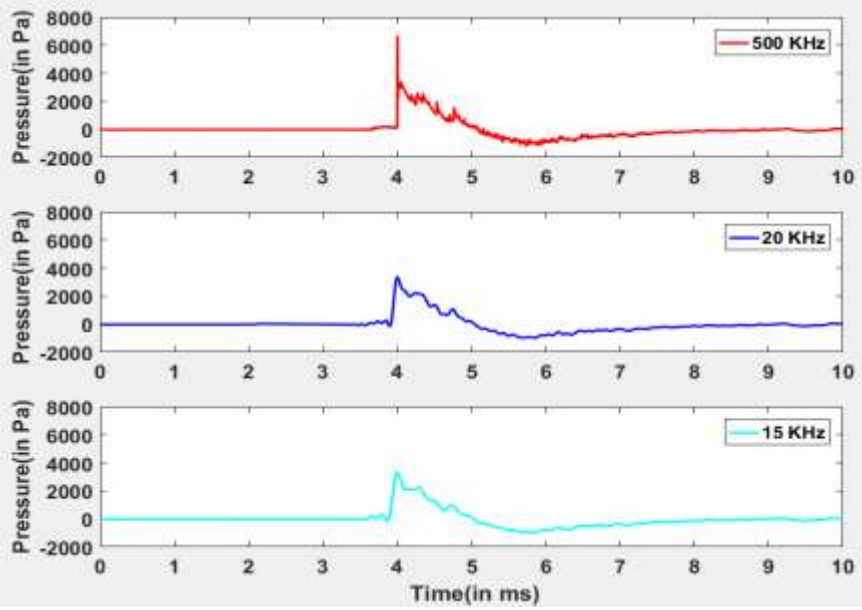

Figure 4.12.12: Muzzle blast portion of 12ga Shotgun: S1: M1 for different sampling rate

4.13 Predicted and Original Data at 49 Degree for Different Firearm and Ammunition

Peak pressure prediction at M4 for Colt 1911A1 (45 ACP) is depicted in figure 4.13.1.

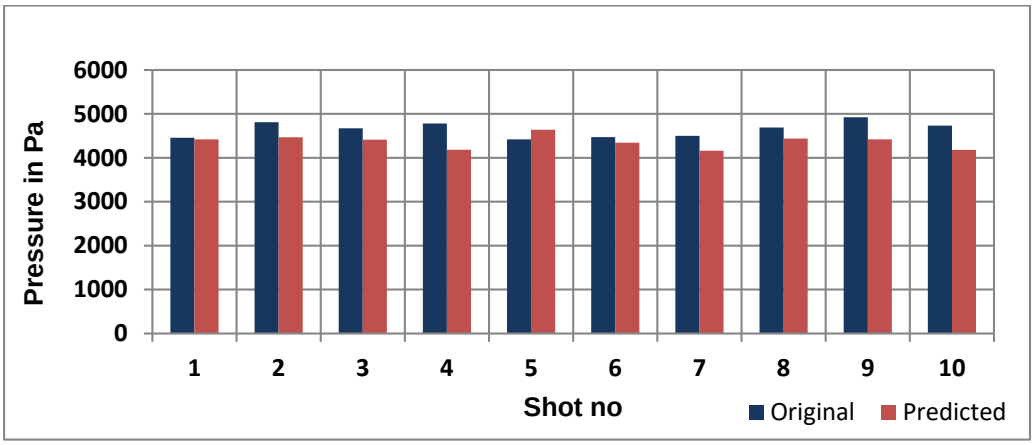

Figure 4.13.1: Peak pressure prediction at M4 position for Colt 1911A1 (45 ACP) (for 10 shots)

Peak pressure prediction at M4 for AR15 is depicted in figure 4.13.2.

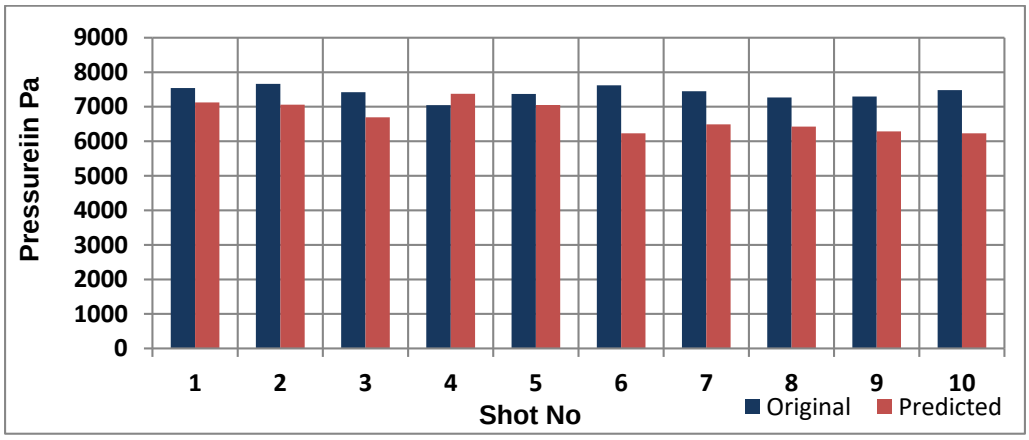

Figure 4.13.2: Peak pressure prediction at M4 position for AR15 (for 10 shots)

Peak pressure prediction at M4 for Glock 23 is depicted in figure 4.13.3.

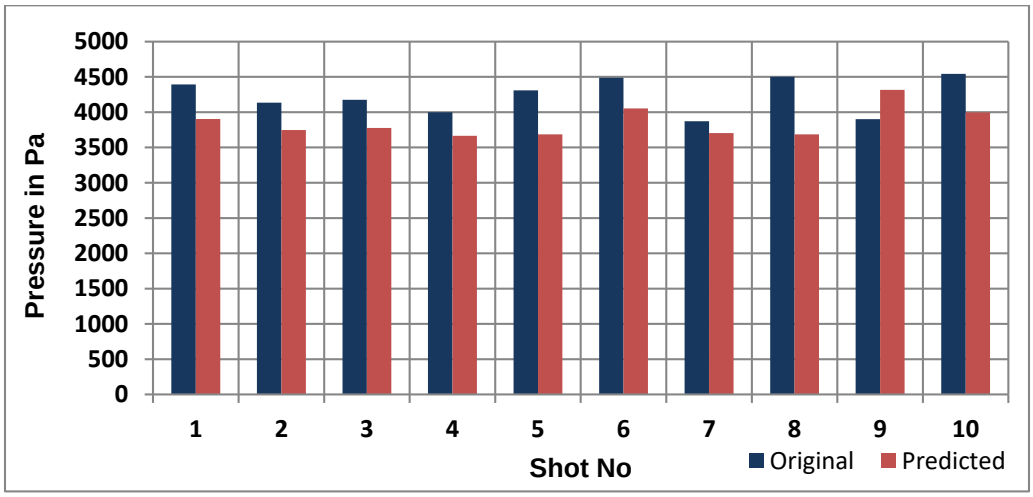

Figure 4.13.3: Peak pressure prediction at M4 position for Glock 23 (for 10 shots)

Peak pressure prediction at M4 for Glock 23 is depicted in figure 4.13.4.

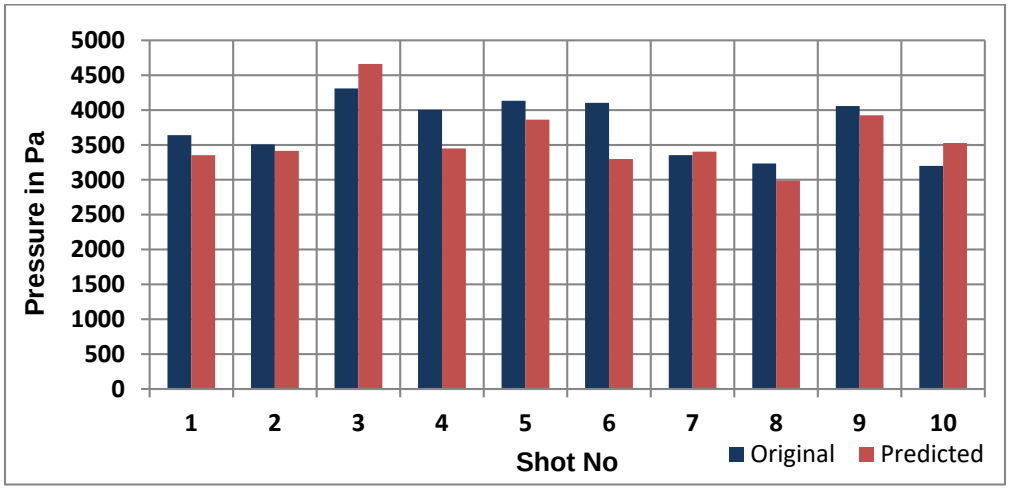

Figure 4.13.4: Peak pressure prediction at M4 positions for Glock 19/135 JHP (for 10 shots)

For Winchester 0.308 caliber, all the predicted values were lower than the original value (figure 4.13.5). The largest error was for S1 (845 Pa).

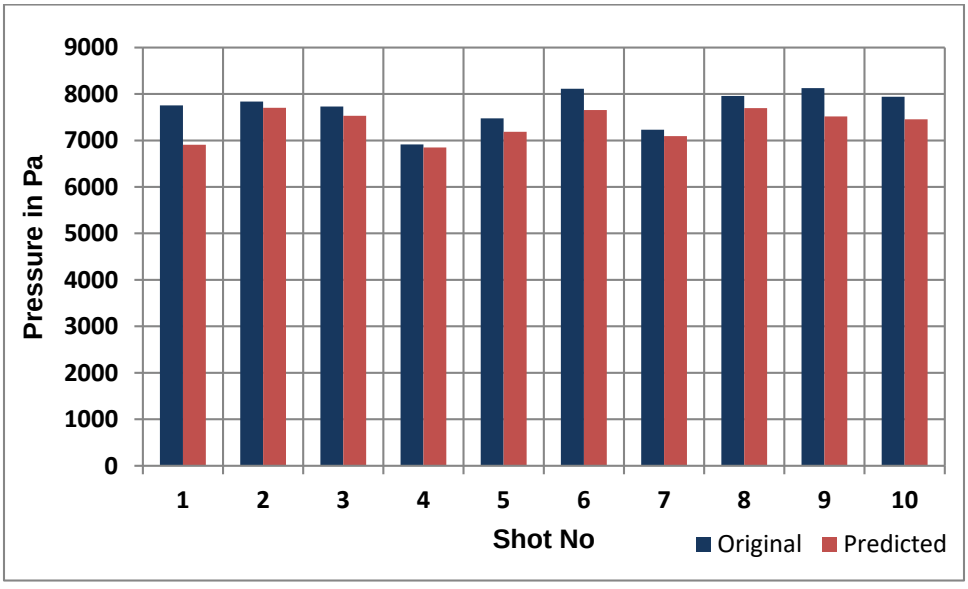

Figure 4.13.5: Peak pressure prediction at M4 positions for Surgeon (for 10 shots)

For Ruger SP 101 with 0.38 caliber bullets, all predicted pressures were less than the recorded pressures. The maximum prediction error was for S8 (1132 Pa), shown in fig 4.13.6.

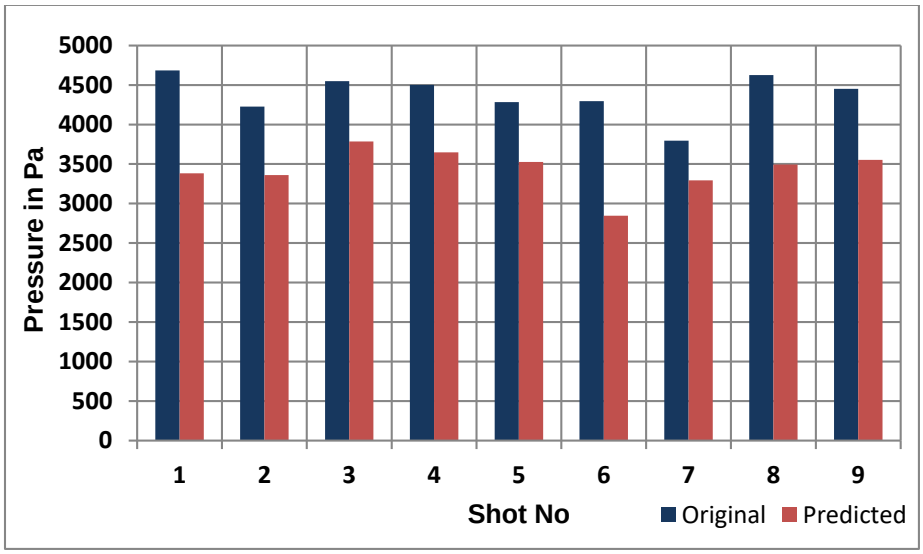

Figure 4.13.6: Peak pressure prediction at M4 positions for Ruger SP101-38 (for 9 shots)

Peak pressure prediction at M4 for Glock 23 is depicted in figure 4.13.7.

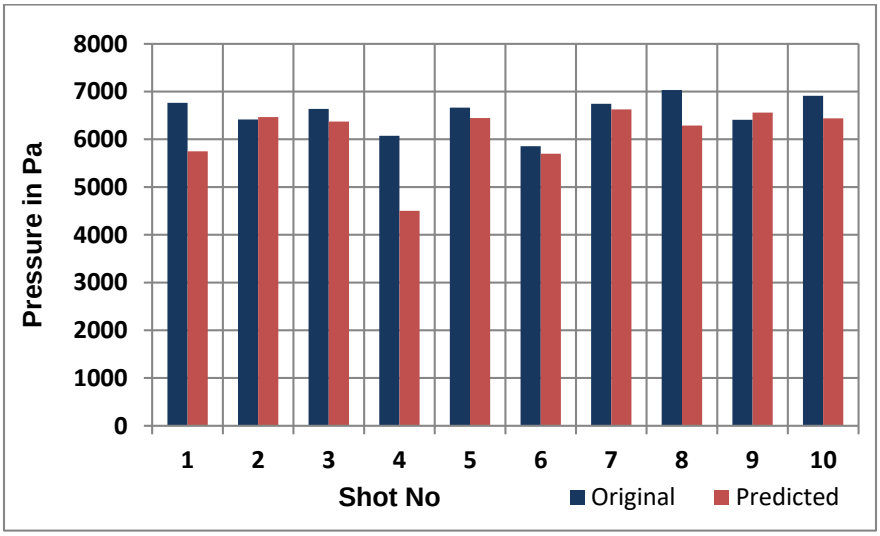

Figure 4.13.7: Peak pressure prediction at M4 positions for Ruger SP101-357 (for 10 shots)

Peak pressure prediction at M4 for Sig 239-357 is depicted in figure 4.13.8.

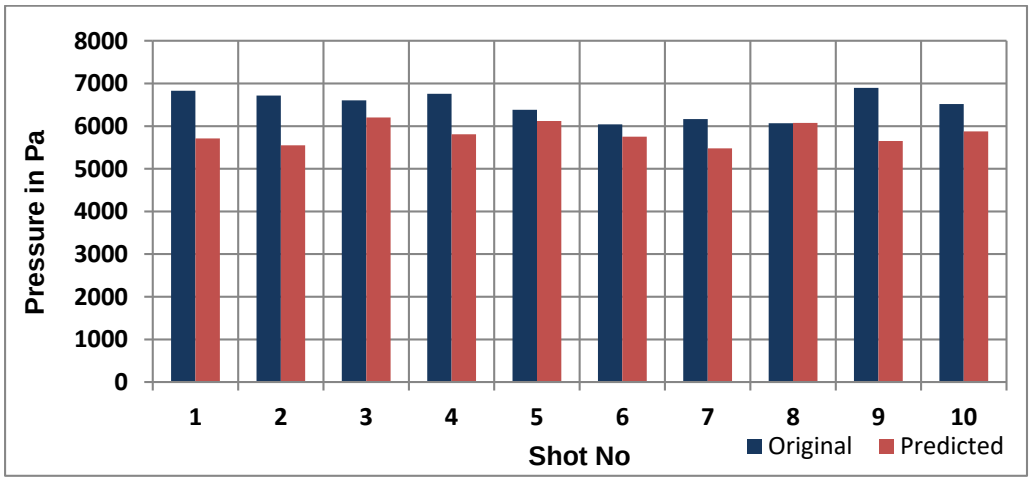

Figure 4.13.8: Peak pressure prediction at M4 position for Sig 239-357 (for 10 shots)

Peak pressure prediction at M4 for 12ga shotgun is depicted in figure 4.13.9.

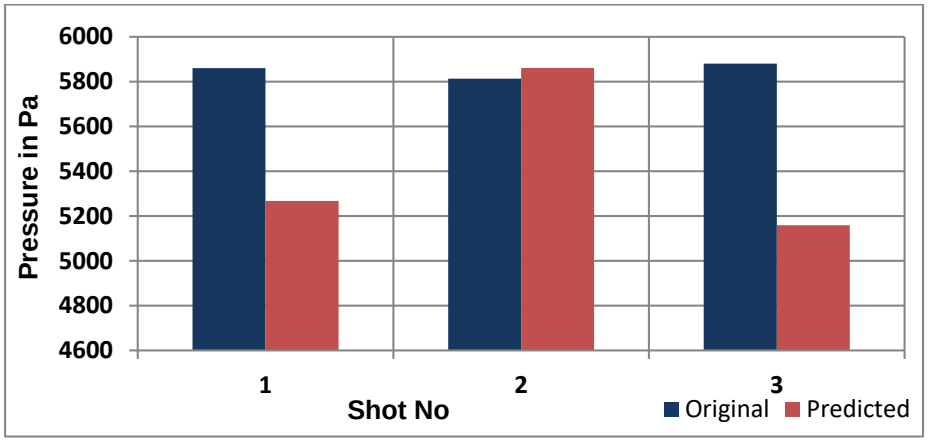

Figure 4.13.9: Peak pressure prediction at M4 position for 12ga (for 10 shots)

For all the shots, the predicted values were lower than the recorded for all the shots with 0.22 caliber rifle. The highest errors were observed for S1 and S9 (figure 4.13.10). Unfortunately, the positioning of the firearms at those two shots could not be located. So positioning may or may not be the reason for these errors.

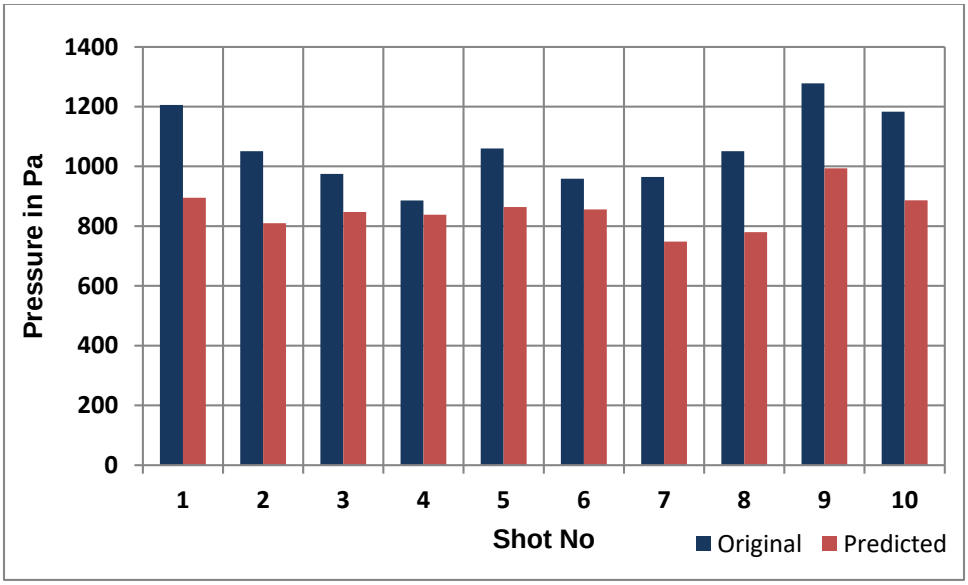

Figure 4.13.10: Peak pressure prediction at M4 position for 22lr (for 10 shots)

4.14 Relationship between Parameters

In this experiment, we have tried to derive a mathematical relationship among the different parameters of the bullet with the peak pressure output of the muzzle blasts. For deriving the relationship, we have taken the highest peak pressure for successive shots at M1 for each of the firearms. The independent variables were bullet mass (in grain), bullet diameter (in inches) and the velocity of the bullets. At first, the relationships were considered for the individual input with the dependent variable. Mathematical relationships that provide the highest correlations were plotted. The relationship formulas and R^2 values (a measurement of how close the observations are in a fitted regression model) are also shown in the graphs.

4.14.1 Relationship between Bullet Mass and Peak Pressure of the Muzzle Blast

Figure 4.14.1 shows the power relationship between these variables. R^2 value is much lower there

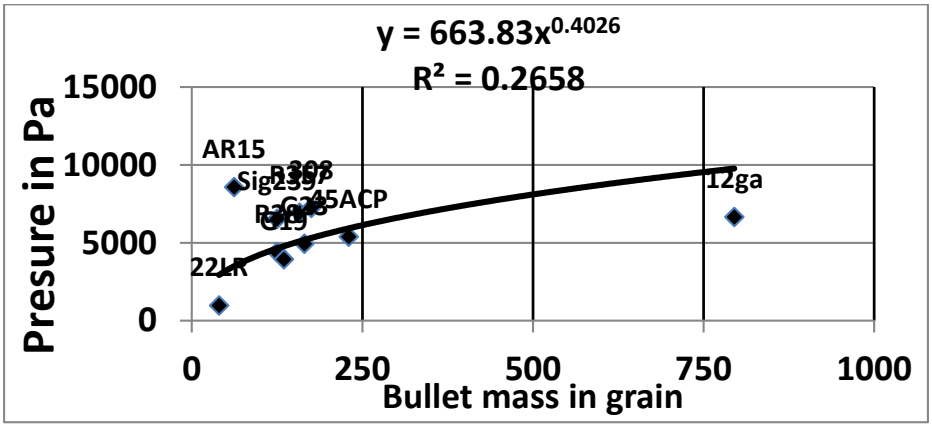

Figure 4.14.1: Power relationship between bullet mass and muzzle peak pressure

4.14.2 Relationship between Bullet
Diameter and Peak Pressure of the Muzzle Blast

The exponential and polynomial relationship between bullet diameter and peak pressure is shown in figure 4.14.2 and 4.14.3.

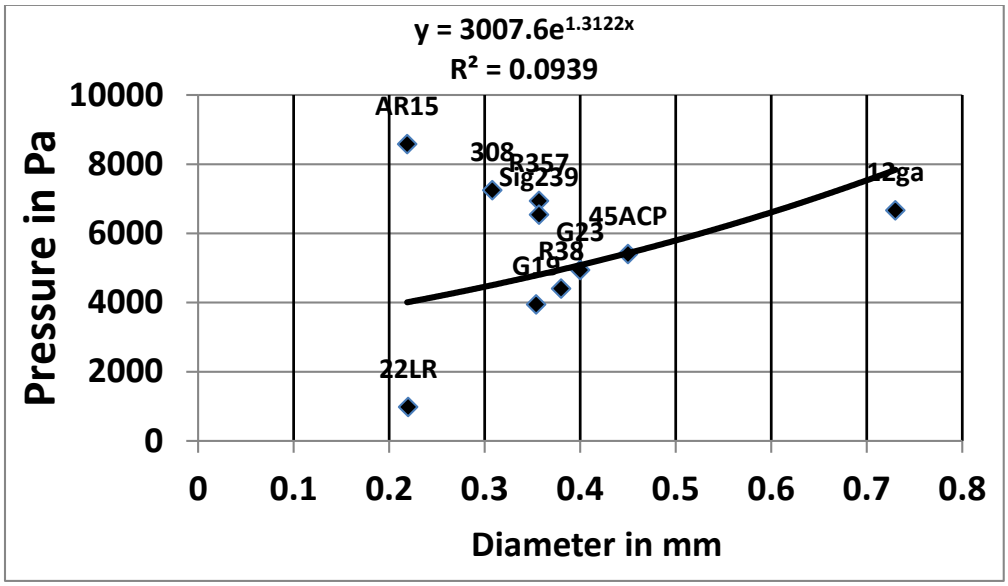

Figure 4.14.2: Relationship between bullet diameter and muzzle peak pressure (using exponential relationship)

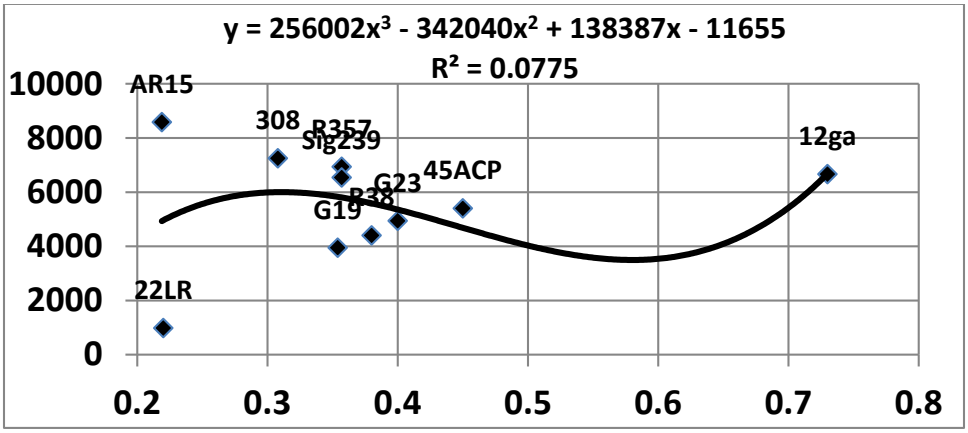

Figure 4.14.3: Relationship between bullet diameter and muzzle peak pressure (using 3rd order poly.)

4.14.3 Relationship between Bullet
Velocity and Peak Pressure of the Muzzle Blast

To observe whether there is any relationship holds in between the speed of the bullet and the peak pressure at the microphone, we have examined the pressure data against the nominal speed of the bullets fired in this experiment. Figure 4.14.4 shows the 4th order relationship between pressure and speed. Logarithmic relationship is shown in figure 4.14.5.

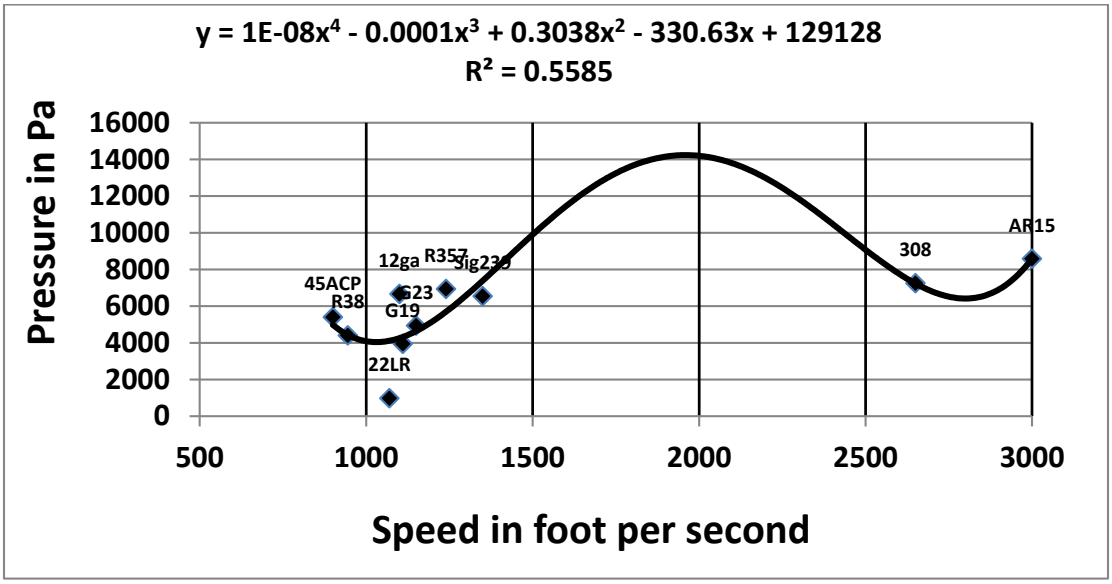

Figure 4.14.4: Relationship between the speed of the bullet and muzzle peak pressure (using 4th order poly.)

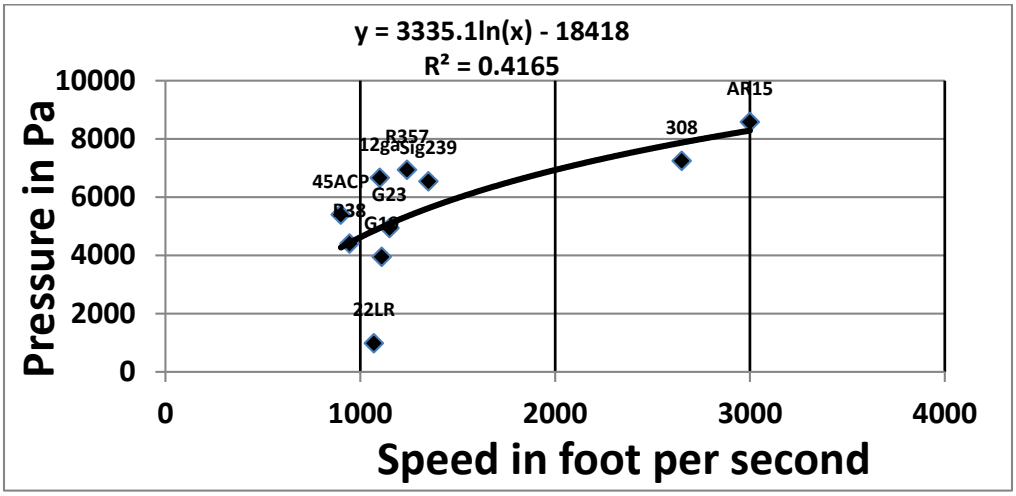

Figure 4.14.5: Logarithmic relationship between the speed of the bullet and muzzle peak pressure

It is possible that bullet mass, diameter, and velocity are contributing jointly to the pressure value at the microphones. We have tried to develop a linear relationship between these inputs with the pressure outputs.

The relationship was found as follows

$$PP = (-95.13) * bs + (-949.20) * bm + (-28292) * bd + (1.14) * bs * bm + (2455.8) * bm * bd + (310.20) * bs * bd + (-2.99) * bd * bs * bm + 86319.5 \quad (4.1)$$

Where,

PP= Peak pressure;

bs = Bullet speed;

bm = Bullet mass;

bd= Bullet diameter;

The R^2 statistic, the F statistic and its p value, and an estimate of the error variance were found to be 0.99, 57.09, 0.173 and 10297. Prediction error for different firearms is shown in figure 4.14.6.

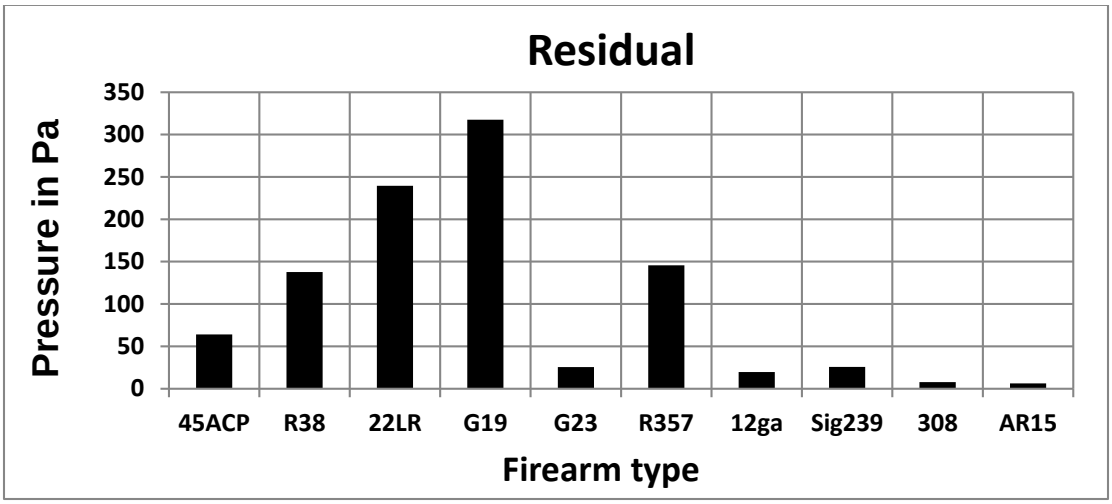

Figure 4.14.6: Residual of the predicted values for peak pressures at M1 for different firearms

5. DISCUSSION

Azimuthal and shot to shot discrepancies for each firearm are discussed below.

5.1 Colt 1911A1 (45 ACP)

While there appears to be good shot-to-shot consistency, some shots show relatively high peak sound pressure. Shot S3 is one example. There can be several explanations behind that.

As muzzle blast signals are extended only for a few milliseconds, one of the explanations may be that even a 500 kilohertz sampling rate is not sufficient to capture the brief instantaneous peak pressure impulse. To assess this possibility, we have digitally up sampled the muzzle blast recording to produce a 5 MHz sampling rate via bandlimited interpolation with MATLAB (10 times higher than the original recording rate). The up sampled observation is plotted in figure 5.1.1. Also after resampling, there are non-uniformities in peak pressure (for example shot S9, M3). So, simply up sampling the recording does not eliminate differences in azimuthal peak pressure for successive recordings of the Colt 1911A1 (45 ACP).

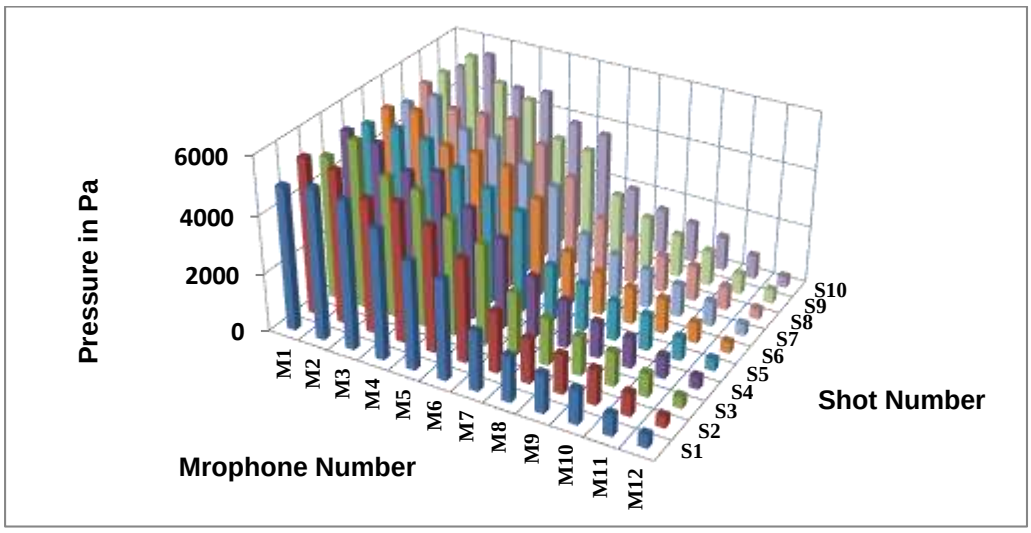

Figure 5.1.1: Re-sampled peak pressure for the Colt 1911A1 (45 ACP) muzzle blast as a function of azimuth (10 shots)

Maximum peak pressures at M1 were observed for S2 and S4. But as seen from figure 5.1.2, S2 and S4 were not the shots that were the closest to M1. So it is hard to deduct that shots that were closer to the microphone always create higher pressure values at different azimuths for Colt (45 JHP).

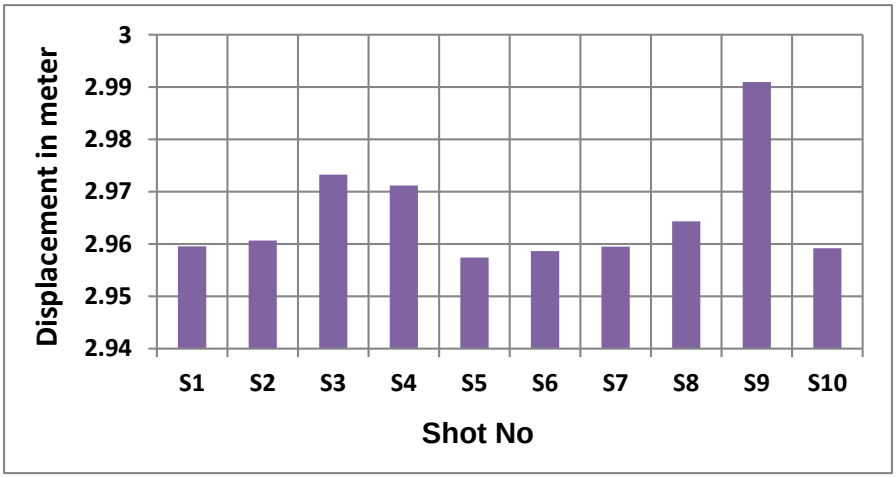

Figure 5.1.2: Distance of the firearm from M1 for Colt 1911A1 (45 ACP) (10 shots)

A closer look at peak pressure variation reveals that the pressure variation is random in nature and varies from one shot to another. For example, M2 (located nearly at 16◦), records higher pressures values than M1 (nearly at the line of fire) for a few shots (shown in figure 5.1.3). A similar variation is observed for different shots in M3 and M4 (figure 5.1.4).

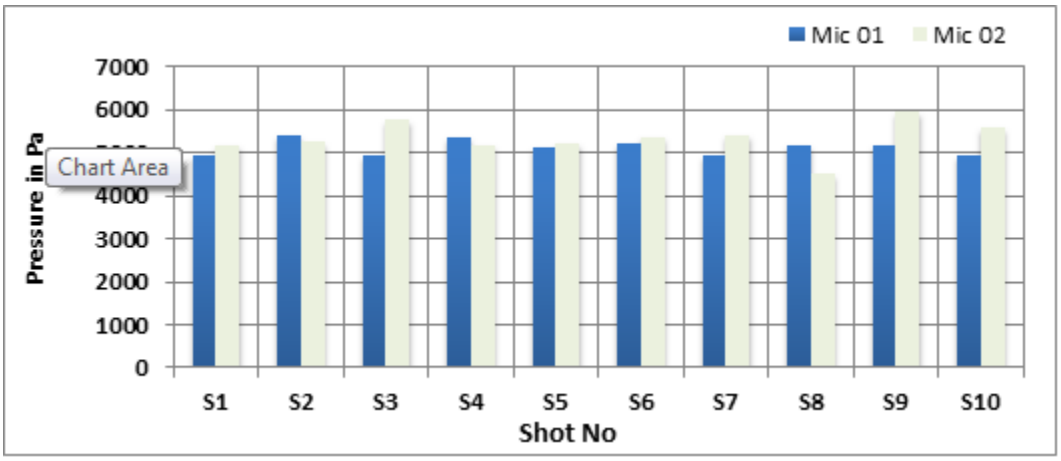

Figure 5.1.3: Peak pressure variations at M 1 & M 2 for Colt 1911A1 (45 ACP) (10 shots)

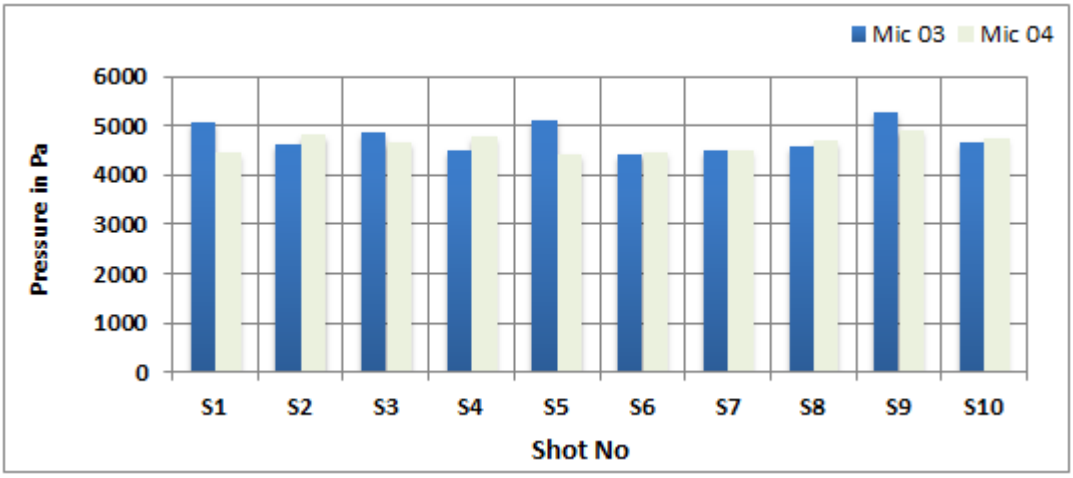

Figure 5.1.4: Peak pressure variations at M3 & M4 for Colt 1911A1 (45 ACP) (10 shots)

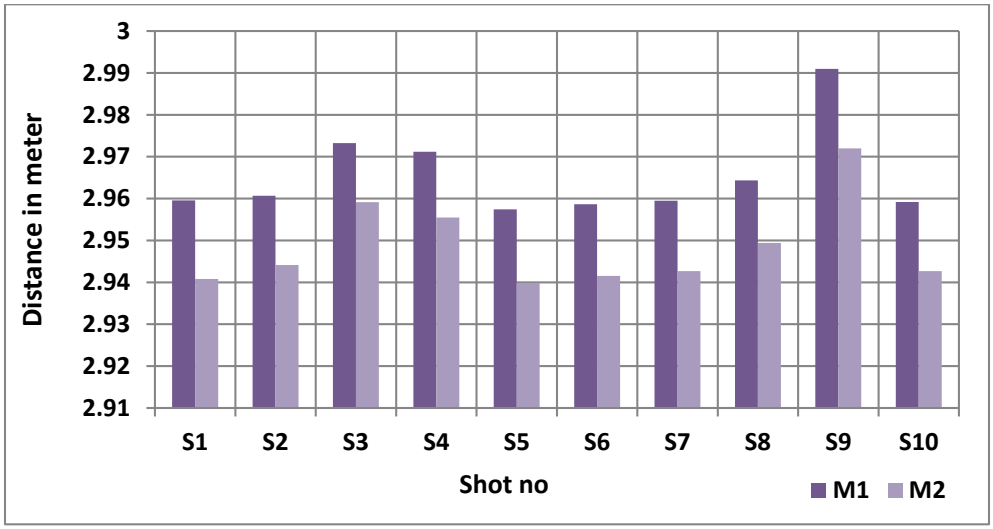

Figure 5.1.5: Distance of the firearms from M1 and M2 for Colt 1911A1 (45 ACP) (10 shots)

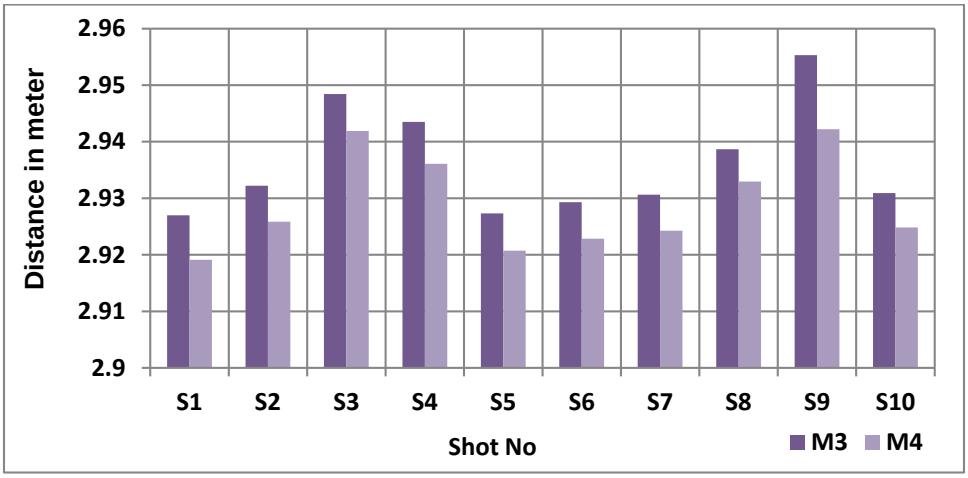

Figure 5.1.6: Distance of the firearms from M3 and M4 for Colt 1911A1 (45 ACP) (10 shots)

As seen from figure 5.1.5, for all the shots, the radial distance of M1 from the firearm was higher than M2; similar observation is shown in figure 5.1.6, where M4 was nearer than M3 for all the consecutive shots. So, firearm position cannot be the only reason for such shot to shot pressure variations at those azimuths.

At M2, the blast duration of S2 (0.958 ms) is higher than S1 (0.826 ms) and S2 (0.756 ms) (using waveform observation method). As seen from figure 5.1.7, for S1 and S3, the muzzle blast segments travel larger distance to get back to the base level. The peak pressure value of at M2 for S2 was also different from S1 and S3. As the other parameters stayed the same, there can be other reasons like atmospheric noise that led these high frequency fluctuations.

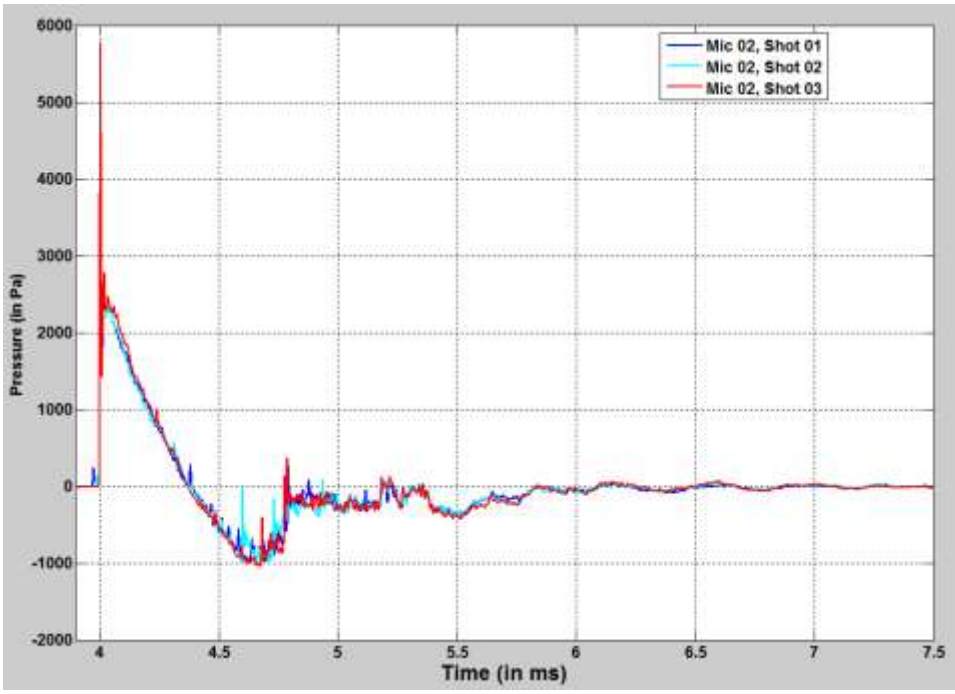

Figure 5.1.7: Muzzle blast segments of different shots recorded at M2 using waveform observation method

Energy accumulation based method was also tried. 93% was chosen in this case, as this percentage shows the minimum shot to shot variation. Overall, the durations are much uniform now, for example, the durations of the previous example were found to be 0.768 ms, 0.752 ms and 0.75 ms. At larger azimuths, there are some fluctuations for successive shots in this method. As the signal strength decreases at higher angle, they get much affected by the surrounding disturbances, which is random in nature.

5.2 Glock 19

Figure 5.2.1 shows the muzzle blast peak pressure variation at M2 for different shots of Glock 19/ 135 JHP. For S2 and S8, the pressure values were much less in all azimuths including M2. To figure out whether that has been occurred for insufficient

sampling rate, we tried with the resampled version and observed the variation as shown in figure 5.2.2. As observed from 5.2.3, the scenario remains almost the same. So sampling rate was not an issue for such discrepancy in Glock 19/135 JHP.

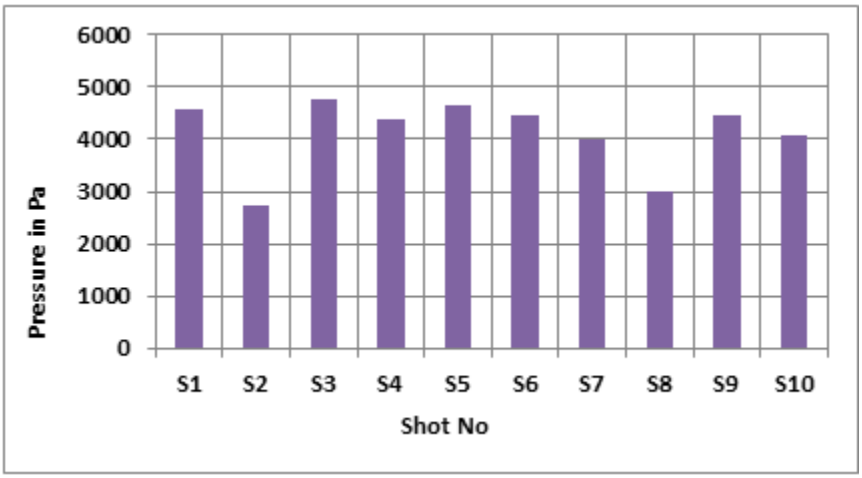

Figure 5.2.1: Peak pressure variation at M2 for 10 consecutive shots

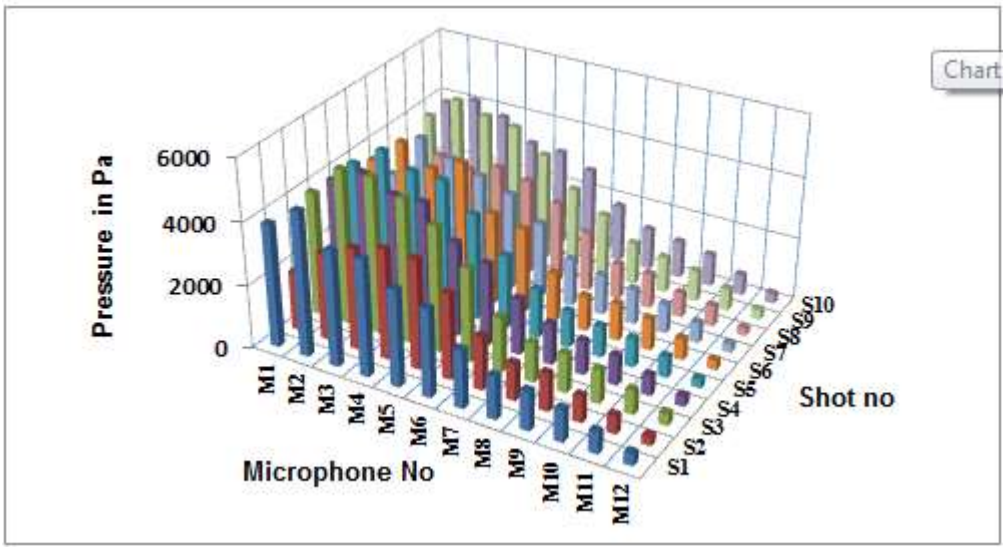

Figure 5.2.2: Re–sampled (5 MHz) muzzle blast peak pressures at 3 meter distance for Glock 19/135 JHP as a function of azimuth (10 shots)

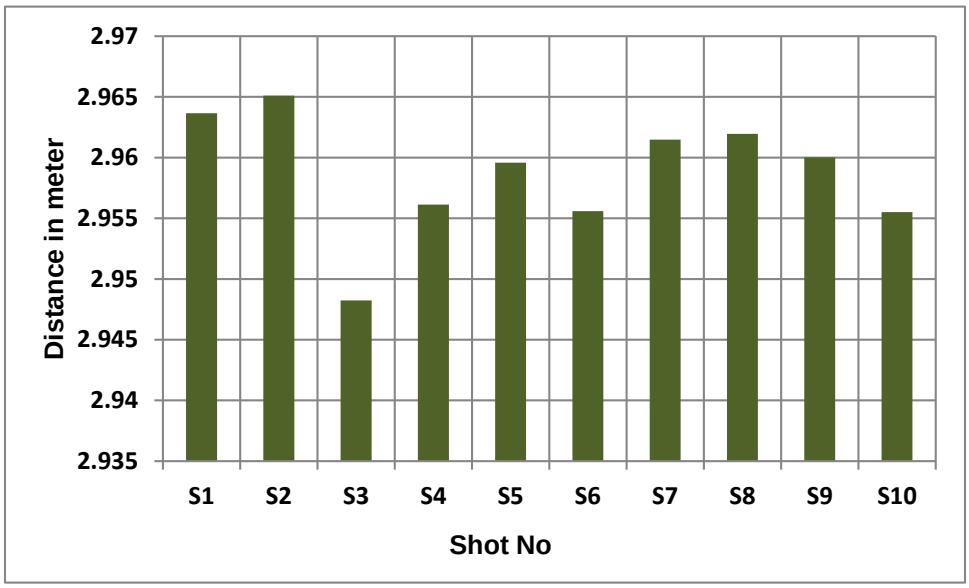

Figure 5.2.3: Distances from the firearm to M2 at various shots of Glock 19/135 JHP

The highest and lowest pressure values that were observed at M2 were for S3 and S2, which is justifiable from figure 5.2.3, as S2 was the farthest shot and S3 was the closest. But S9 generated a higher pressure than S10 at same azimuth, although S9 was at a higher distant than S10 from M2. So it is hard to describe the pressure variation for Glock 19/135 JHP only from the positioning of the firearm.

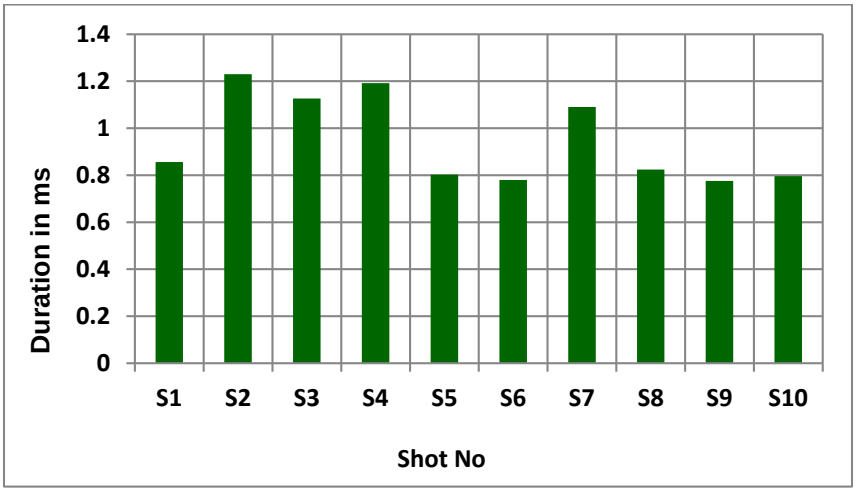

Figure 5.2.4: Muzzle blast duration variation at M2 from successive shots of Glock 19/135 JHP (waveform observation)

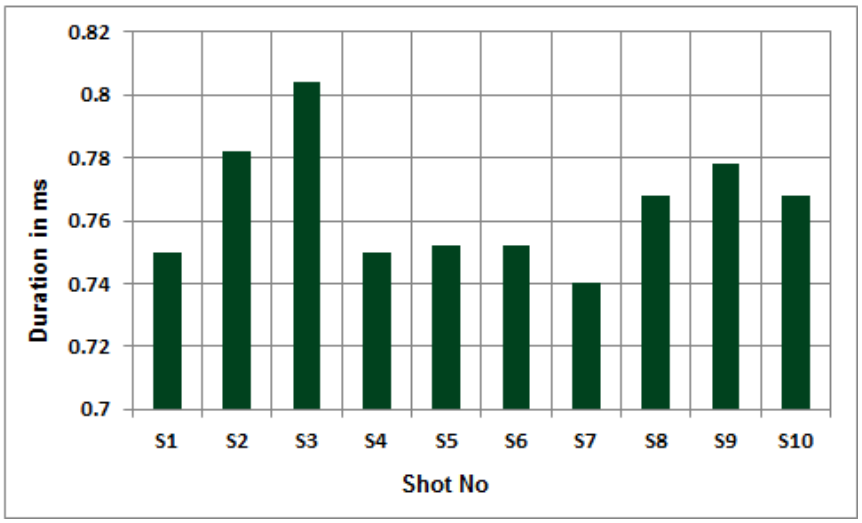

Figure 5.2.5: Energy accumulation based muzzle blast duration variation at M2 from successive shots of Glock 19/135 JHP

Muzzle blast duration variation at M2 is observed with both waveform observation and energy accumulation techniques (shown in figure 5.2.4 and 5.2.5). The muzzle blast segment for different shots at M2 is shown in figure 5.2.6. For S2, there is an additional peak before reaching to the muzzle peak, which resulted a higher duration

at S2 using waveform based observation. For S4, the peak pressure level is much higher than S2 and S3. This peak pressure contributes the major portion of the total energy, which results in much smaller duration than other two shots using energy accumulation method.

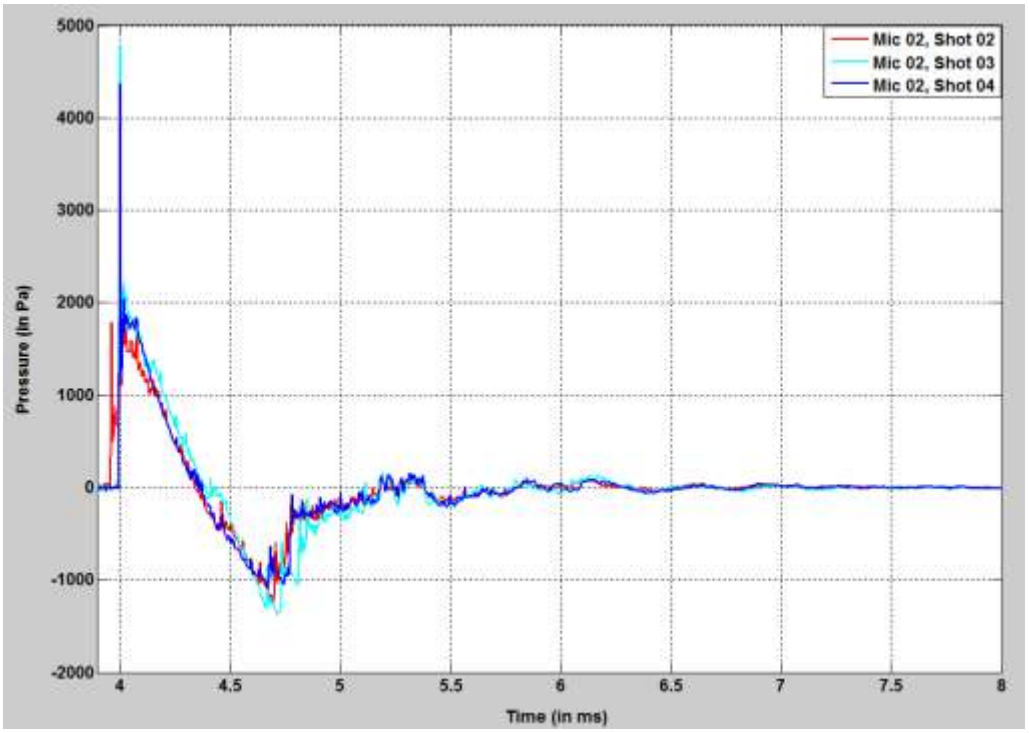

Figure 5.2.6: Muzzle blast duration variation for several shots at M2 for Glock 19/135 JHP

5.3 Glock 23

Although Glock 19 and Glock 23 are similar pistols, they display differences in peak pressure levels. Perhaps the reason was the different types of bullets used during the shots. As the pressure graph suggests, the peak pressure level is higher in M2 than M1 and M3, also the pressure level is higher in M4 than neighboring microphones. For S4, at M2, there is an unusual pressure rise. These pressure signals were resampled to have a look at a higher sampling rate (5 MHz) and to capture the pressure peaks more accurately.

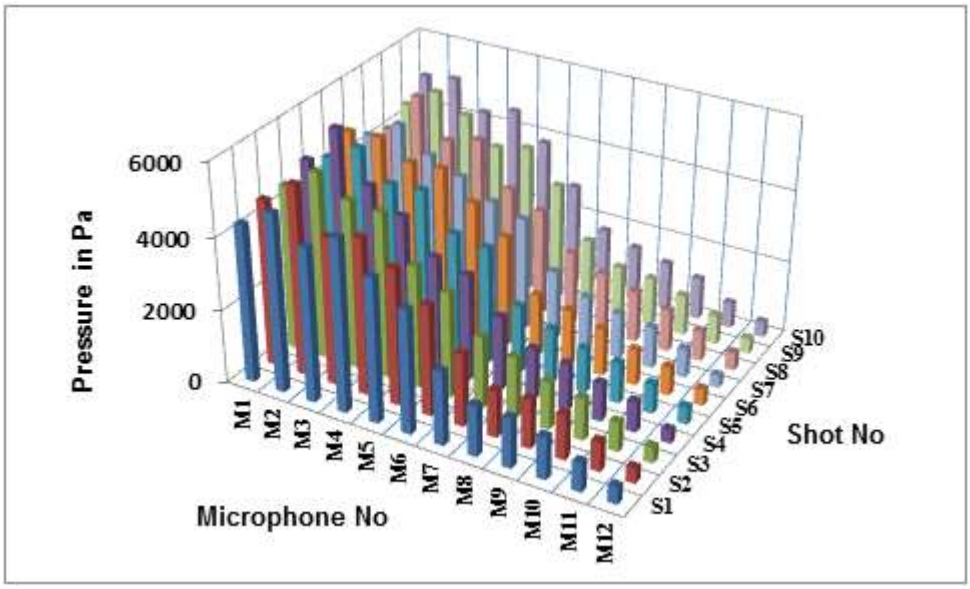

Figure 5.3.1: Re-sampled peak pressure for the Glock 23 muzzle blast as a function of azimuth (10 shots)

Figure 5.3.2 depicts the peak pressure variation in different shots for M3 and M4 with 500 kHz sampling rate. For a few shots, the pressure values were higher at M3 and lower at M4 and vice versa. After the signals being resampled, the pressure variation is shown in figure 5.3.3. As seen, the asymmetry has not been improved for higher sampling rate. So sampling rate was not an issue for such dissimilarities in different shots for Glock 23.

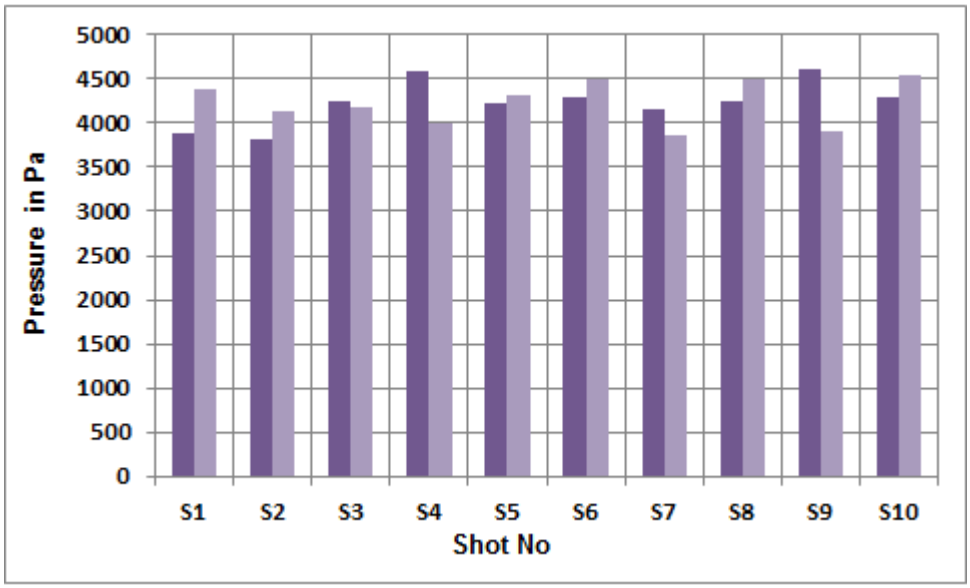

Figure 5.3.2: M3 and M4 peak pressure variation for Glock 23 (for 10 shots)

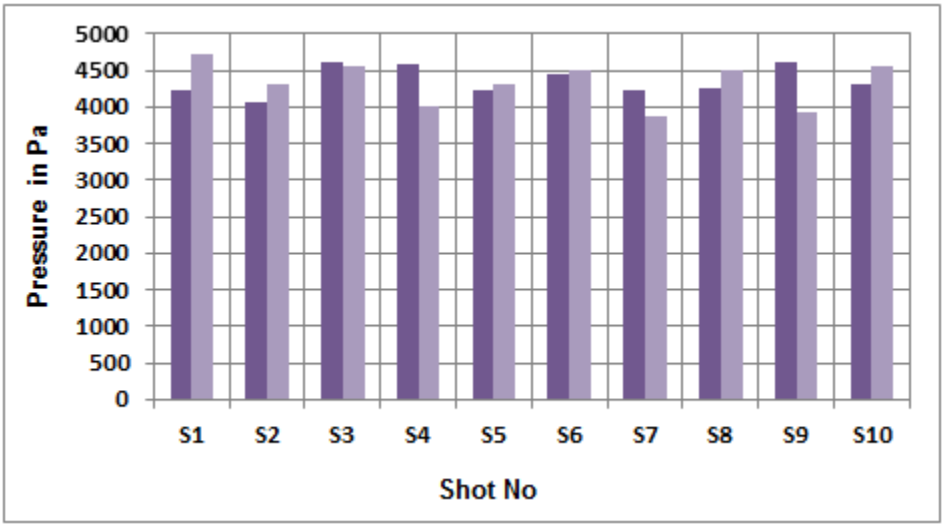

Figure 5.3.3: Re- sampled M3 and M4 peak pressure variation for Glock 23 (for 10 shots)

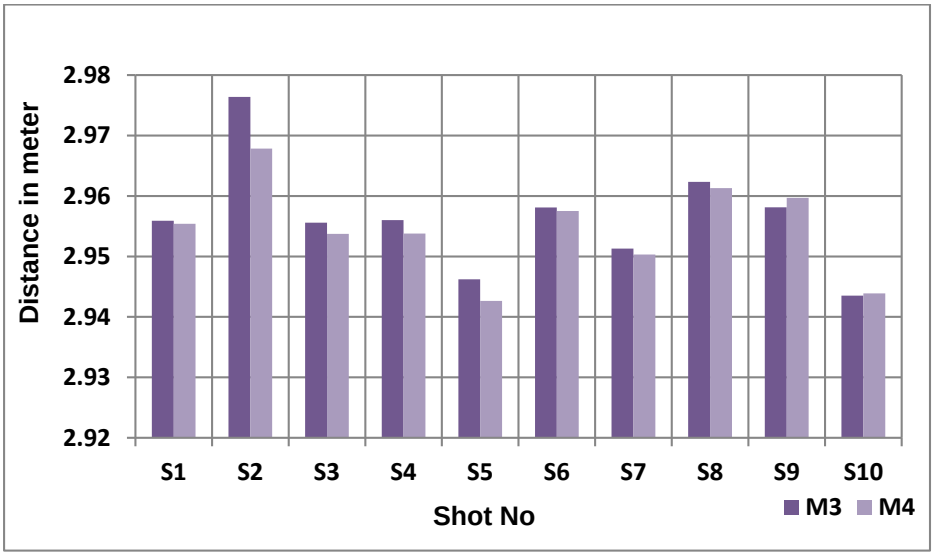

Figure 5.3.4: Distance from the firearm to M3 and M4 for different shots

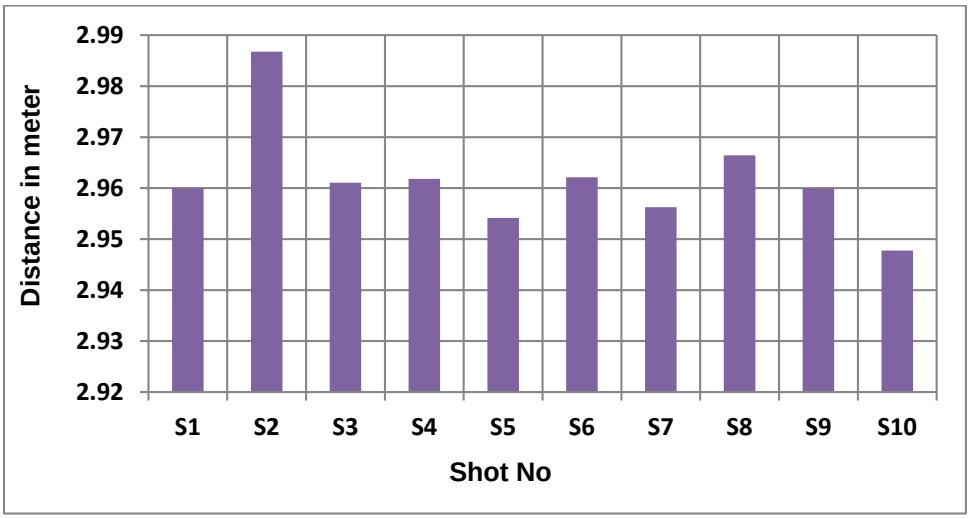

Figure 5.3.5: Distances from the position of the firearm to M2 for different shots

The pressure values at M4 was higher than M3 were for S1, S2, S3, S6, S8 and S10. As seen from figure 5.3.4, apart from S10, in all those shots, M4 was nearer to the firearm than M3. M4 was also nearer for S3 and S4, but the pressures at M3 were higher.

Again from figure 5.3.5, it cannot be d out for what reason there was an increased pressure for S4 at M2, as it was not closer from the other shots. So it is difficult to draw any conclusion on the muzzle blast peak pressure variation of Glock 23 based on firearm position.

There are some asymmetries also in blast duration for successive shots. For example, M3 exhibits variation in duration from one shot to another. As shown in figure 5.3.6, for S2 (blast duration 1.216 ms), the muzzle blast segment returns to the base voltage later than S1 (0.894 ms) and S3 (0.894 ms).

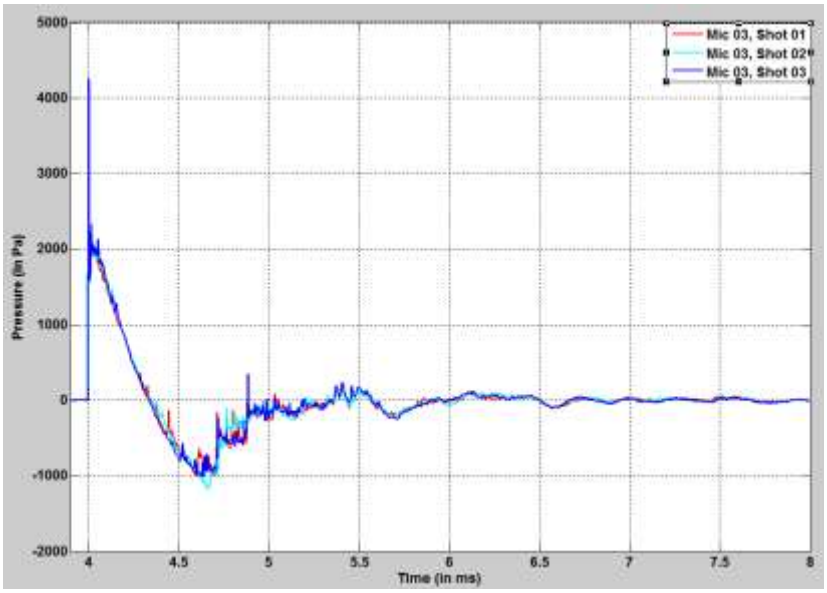

Figure 5.3.6: Muzzle blast duration variations for Glock 23 at M3 for different shots

This variation may be a result of the introduction of external disturbances. The durations based on energy accumulation method at M3 for consecutive shots are more symmetrical than the previous case (0.758 ms, 0.712 ms, and 0.742 ms).

5.4 Sig 239

At M1, the peak pressure level is higher in S1 and S3 than other shots. Higher pressure variation for different shots is also noticeable at M5.

To observe whether our sampling rate was high enough to capture this brief pressure period, we resampled muzzle blast segments. The results are shown in figure 5.4.1. Again, the pressure variation is observed after resampling. The pressure values at M1 and M5 after resampling the portion is depicted in figure 5.4.2 and 5.4.3. As seen from those figures, shot to shot variation has not improved after resampling. So, sampling rate was not an issue for Sig 239 for non-uniform pressure values for different shots at particular azimuths.

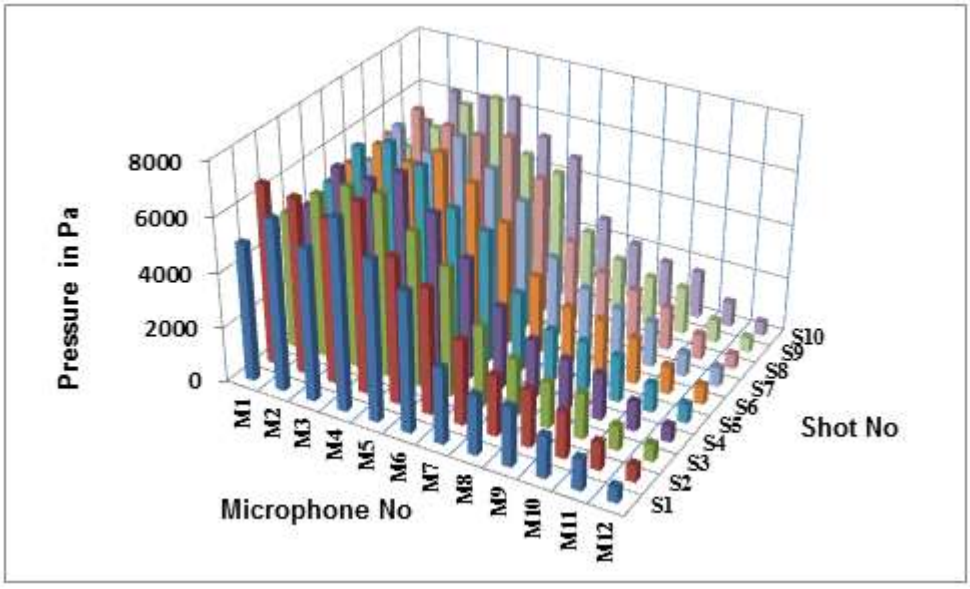

Figure 5.4.1: Re-sampled peak pressure for the Sig 239 muzzle blast as a function of azimuth (10 shots)

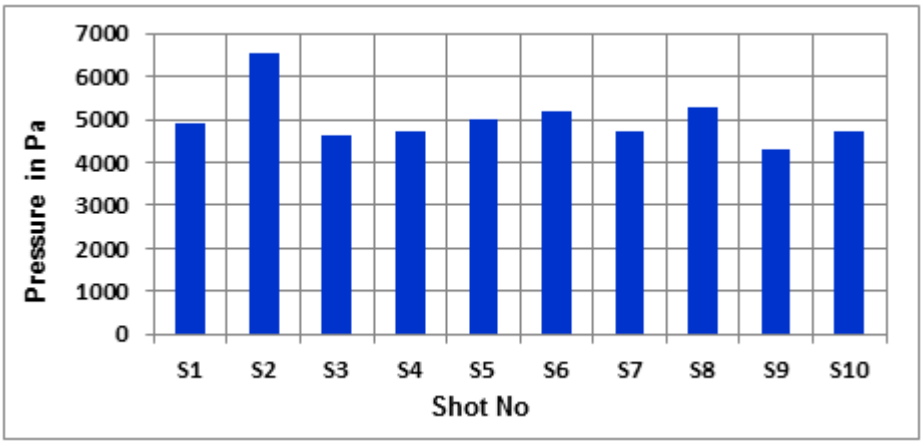

Figure 5.4.2: Peak pressure variation at M1 for Sig 239 after resampling

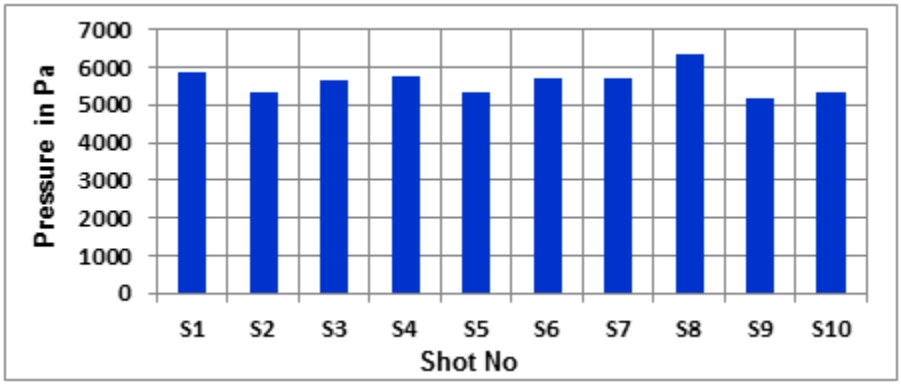

Figure 5.4.3: Peak pressure variation at M5 after resampling for Sig 239

If the positions of the firearm were not the same for different shots at those azimuths, it can cause such variation. Radial distances from the firearm to the microphones are observed in figure 5.4.4 and 5.4.5.

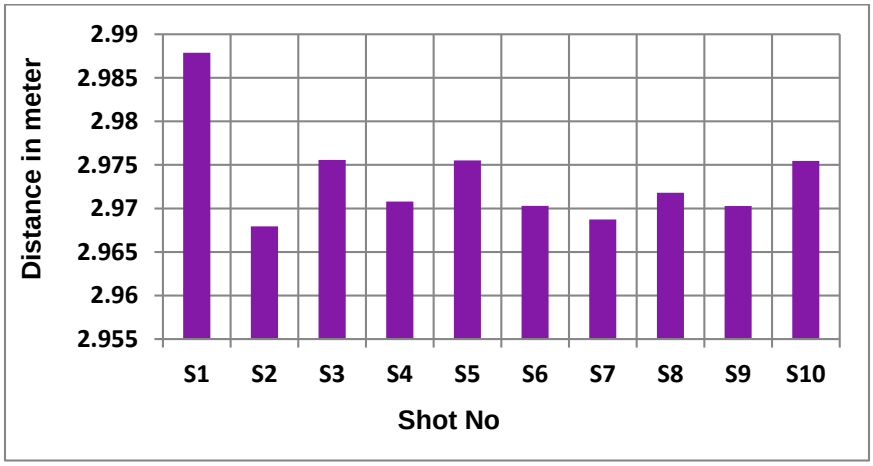

Figure 5.4.4: Distance of the firearm from M1 at different shots of Sig 239

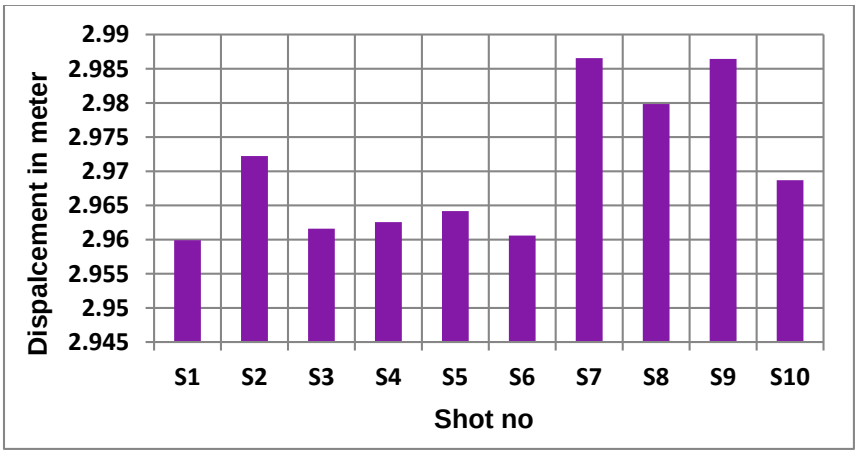

Figure 5.4.5: Distance of the firearm from M5 at different shots of Sig 239

The highest pressure at M1 was observed at S2, S6 and S8 which goes with the observation as the lowest distances from the firearm were also at those shots (figure 5.4.4). S7 and S9 were nearer than S8, but fail to record pressure values that are higher than S8. Again at M5, larger pressure values were observed at S8, which was not the nearest shot to M5. As seen from these observations, there can be some other issues other than the firearm positioning regarding such variations from one shot to other for Sig 239.

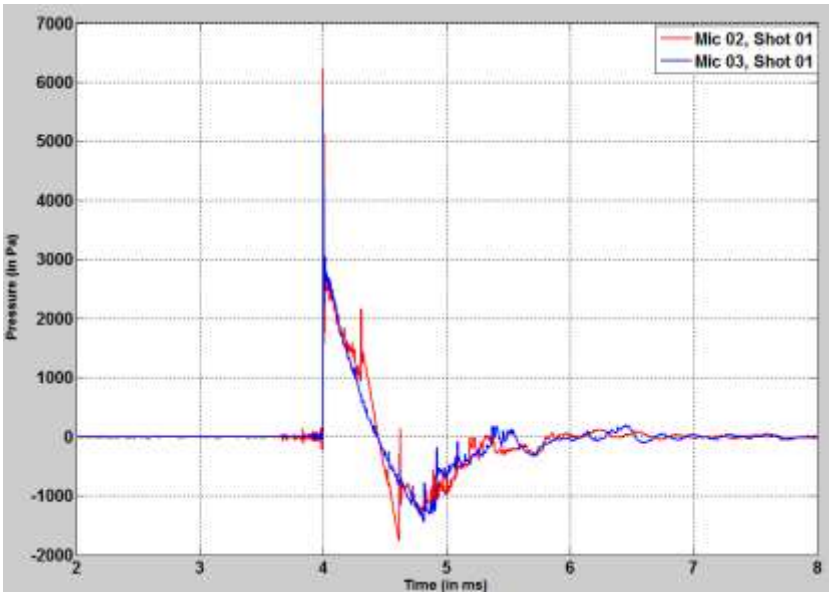

Figure 5.4.6: Azimuthal muzzle blast variations for S1 of sig 239 at M2 and M3

Figure 5.4.6 shows the muzzle blast duration wave at 2 different azimuths for S1. At M2, the signal returns to the base level before the end of negative phase duration, causing the very small duration of the blast (0.636 ms compared to 1.378 ms). These variations may occur due to the presence of some kind of external chaos. That's why; energy accumulation based approach was also tried. The durations show better consistency than the previous method for the prr example (1.016 ms and 0.992 ms).

5.5 Surgeon/AI

For 10 successive shots, there are shot to shot consistencies for this firearm except some cases. For example, if we take a look at M3, M4 and M5 for S1, S2 and S3, we can figure that for the first shot, M3 records a lower peak pressure than M4 and M5, which is not the case for other shots (figure 5.5.1).

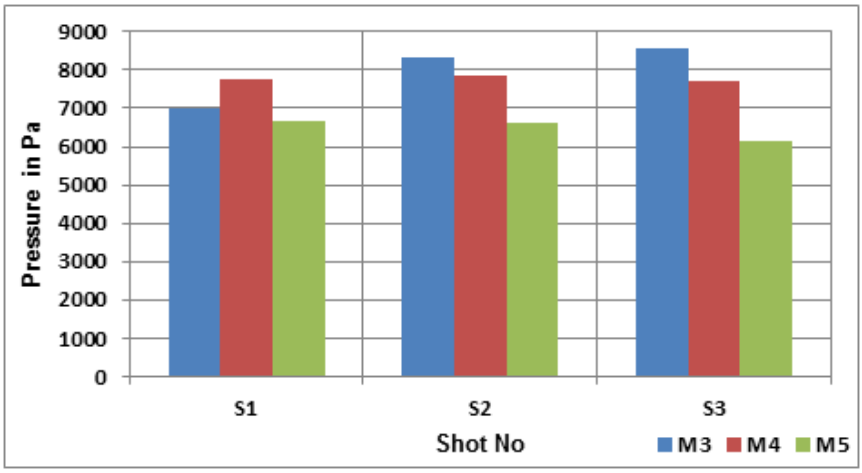

Figure 5.5.1: Shot to shot variations of Winchester 0.308 caliber bullets at 3 different azimuths

One of the reasons can be insufficient sampling rate that could not record the peak pressures. We have resampled the pressure waves (5 MHz) to observe whether higher sample rate can actually answer this low peak pressure (figure 5.5.2).

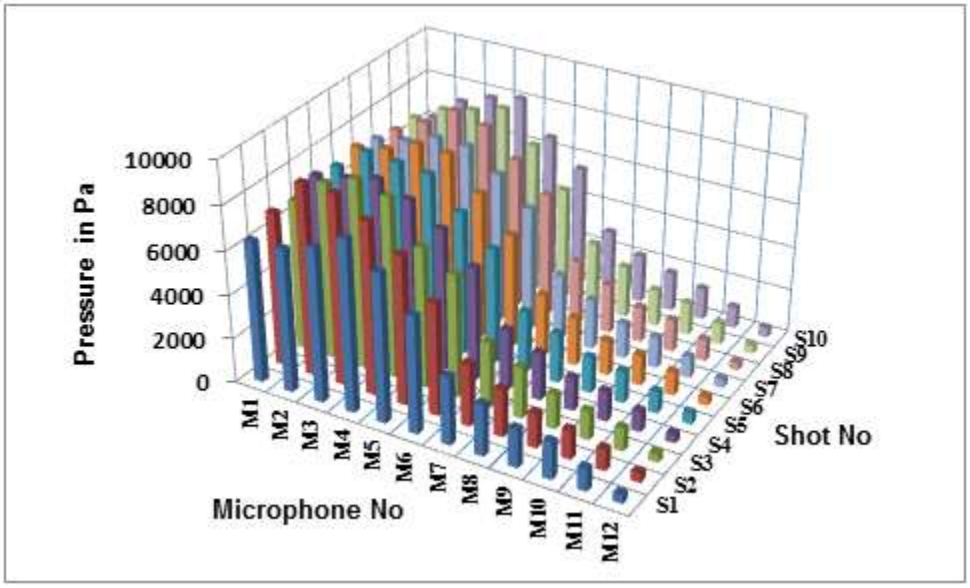

Figure 5.5.2: Re- sampled peak pressure at 3 meters for the Winchester 0.308 caliber muzzle blast as a function of azimuth (10 shots)

As seen from figure 5.5.3, after resampling, the variation is still there. Another reason may be the firearm displacement during that particular shot from M3 which caused this low pressure.

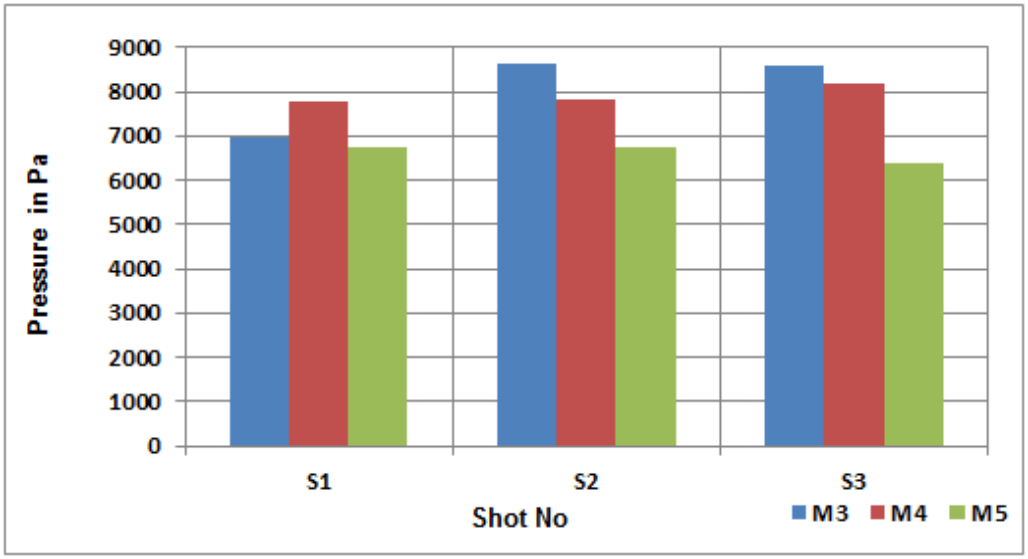

Figure 5.5.3: 3 Shot variations of Winchester 0.308 caliber bullets at 3 azimuths (after resampling)

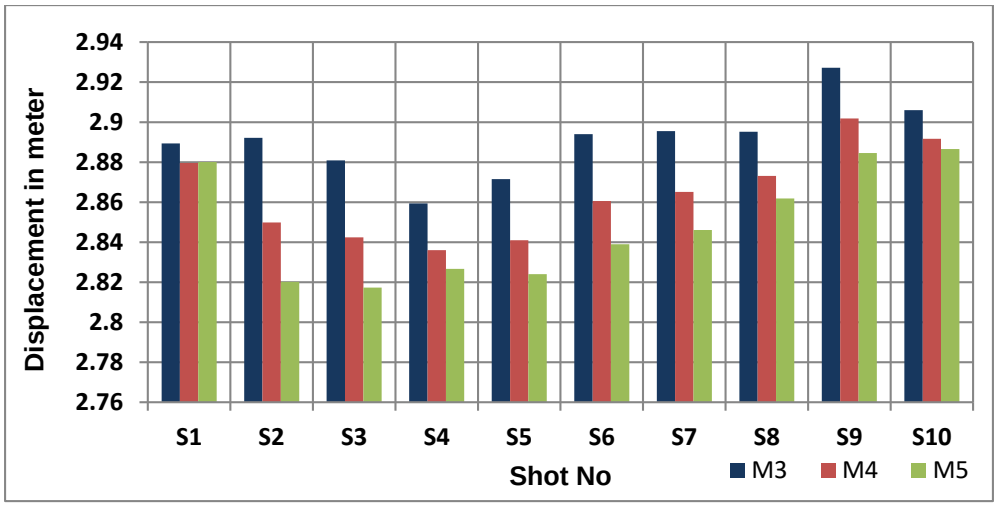

Figure 5.5.4: Radial distance from the firearm to M3, M4 & M5 for 10 shots

It seems from figure 5.5.4, for all the shots, M3 was the farthest microphone from the point of the shooting. So it is not clear from the positioning information that why the pressure value was higher at M3 for some shots.

As seen from muzzle blast variation, for most of the shots, the trend is that the duration reduces from M1 to M6 and then rises again nearly for all the shots. For S1, the duration at M4 is lower (1.272 ms) than both of M3 (2.78 ms) and M9 (2.26 ms). The negative phase returns to base level earlier than other azimuths, as seen in figure 5.5.5. After observing with energy accumulation method, the durations at those azimuths were found to be 1.672 ms, 1.614 ms and 1.141ms.

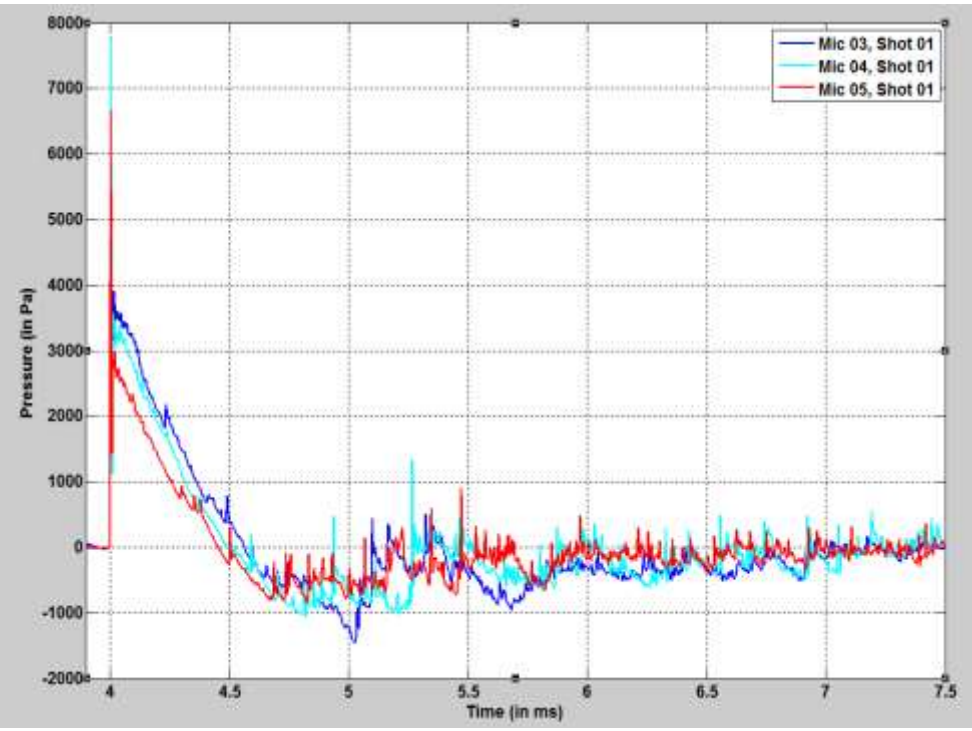

Figure 5.5.5: Muzzle blast segments at different azimuths for S1

5.6 Stag Arms AR15

Among all the firearms categories, the highest pressure values were observed for this category. At M2, the pressure values were different for different shots, as shown in figure 5.6.1. Azimuthal pressure variation for a single shot is also observed (figure 5.6.2).

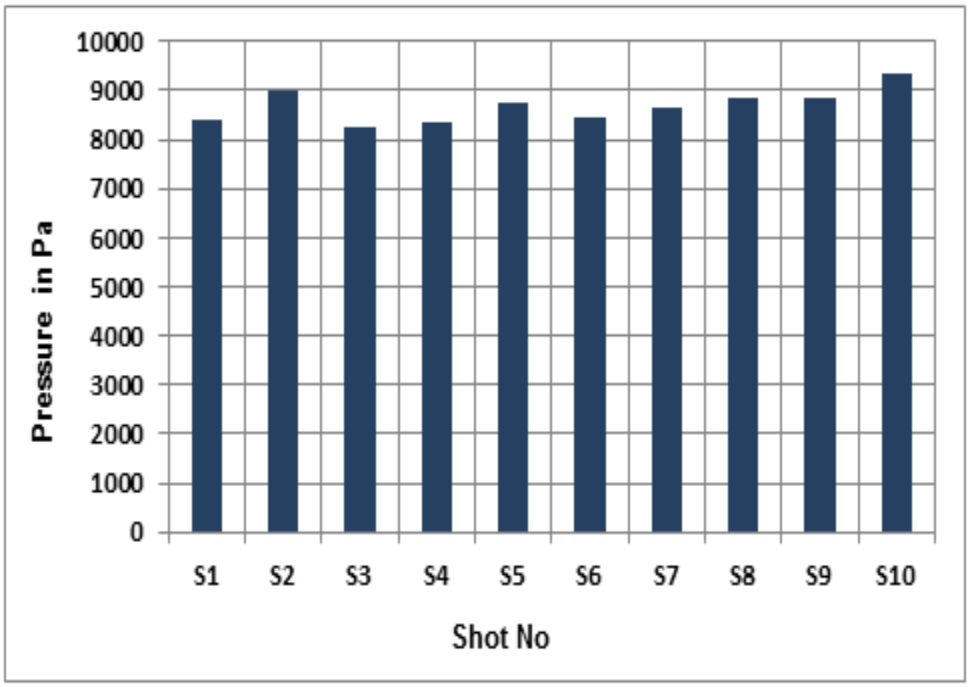

Figure 5.6.1: Peak pressure variation at M2 for AR15 (10 shots)

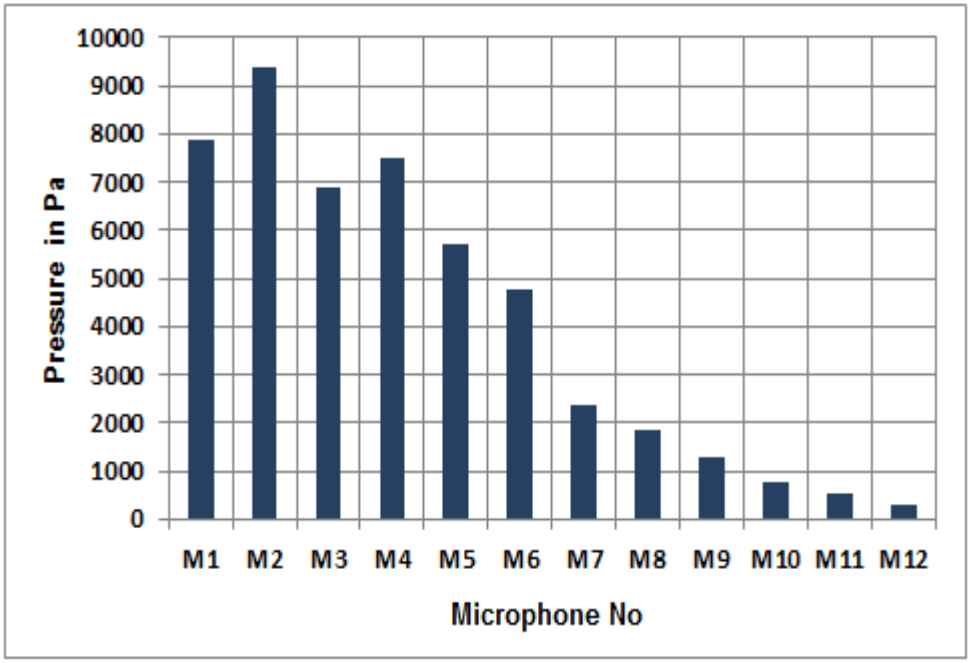

Figure 5.6.2: Azimuthal peak pressure variation for AR15 (S2)

One of the reasons may be the sampling rates; lower sampling rate may cause recording lower pressure values of muzzle blast waves. So the signals were analyzed through resampling them at 5 MHz rate to observe these variations as shown in figure 5.6.3., 5.6.4., and 5.6.5 show the resampled peak pressure variations for different shots at M2 and azimuthal variation for S10. As observed, there are still shot to shot and azimuthal variations as with previous sampling rate. So sampling rate was not an issue regarding this variation.

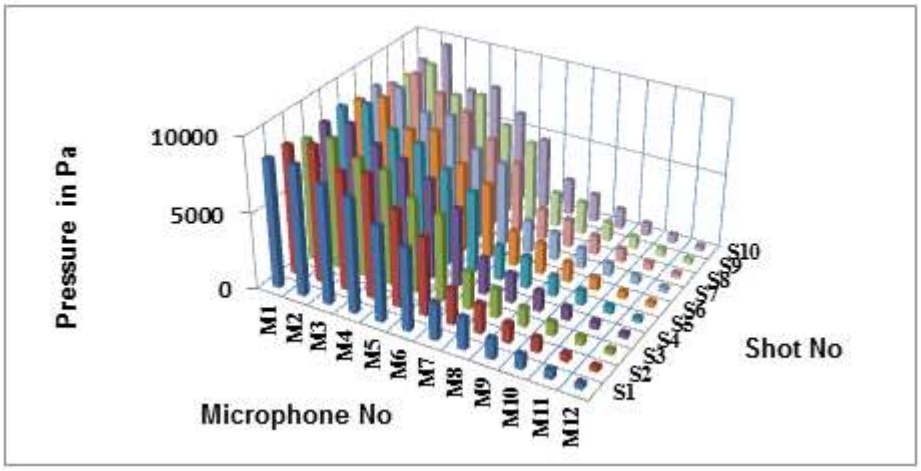

Figure 5.6.3: Re-sampled peak pressure for the AR15 muzzle blast as a function of azimuth (10 shots)

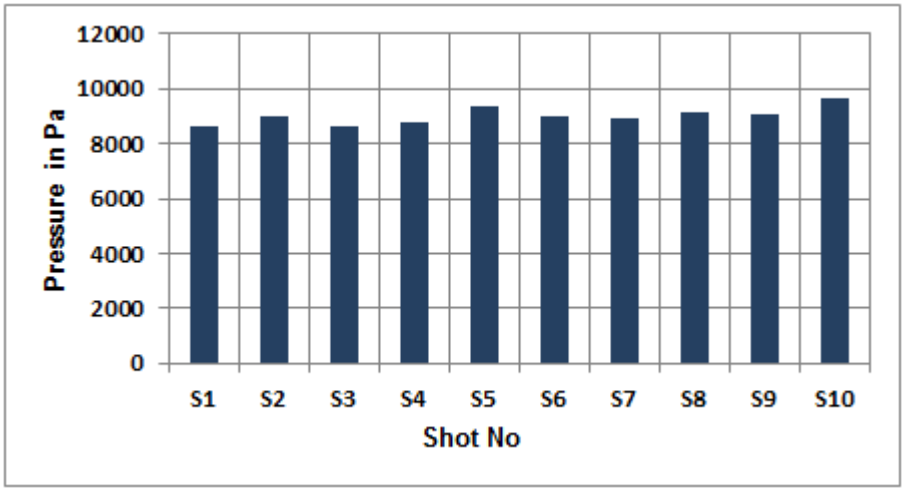

Figure 5.6.4: Resampled peak pressure variation at M2 for AR15 (10 shots)

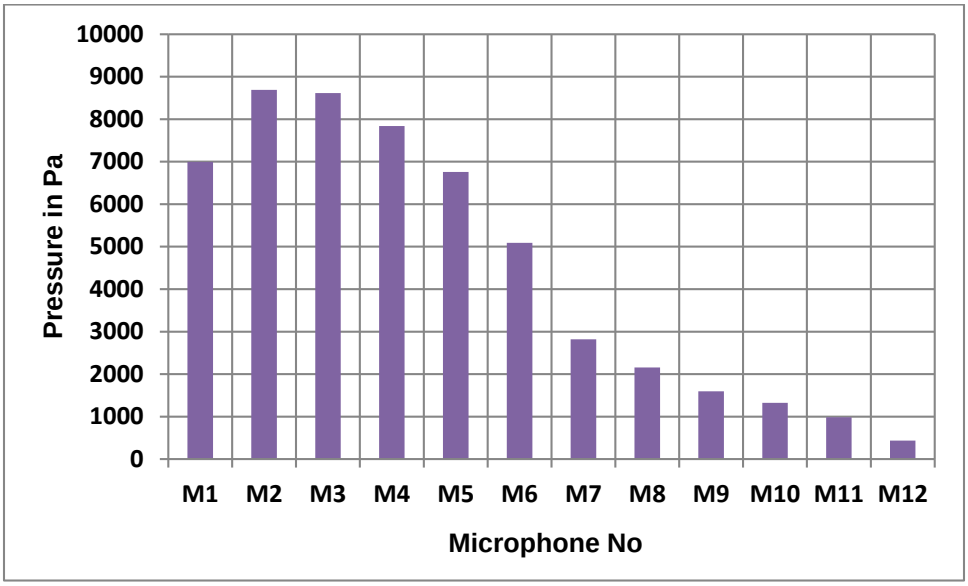

Figure 5.6.5: Resampled Azimuthal peak pressure variation for AR15 (S2)

Another reason may be for that particular shot; M2 was much closer to the shot than other microphones. As seen from the figure 5.6.4, the peak pressure for M2 was observed at S10. But from figure 5.6.6, it is observed that S10 was not the closest shot to M2. Also from figure 5.6.5, the pressure values were higher at M2 and M3. From figure 5.6.7, it has been observed that M2 and M3 were not closest to the firearm to record high-pressure values. So for AR 15, it can be concluded that firearm position was responsible for pressure variation at different azimuths.

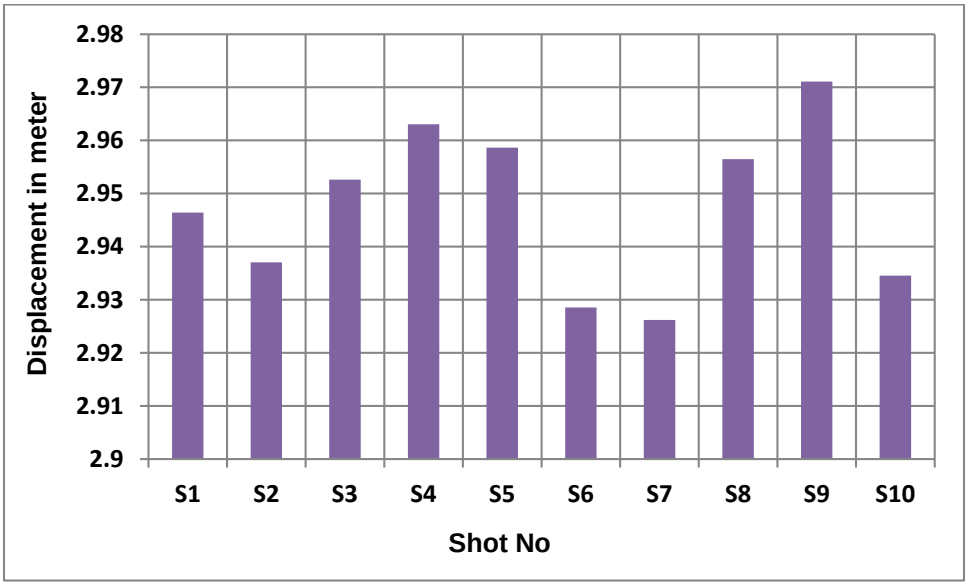

Figure 5.6.6: Radial distance from the firearm to M2 for 10 shots

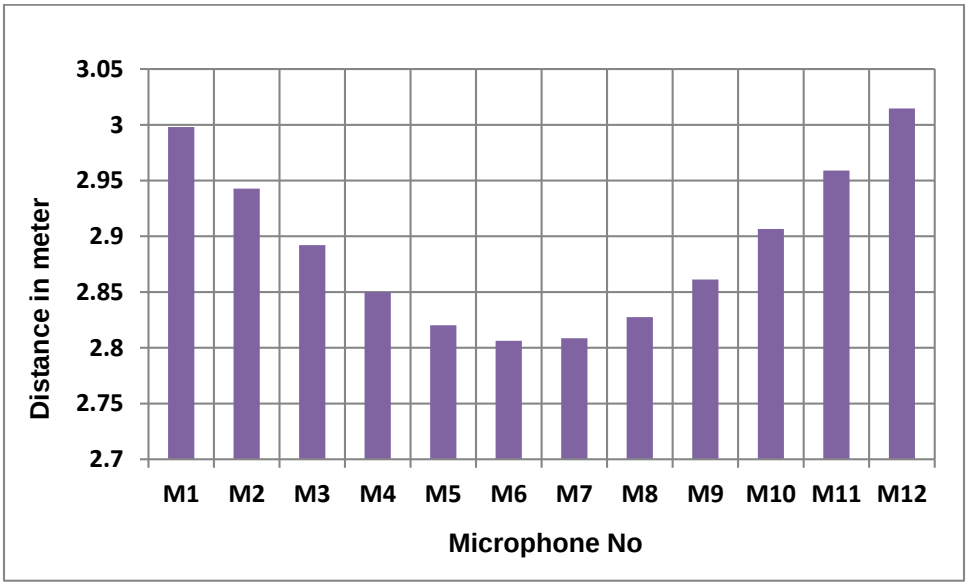

Figure 5.6.7: Radial distance from the firearm to different azimuths for S2

The nature of the muzzle blast duration seems that it is higher for smaller azimuths, tends to decrease up to M7 and then rises again from M8. There are sudden rises of durations at the position of M9 and M11.

To find out whether this particular nature are signatures of AR15 or whether there is the presence of some disturbance at that particular azimuths which are governing this behavior, we also tried to take a closer look at particular blast waveforms.

For example, in case of S1, greater amount of high frequency fluctuations is observed at M11 than M12 (figure 5.6.7). Moreover, the negative phase duration is smaller at M11 than M12. It results in higher muzzle blast durations in both methods at M11 than at M12.

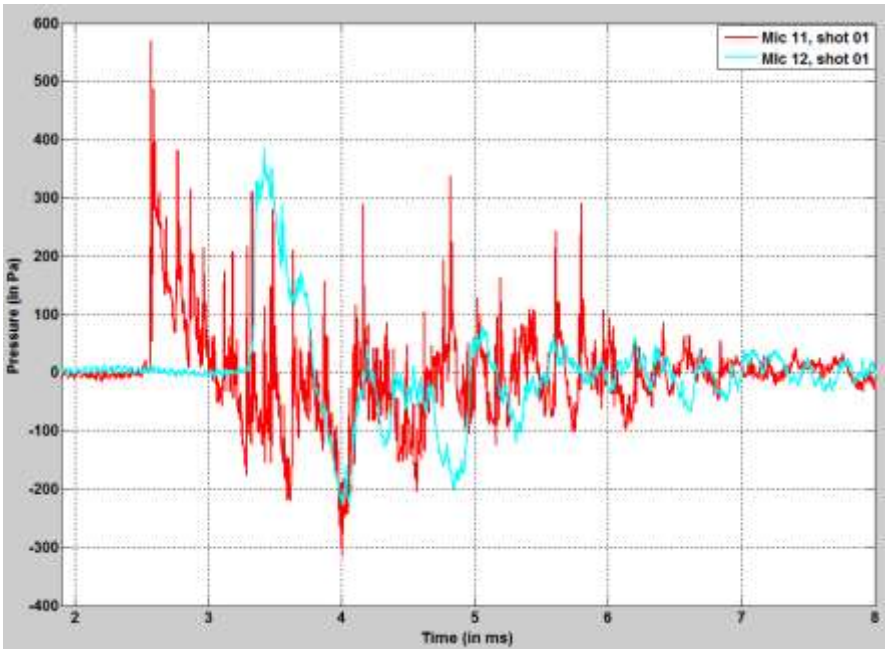

Figure 5.6.7: Muzzle blast duration variations at M11 and M12 for S1 of AR 15 rifle

5.7 CZ 452 (Ceska Zbrojovka) (.22 Caliber)

During capturing gunshots from this particular firearm, the gains of the amplifiers (both 12 AG and 12AA) were increased by an amount of +20dB (a total attenuation of 0

dB); by considering their small amplitudes. Even then, at higher azimuths, the peak pressure levels are much lower (nearly of single digit). The total number of shots was 11 this time, but due to excessive noise was present at S6, we have not included that shot in our analysis.

It is observed that 0.22 caliber long rifle bullets generate much smaller muzzle blast pressure than other firearms. The reason is that all the bullets used in this experiment were center fire, only these bullets were rim fire bullet. For rim fire bullets, the priming compound stays within the rim of the cartridge. The cartridge is thin walled. After pulling the trigger, rim ignites the gunpowder. As the primer is in very well contact with the gunpowder, the ignition is much guaranteed in case of rim fire (5.7.1)(Heard 2008) . The complexity of rim fire is much less. Rim fire bullets are constructed with much less amount of gunpowder and that's why they generate a much smaller amount of muzzle pressure compare to centerfire (Blackstone Shooting Sports) .

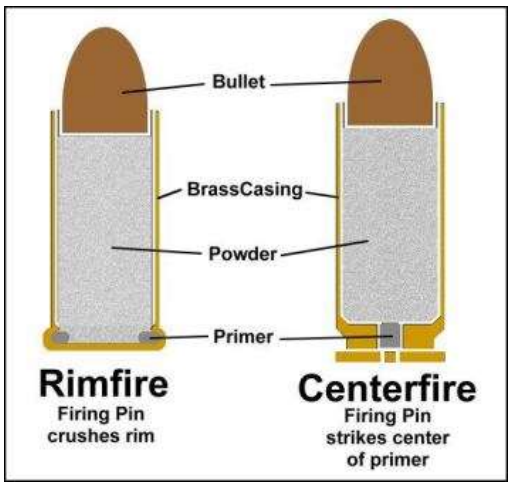

Figure 5.7.1: Difference between rim fire and centerfire bullet (Blackstone Shooting Sports)

However, for some pressure level, 0.22 LR exhibits some discrepancies from one shot to another. For example, if we take a look at the peak pressure levels at M4, we observe that the pressure level varies from 1206 pa for S1 to 887 Pa for S4 as seen in figure 5.7.2.

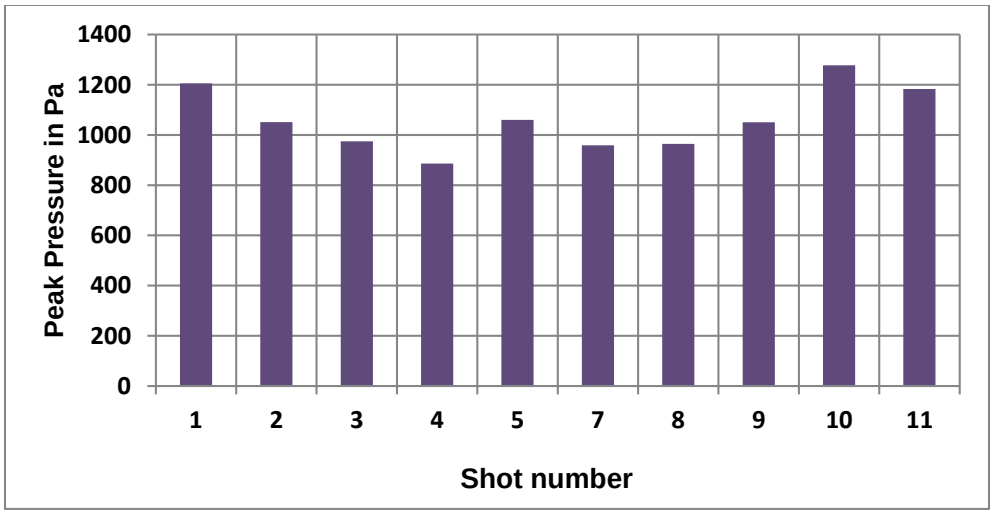

Figure 5.7.2: Muzzle blast peak pressure variation at M4 for 10 shots with 0.22 LR

Again, a resampled version (5 MHz) of these pressure waves was observed. The result is depicted in figure 5.7.3.

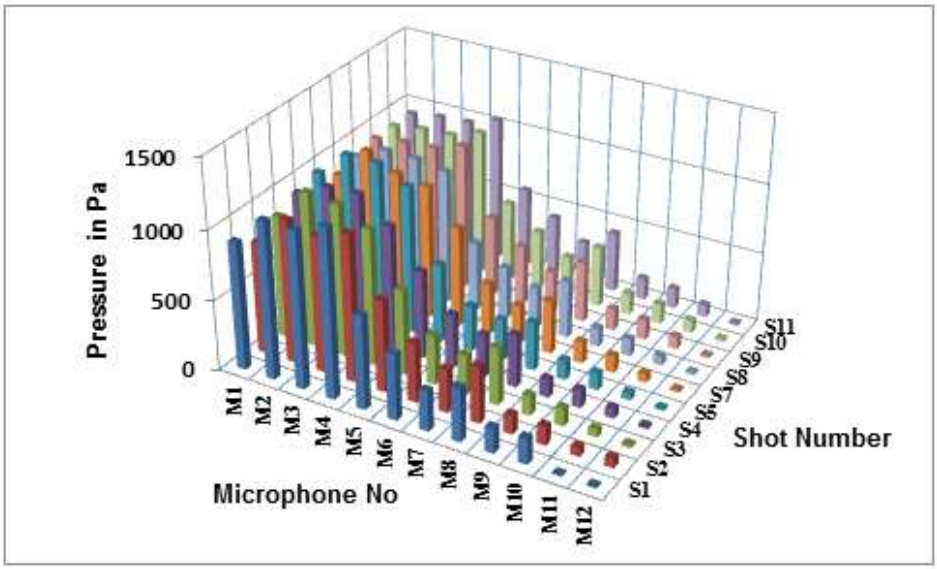

Figure 5.7.3: Re–sampled peak pressure at 3 meters for the 0.22 caliber long rifle muzzle blast as a function of azimuth (10 shots)

For the resampled version, the pressure variations do not change a lot. As seen from figure 5.7.4, the peak pressure levels at M4 still shows similar irregularities from consecutive shots.

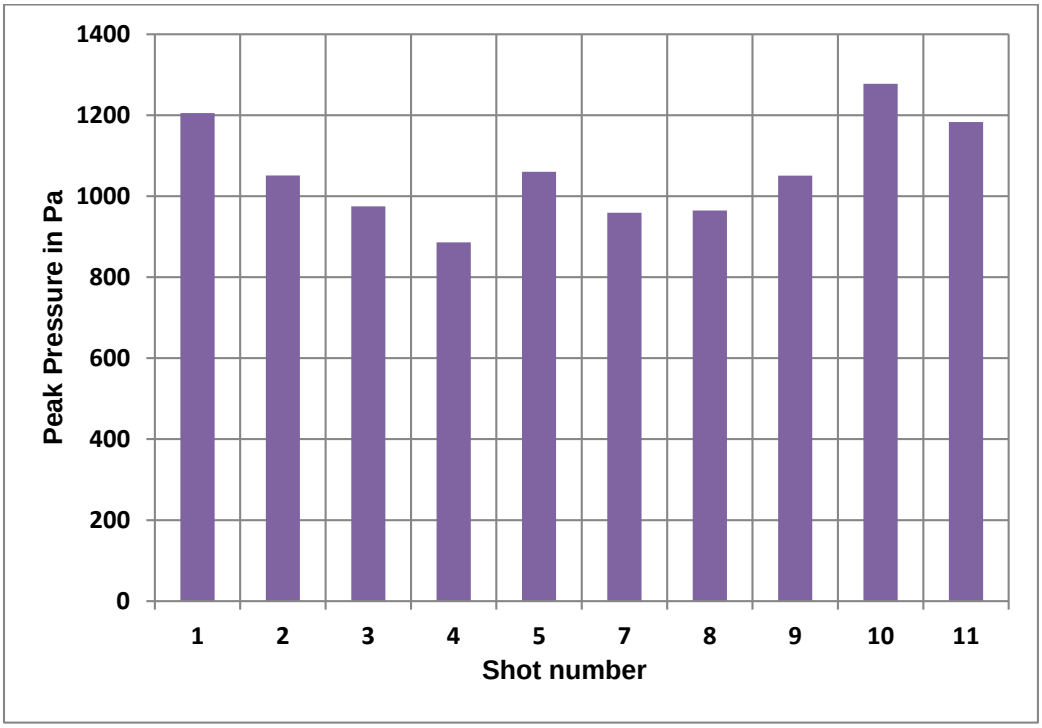

Figure 5.7.4: Re–sampled muzzle blast peak pressure variation at M4 for 10 shots with 0.22 LR

It seems that S1 and S10 records higher pressure than other shots. It may happen that during the firing S1 and S10 was much closer to the M4 than the other shots.

As seen from figure 4.7.7, peak pressure at M4 was higher at S5 than S4 and S6. Figure 5.7.5 exhibits that for S5; M4 was not at a nearer distance from the firearm for that particular shot. So pressure variation for 0.22 LR does not only depend on the positioning of the firearm.

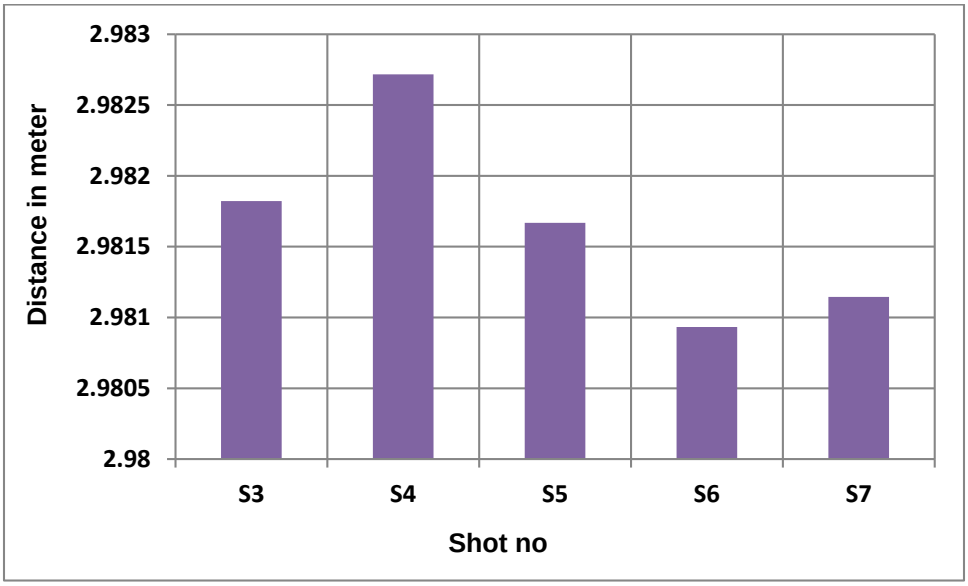

Figure 5.7.5: Radial distances of M4 from the position of the firearm for 5 different shots

Muzzle blast duration for 0.22LR varied a lot due to random low frequency contents in the signals; it is difficult to precisely detect the durations for this firearm even with energy accumulation method. Our plan is to record the same shot again with higher gain.

5.8 Ruger SP 101 with 0.38 Caliber Bullets

Ruger SP 101 with 0.38 caliber bullets show irregularities from one azimuth to another (the azimuthal variation in shot 1 is shown in figure 5.8.1), as well as one shot to another for the same microphone (variation at M4 is shown in figure 5.8.2).

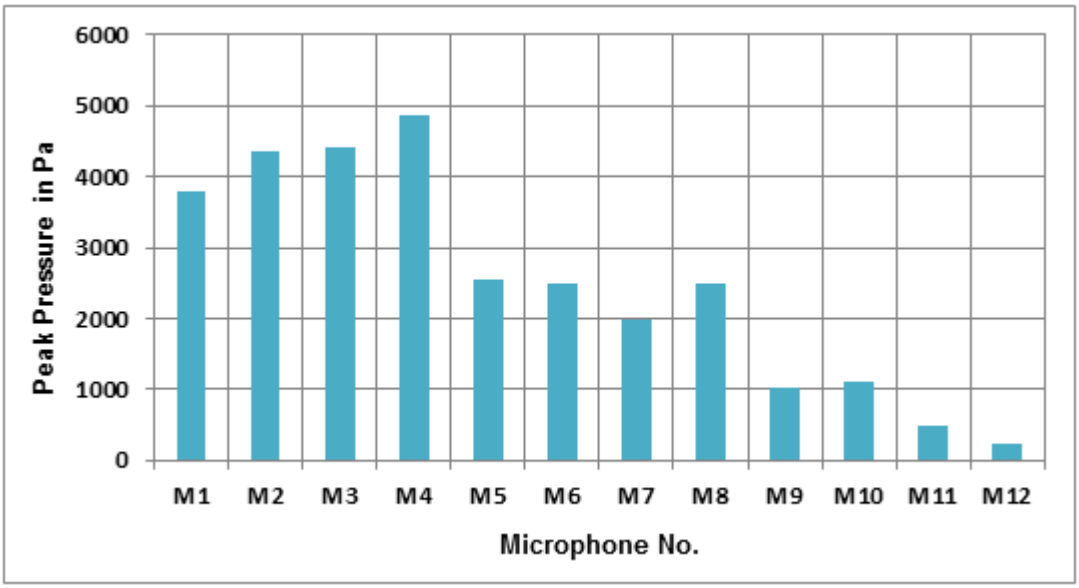

Figure 5.8.1: Azimuthal variation of peak pressure for Ruger SP101 with 0.38 caliber bullets (first shot)

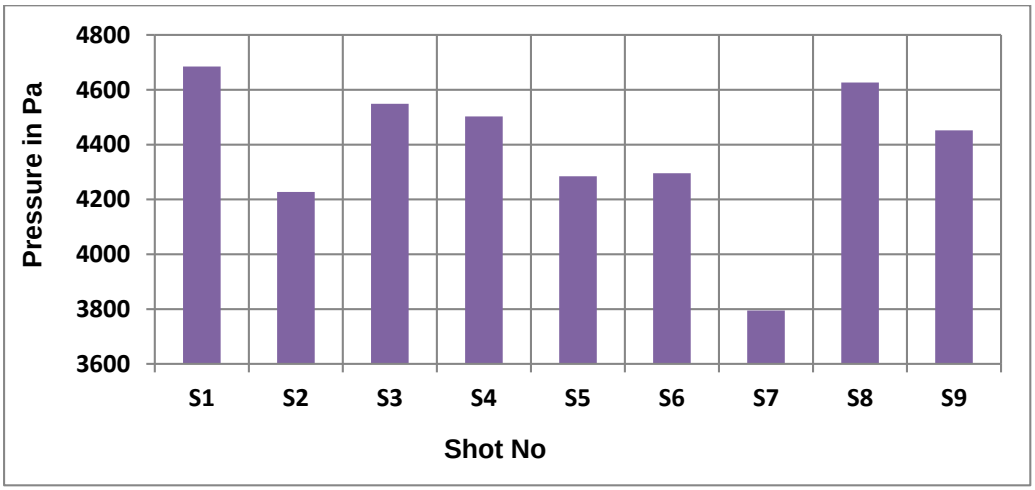

Figure 5.8.2: Shot to shot variation of peak pressure at M4 for Ruger SP101 with 0.38 caliber bullets (9 shots)

Again, to capture the small duration muzzle blast variation, peak pressure waves were analyzed using 5 MHz sampling rate. The results are depicted in figure 5.8.3. Azimuthal

variation for the same shot and shot to shot variation at the same azimuth were observed for the resampled version (figure 5.8.4 and 5.8.5).

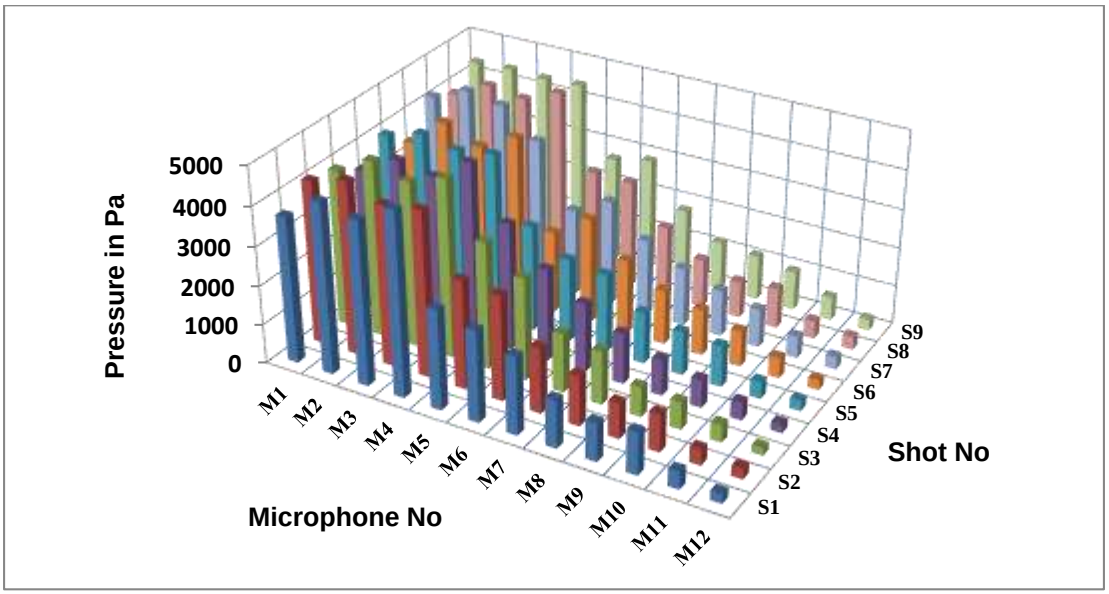

Figure 5.8.3: Re-sampled peak pressure of Ruger sp101 with 0.38 caliber muzzle blast as a function of azimuth (9 shots)

As seen from the figures, the scenario for the variation has not changed much. So, sample rate was not an issue for such irregularity.

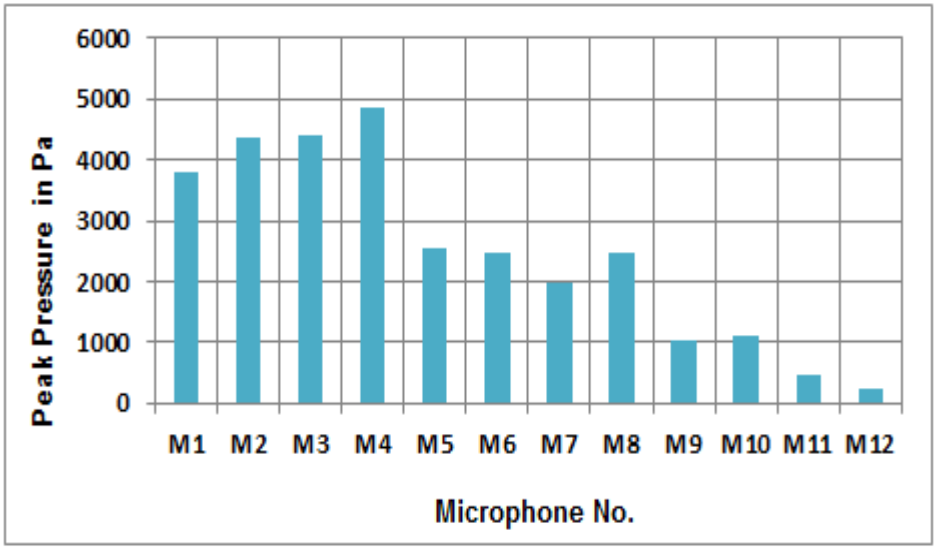

Figure 5.8.4: Azimuthal variation of peak pressure for after resampling (first shot)

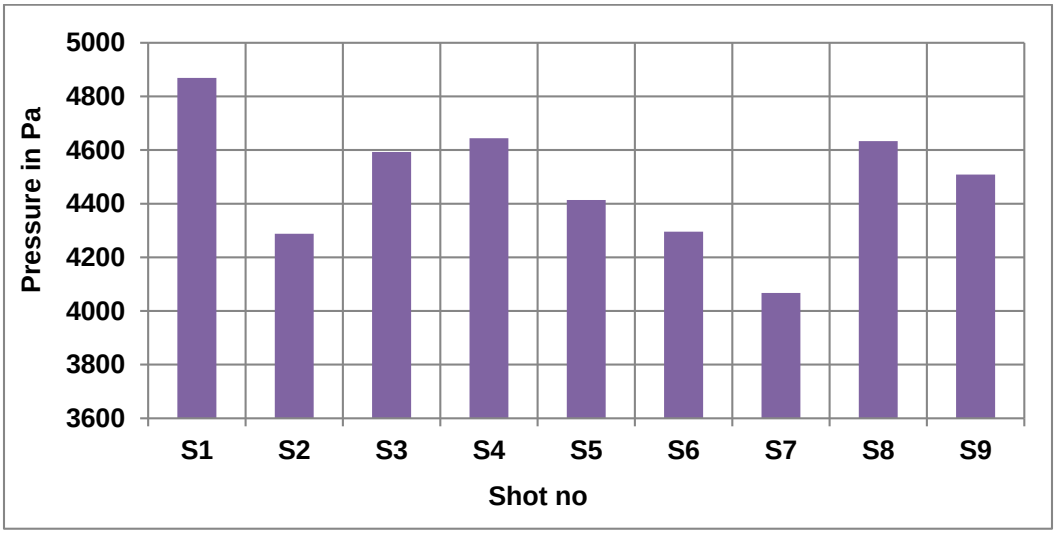

Figure 5.8.5: Shot to shot variation of peak pressure at M4 after resampling (9 shots)

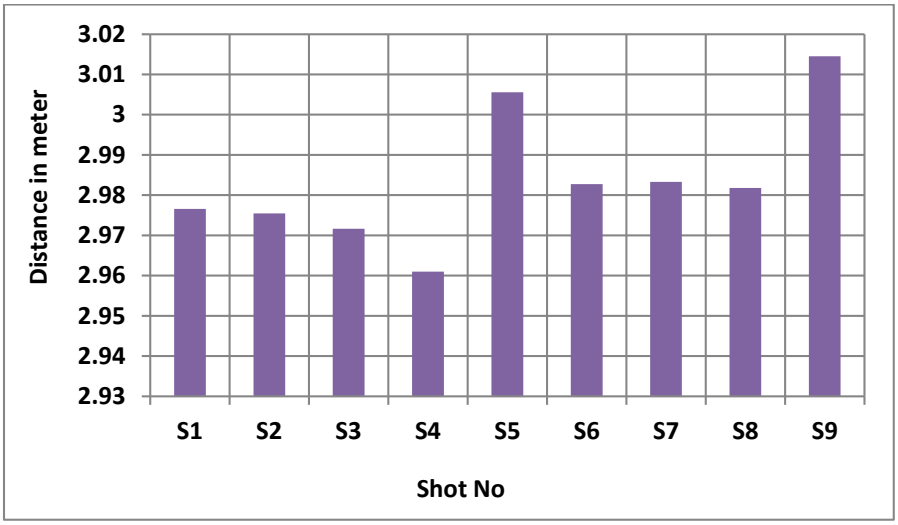

Figure 5.8.6: Radial distance from the firearm to M4 for successive shots with Ruger SP101 (0.38 caliber bullets)

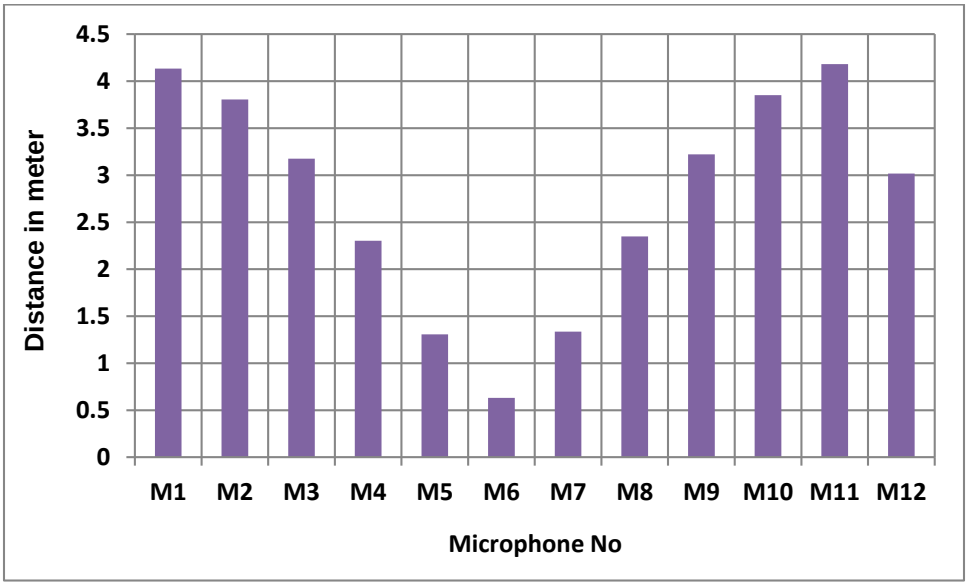

Figure 5.8.7: Firearm distances at several azimuths for S1

From 5.8.4, the highest peak pressures for S1 were observed at M3 and M4, and then there is a sudden drop in peak pressure at M5. As seen from figure 5.8.7, M4 was not the closest to the firearm but recorded the highest peak pressure. The nearest

microphone from the firearm for S1 was M6, which recorded much lower pressure. The highest and lowest pressure values were observed at M4 was for S1 and S7. As observed from figure 5.8.6, M4 was neither the closest nor the farthest from the firearm for those two shots. So it cannot be concluded for Ruger SP101 with 0.38 caliber ammunition, closer shots record higher muzzle blast peak pressures at the microphones.

The trend of duration seems to be the duration is higher at higher azimuths; the exception is the azimuth of M7. As seen from figure 5.8.7, there are multiple peaks at that azimuth. This may have caused by any particular disturbance in that direction. So Ruger SP101 with 0.38 caliber ammunition exhibits random shot to shot and also azimuthal muzzle blast duration variation.

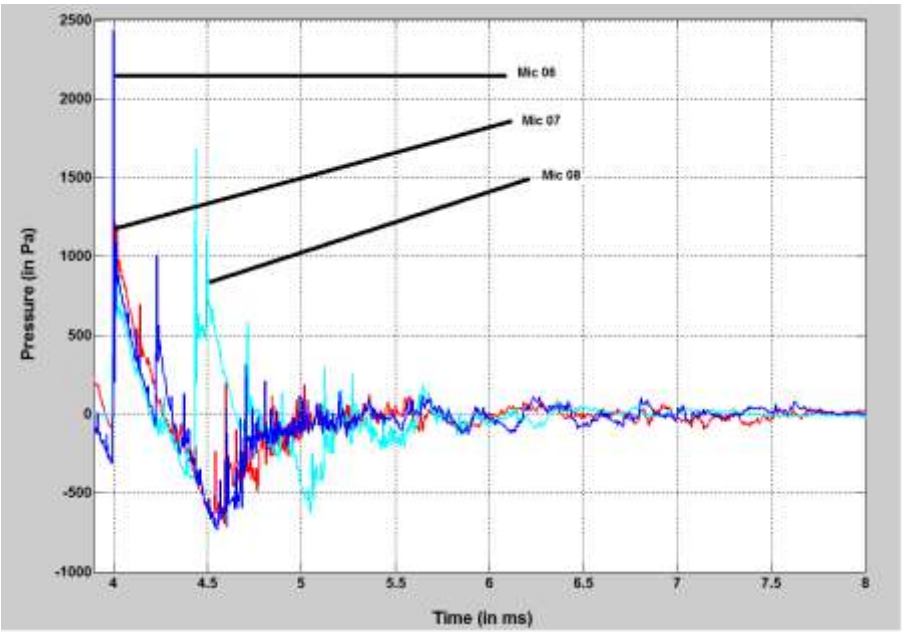

Figure 5.8.7: Muzzle blast duration variation at different azimuths for S1

5.9 Ruger SP 101 with 0.38 Caliber Bullets

If we look at the peak pressure variation for Ruger SP 101 revolver with 0.38 diameter bullets, we will find that peak pressure varies greatly in between different azimuths at the same shot and in between shots. For example, azimuthal variation for S1 is depicted in figure 5.9.1 and shot to shot variation at microphone 05 is showed in figure 5.9.2.

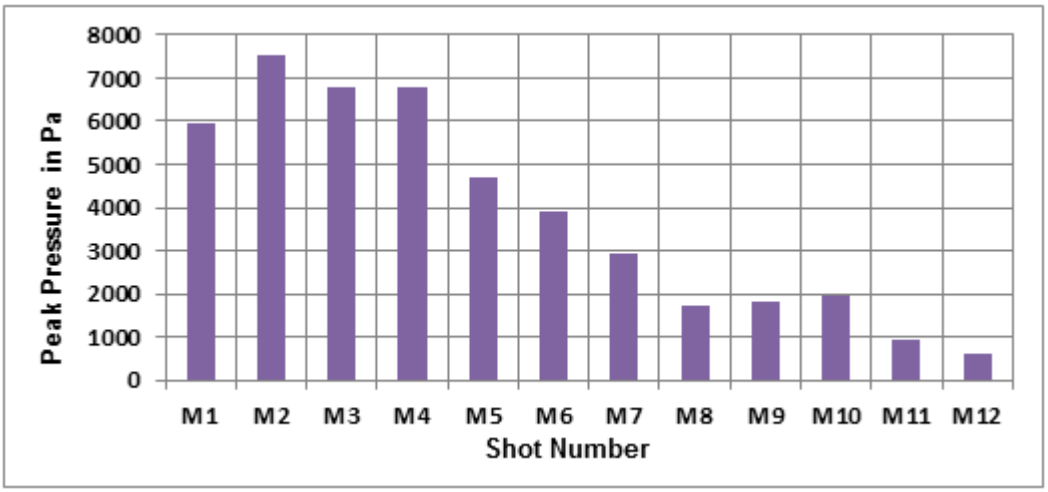

Figure 5.9.1: Azimuthal variation of peak pressure for Ruger SP101 with 0.357 caliber bullets (first shot)

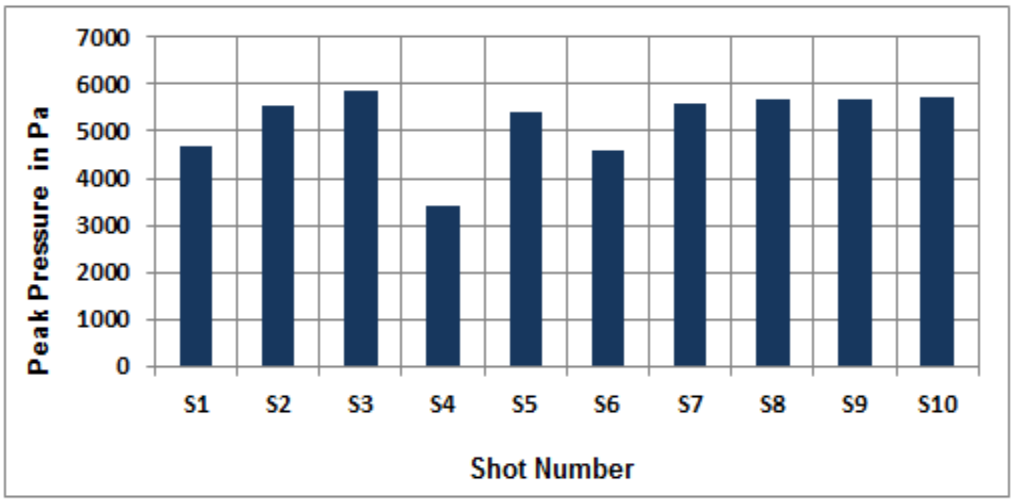

Figure 5.9.2: Shot to shot variation of peak pressure for Ruger SP101 with 0.357 caliber bullets at the M4 (10 shots)

As it is seen, M2 records higher peak pressure than M1 and M3 for the first shot (figure 5.9.1). This is true for all shots except S5. For S5, the firearm may be closer to M3 than M2. Again, according to figure 5.9.2, S4 records the lowest pressure at M4. If we have a look at the re-sampled version of the pressure waves to capture the peak pressure level more precisely (figure 5.9.3), we see that the picture does not change (figure 5.9.4 and figure 5.9.5). That means sampling rate was not an issue for this variation.

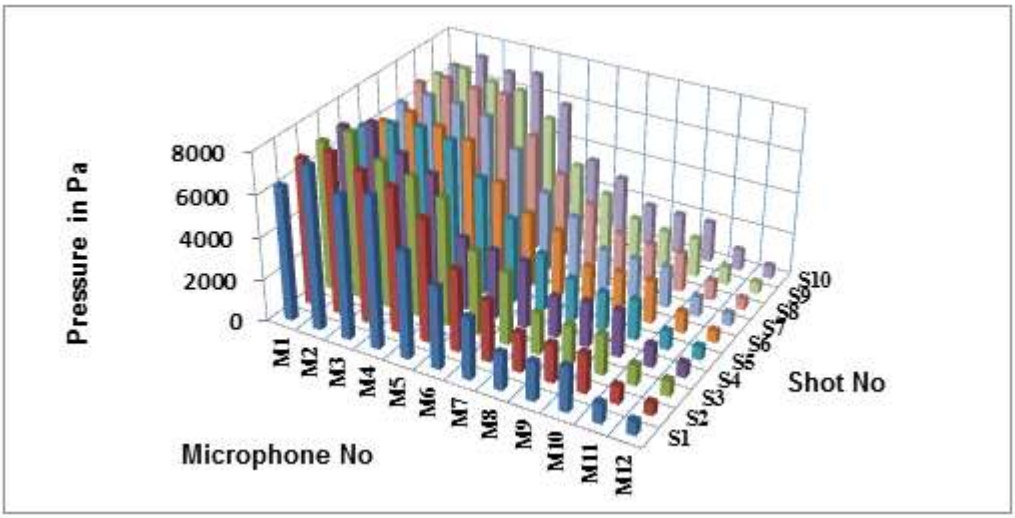

Figure 5.9.3: Re-sampled peak pressure of muzzle blasts of Ruger sp101 with 0.357 caliber bullets as a function of azimuth (10 shots)

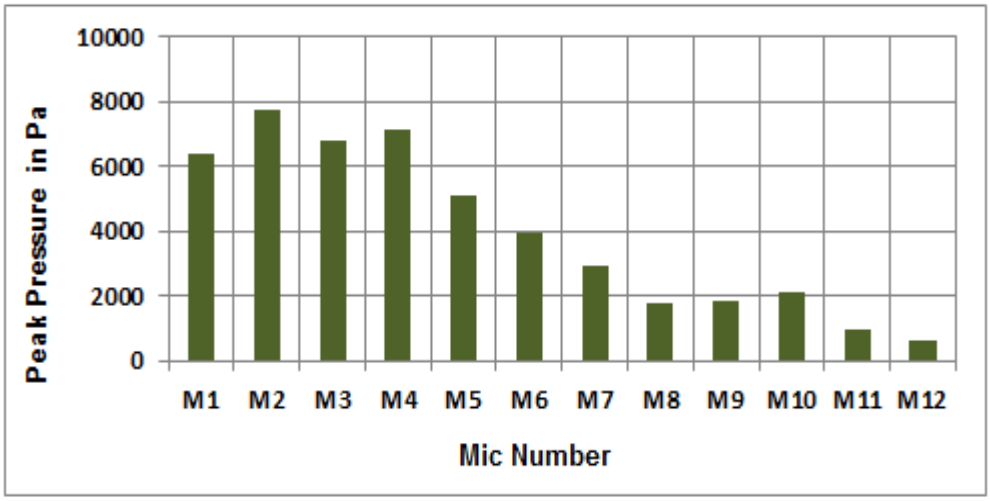

Figure 5.9.4: Re- sampled azimuthal variation of peak pressure for Ruger SP101 with 0.357 caliber bullets (first shot)

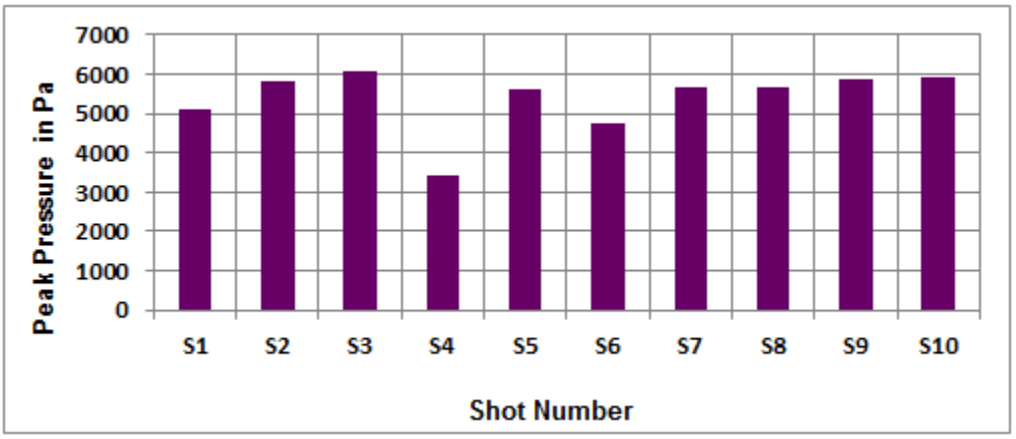

Figure 5.9.5: Shot to shot variation of peak pressure for Ruger SP101 with 0.357 caliber bullets at M4 (10 shots)

`

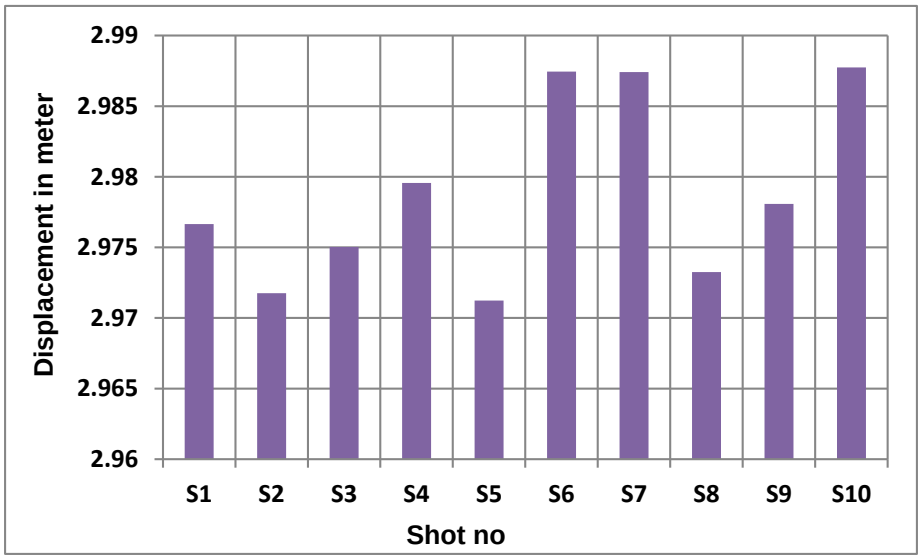

Figure 5.9.6: Distance from the firearm to M4 for various shots

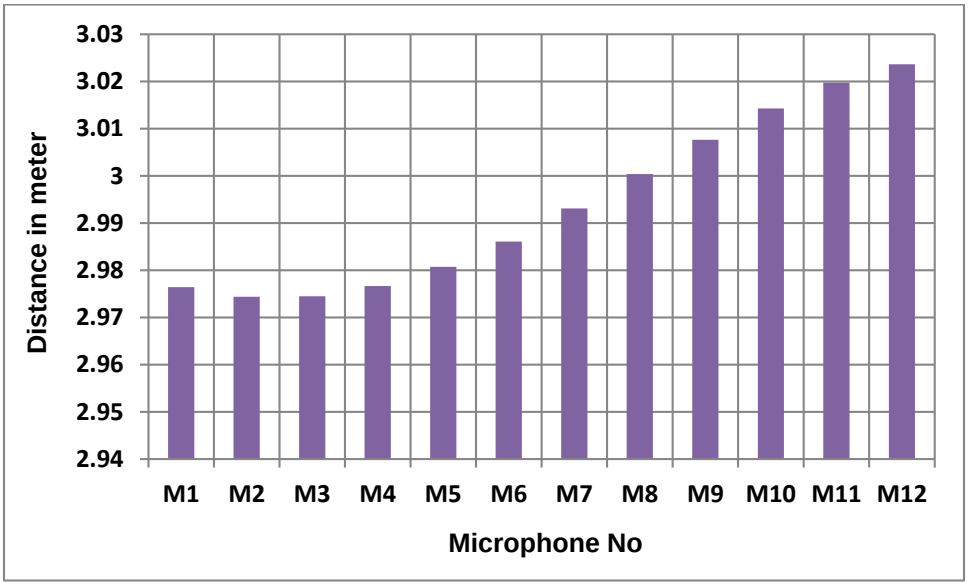

Figure 5.9.7: Distance from the position of the firearm at different microphones S1

For S1, the pressure at M2 was higher than M1 and M3, which is realizable as this microphone was closer than the other two for that shot. Figure 4.9.5 shows that S3 generated the highest pressure output at M4, but as observed from figure 4.9.6, it was not the closest shot. So there are factors other than position of the firearm which regulates the behavior of the peak pressure.

The muzzle blast durations exhibit many asymmetries from shot to shot and azimuth to azimuth. For example, at M1, the durations varied from one shot to the other. Waveform based approach durations were found 0.77ms, 1.52 and 0.652 ms consecutively. For S2, the blast signal nearly touches the base level at 0.67 ms, as seen from figure 5.9.8. The duration based on energy accumulation seems much symmetric; the durations were recorded as 0.996 ms, 0.982 ms and 0.966 ms.

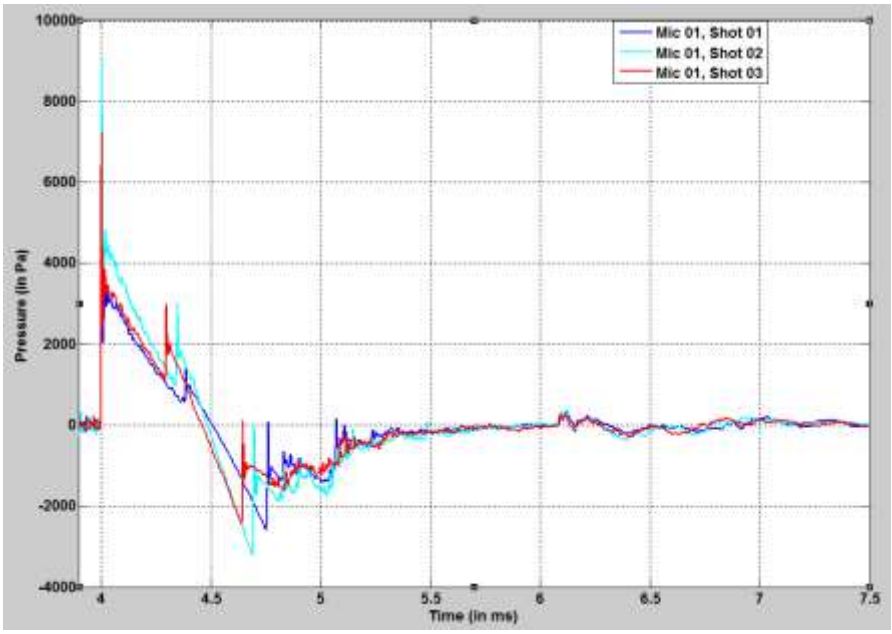

Figure 5.9.8: Muzzle blast duration variation at different azimuths for the first shot

5.10 12ga Shotgun

Remington 00 buckshot contains a total number of 15 pellets, each having a weight around nearly 3.43 grams. So the thrust from gunpowder explosion needs to push a total mass of nearly 51 grams outside the barrel and ensure enough penetration. The recorded muzzle blast pressure value may be high in these shots for this reason (comparable to the rifle category).

The trend is that the peak pressure decreases as we move at higher azimuths. As observed from the pressure graph, recorded pressure at M3 was not consistent for successive shots. Figure 5.10.1 shows the pressure difference between M3 and M4 for three different shots.

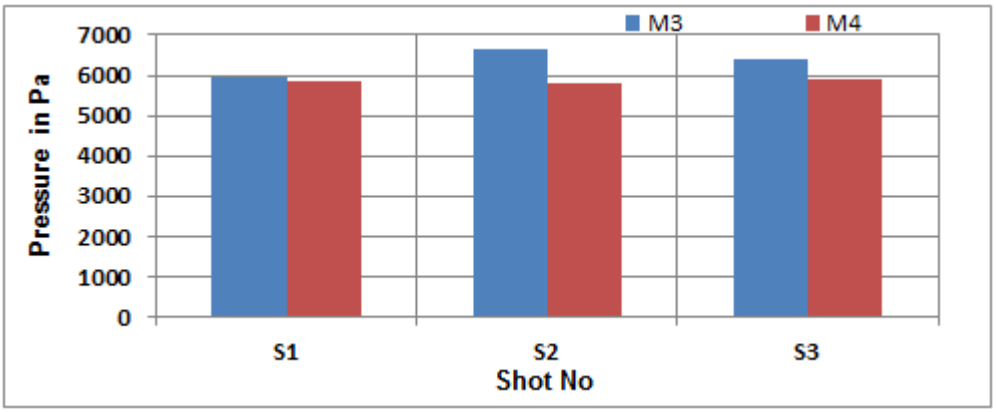

Figure 5.10.1: Peak pressure variation in three different shots at M3 and M4

We have considered a resampled version of the pressure wave to have a closer look at these muzzle blast signals (figure 5.10.2). The scenario has not changed for a resampled version as seen from figure 5.10.3.

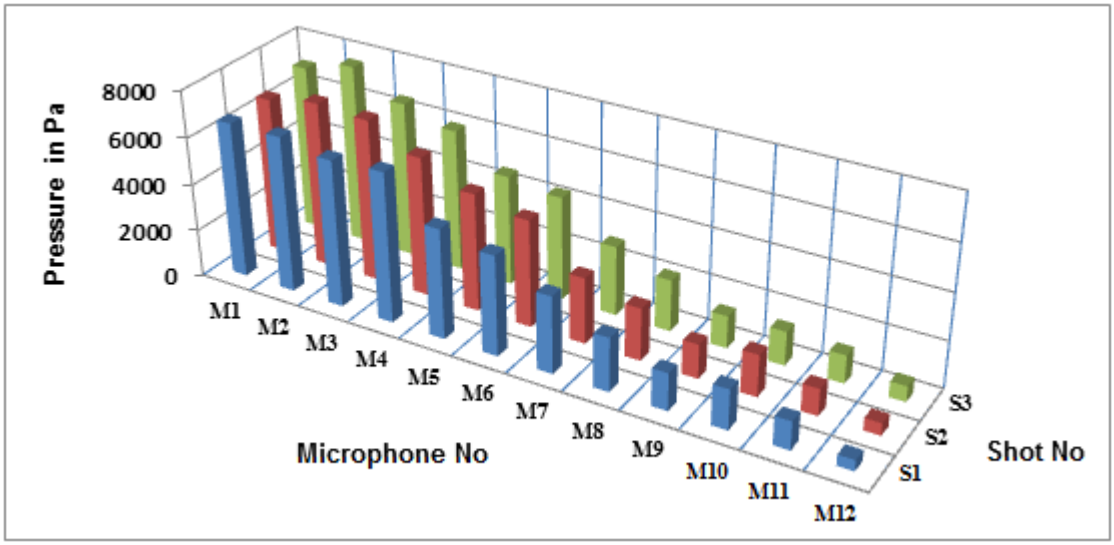

Figure 5.10.2: Re-sampled (5 MHz) peak pressure for 12ga muzzle blast as a function of azimuth (3 shots)

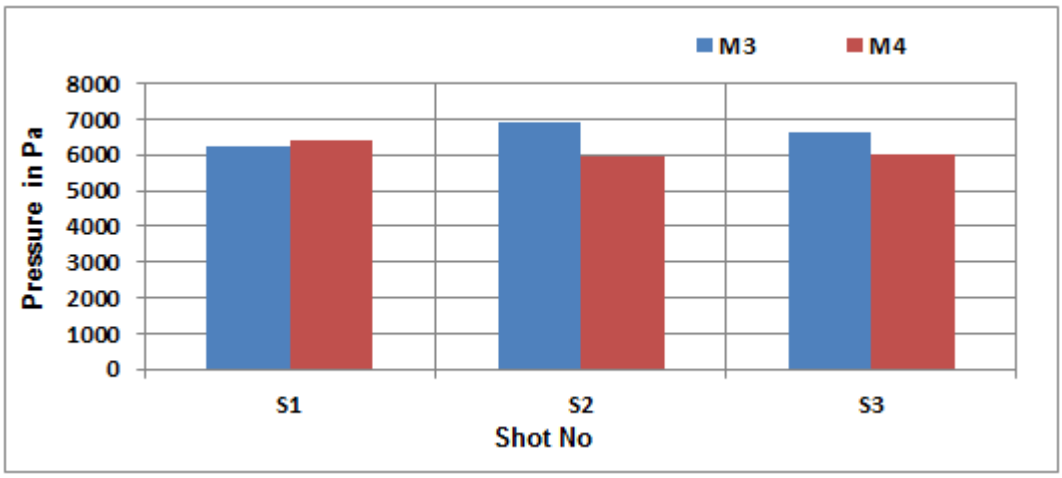

Figure 5.10.3: Resampled peak pressure variation in three different shots at M3 and M4

For the resampled version, again it is observed that, the pressure at M3 varies from one shot to the other.

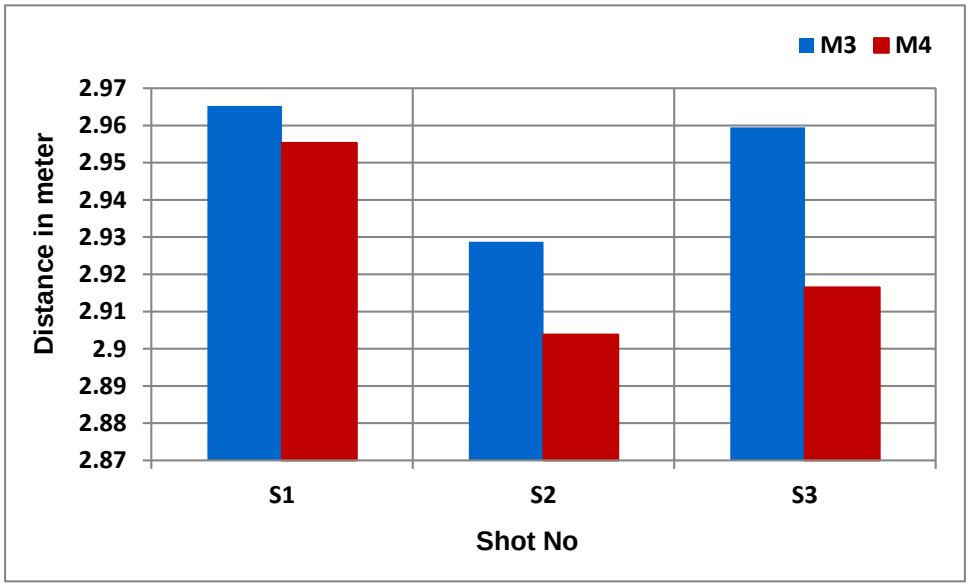

Figure 5.10.4: Distances from the position of the firearm to M3 and M4 for several shots of 12ga

As observed, the ascending order of pressure values at M3 was S2, S3 and S1. Figure 5.10.4 shows that for all the shots, M4 was nearer to the firearm than M3. Therefore, analyzing distances from the firearm to microphones, it cannot be described what is causing the pressure variation during various shots.

As seen from figure 5.10.5, the positive phase duration segment covers a very small portion of the total Muzzle blast duration in all the cases (for example, 1.9 ms for a total Muzzle blast duration 5.08 ms).

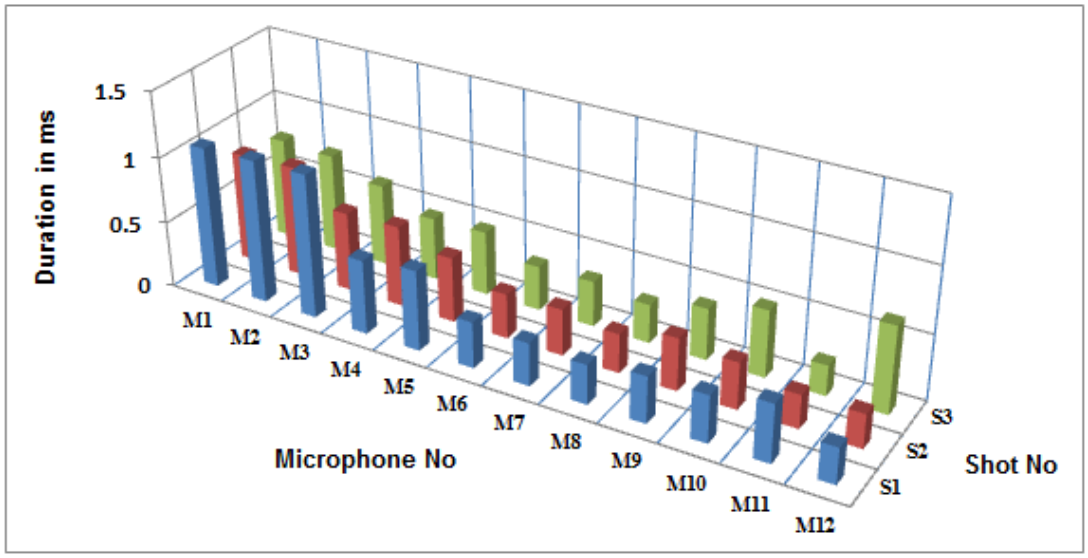

Figure 5.10.5: Shot to shot azimuthal variation of the positive phase duration for 12ga (3 shots)

Non uniformity in blast durations was observed for 12ga gunshots in several cases. Here we will discuss two. For S1, blast duration at M6 is less than M5 and M7 (figure 5.10.6). Muzzle blast signal from M6 goes below the zero line and comes out

much earlier than M5 and M7 (durations are 2.13 ms, 1.946 ms and 2.712 ms respectively).

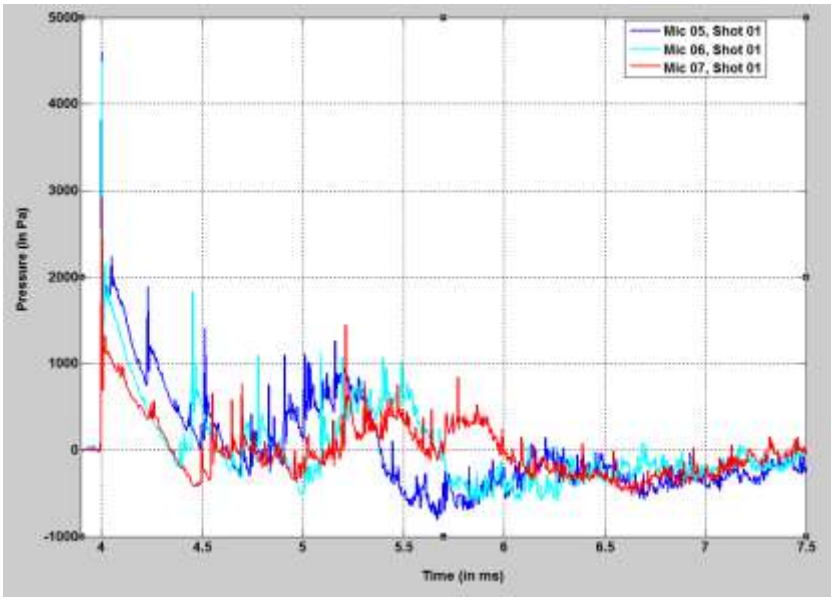

Figure 5.10.6: Muzzle blast duration variation at different azimuths for S1

For M4, the duration also varies from one shot to other as shown in figure 5.10.7. In this case, the blast duration for S2 was less than S1 and S3 (3.884ms, 2.282 ms and 3.066 ms respectively).

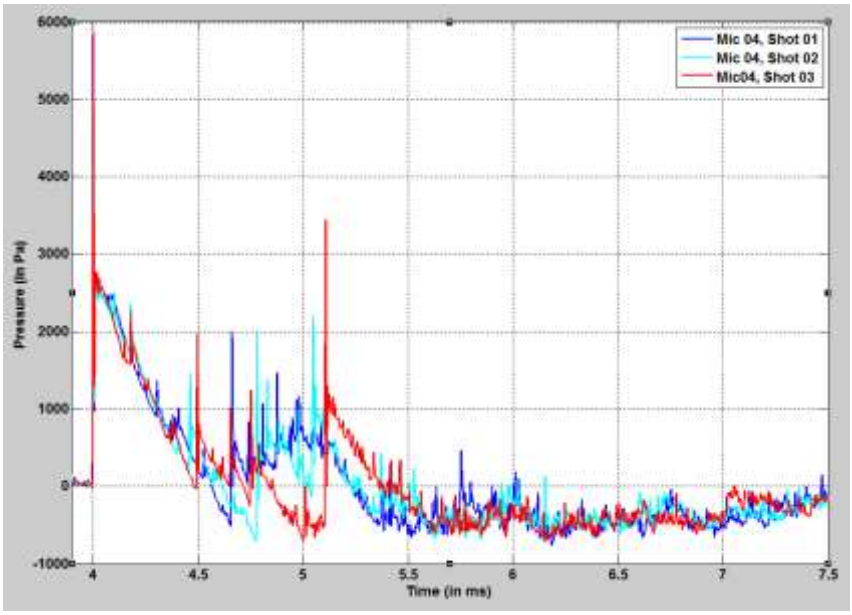

Figure 5.10.7: Muzzle blast duration variation at M4 for 3 successive shot

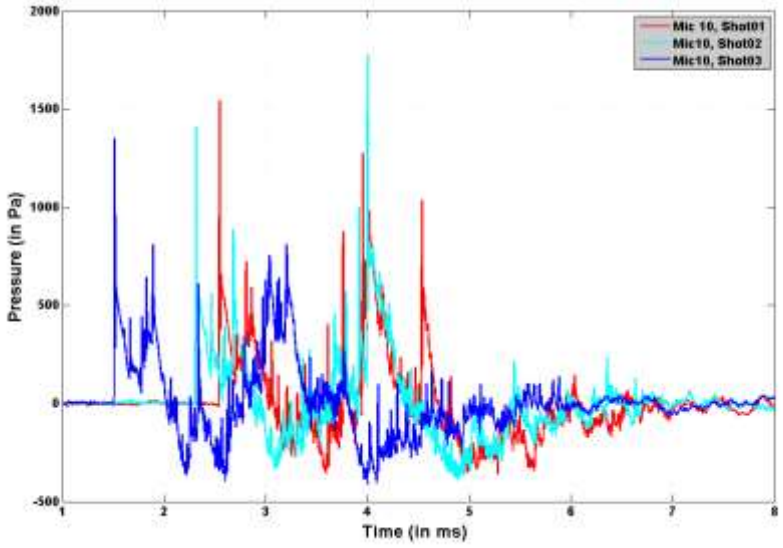

Figure 5.10.8: Energy accumulation based muzzle blast duration variation at M10 for different shots

Variation in duration was also observed at M10 (figure 5.10.7). For shot 3, the number of spikes before settling down to the base level was higher than the other two cases, which may lead to this high blast duration. These high frequency fluctuations might have been inherent for this firearm at that particular azimuth. The similar case occurs also for M11 for different shots. So it is not conclusive from this study that why the blast durations vary for 12ga shotguns.

5.11 Correlation of Gunshots Compare to Colt 1911A1 (45 ACP)

Figure 5.11.1 shows the comparison between two signals captured at M1 at two different shots: S1 and S8. As observed, the negative phase of the muzzle blast signal of S1 reaches to higher peak value than S8 after crossing the mean voltage; such dissimilarity causes a lower value of correlation factor.

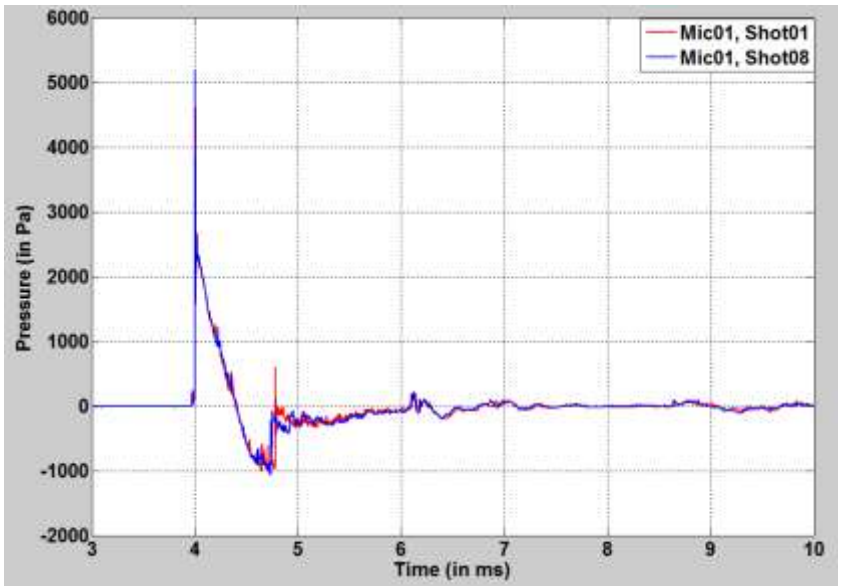

Figure 5.11.1: Variation of muzzle blast waveform at M1 for two different shots of Colt 1911A1 (45 ACP)

The lowest correlation in between Colt 1911A1 (45 ACP) and other pistols were found with Sig 239 pistol. The negative phase of the blast portion was much longer; also there was more than one peak at the peak pressure region for Sig 239; as seen in figure 5.11.2.

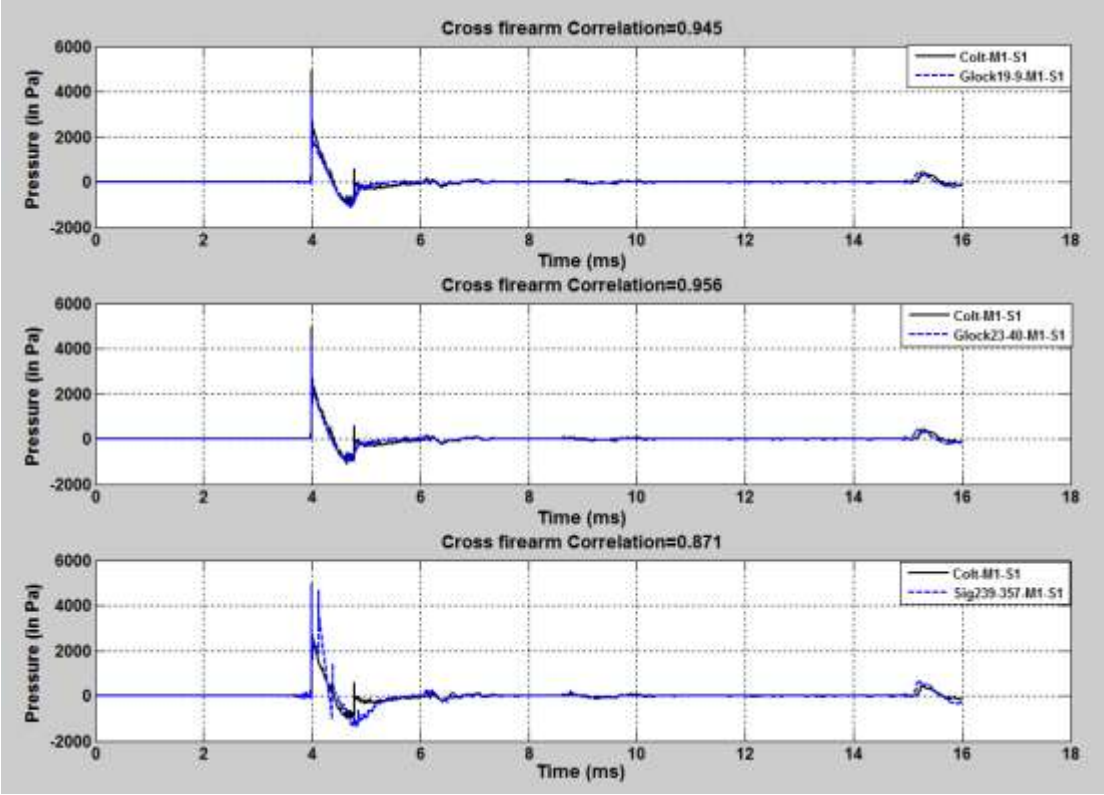

Figure 5.11.2: Comparison of muzzle blast waveform of Colt (45ACP) with other pistols

Figure 5.11.3, compares the muzzle blast portions of various rifles with Colt (45ACP). AR 15 and Surgeon were fired with supersonic bullets, as seen from the shockwave portion of figure 5.11.3. The muzzle blast portions for these two seem to be longer than Colt 1911A1 (45 ACP).

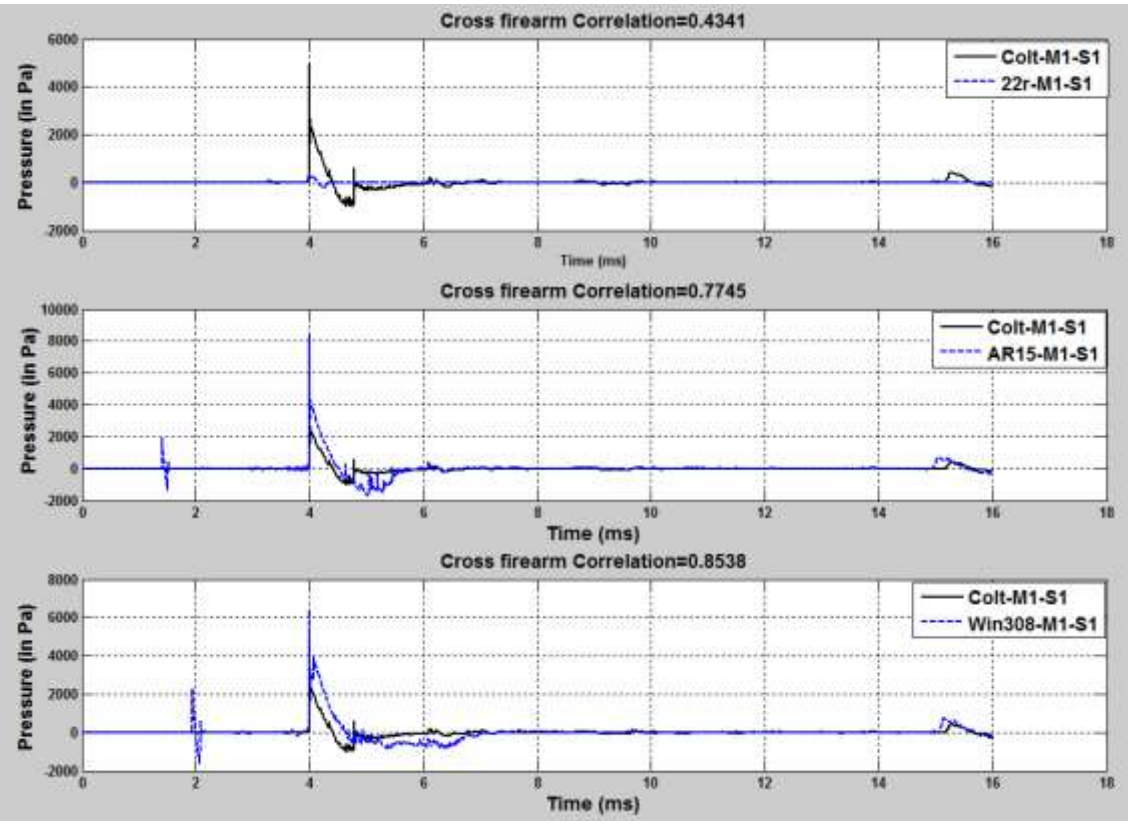

Figure 5.11.3: Variation of correlation factor of Colt (45ACP) with rifles

Comparison between Colt (45ACP) and revolver gunshot signals are shown in figure 5.11.4. The correlation was higher with 38 special than 357 magnums, fired with Ruger SP101.

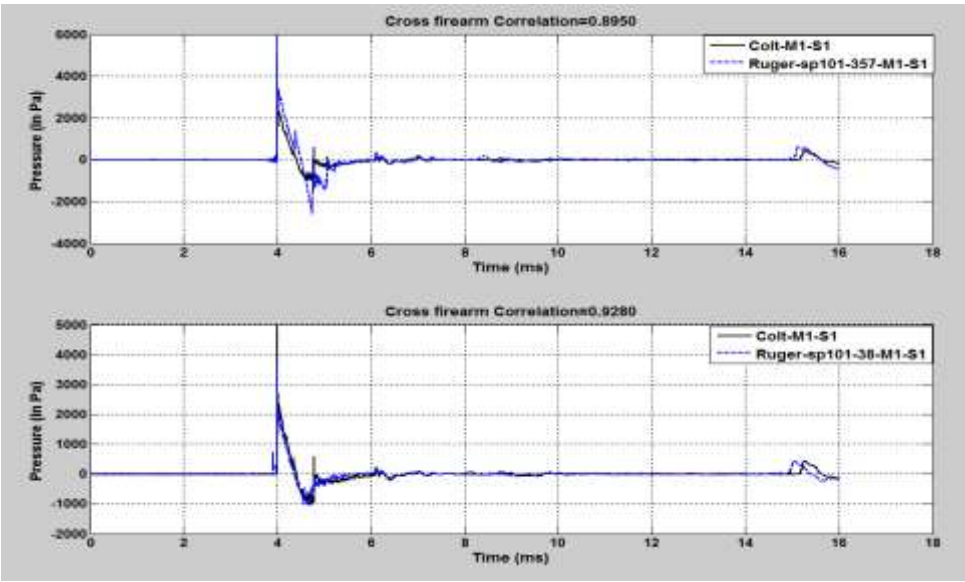

Figure 5.11.4: Successive shot variation of correlation factor at M1 of Colt (45ACP)

Figure 5.11.5 shows the comparison between Colt (45ACP) and 12ga shotgun. The values were found lower than other categories, as muzzle blast portions are much longer in shotgun than the pistol.

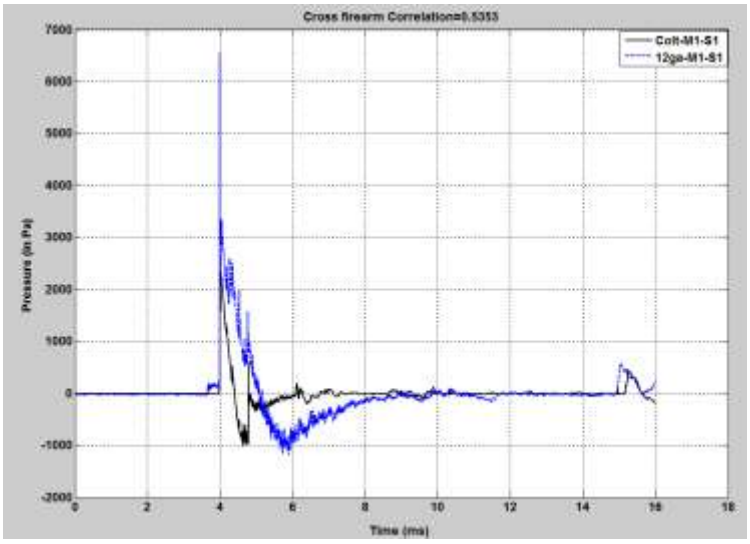

Figure 5.11.5: Comparison of muzzle blast waveform of Colt (45ACP) with 12ga shotgun

5.12 Predicted and Experimental Data at 49 Degrees for Different Firearm and Ammunition

Peak pressure prediction at M4 for Colt (45ACP) was less than the experimental measurement, apart from S5 for Colt 1911A1 (45 ACP). The highest error was for S4, near about 598 Pa. For S5, the firearm displacement was the highest. For S5, the pressure value at M4 was recorded 4417.3 Pa, which was the lowest among 10 shots. One of the reasons may be for that shot the M4 was at the highest distance among 10 shots. The distance from the firearm to M4 for that particular shot was 2.921 m, where the lowest was for S1 (2.919 m). So we could not conclude what exactly caused this original lower pressure value for that particular shot at M4.

For S5, predicted value was higher for AR 15. For S4, the original pressure value recorded for S4 at M4 was 7048.326 Pa, which was the lowest among 10 shots. As seen from figure 5.12.1, M4 was not at the nearest or farthest from the firearm during that shot, so the positioning cannot be the reason behind that.

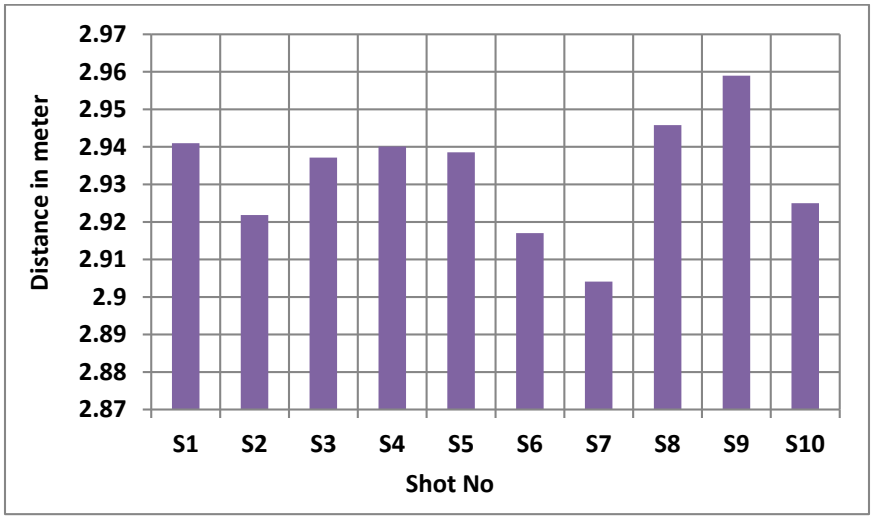

Figure 5.12.1: Distances from the firearm to M4 (for 10 shots of AR15)

For Glock 23, only for S9, the prediction was higher than the real value. This is realizable, as for this shot, M4 was the farthest from the firearm, as seen from figure 5.12.2. But S8 was not the nearest but recorded a very high pressure at M4, provided the largest prediction error.

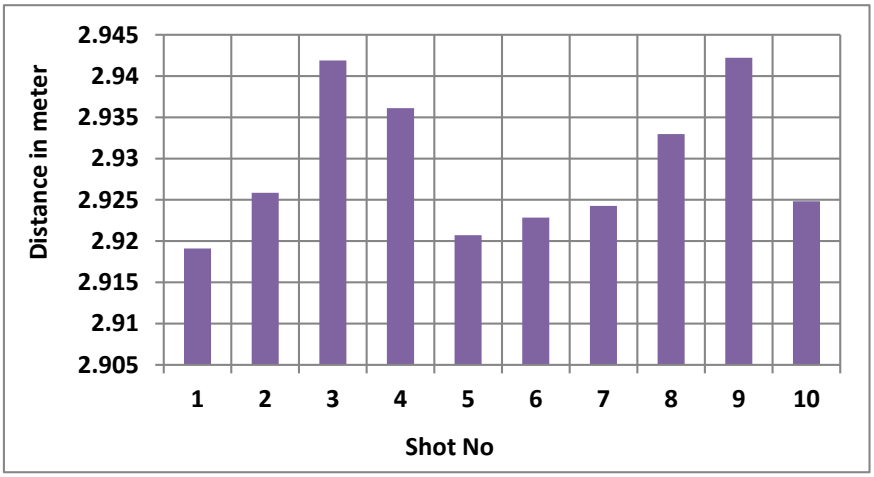

Figure 5.12.2: Distances from the firearm to M4 (for 10 shots of Glock 23)

For Glock 19/135 JHP, the predictions were higher than the recorded pressures in S3, S7 & S10. One of the reasons can be that for those shots, M4 was far from the firearm than the others. But as seen from figure 5.12.3, that has not been the case. S3 was the closest, the recorded pressure was the highest but prediction was even higher. One of the reasons can be other microphones were also nearer to the firearm to interpolate a higher value at that azimuth. Recorded pressure from S5 and S6 were nearly the same, although their distances from the firearm were not.

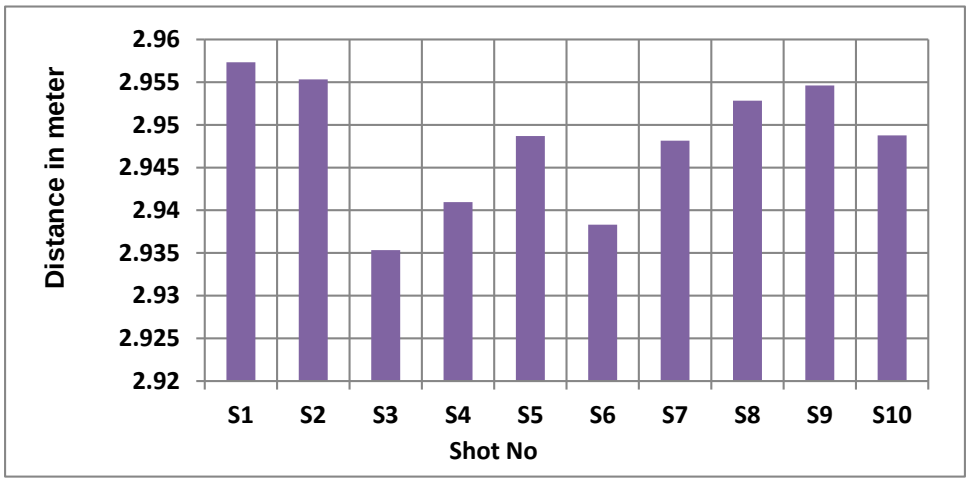

Figure 5.12.3: Distances from the firearm to M4 (for 10 shots of Glock 19/135 JHP)

The predicted pressure values were higher for S2 and S9 for Ruger SP101-357. For both of these shots, distances from M4 to firearm were neither the highest nor the lowest. S10 was one of the farthest shots from the firearm for M4, but generates a high pressure value.

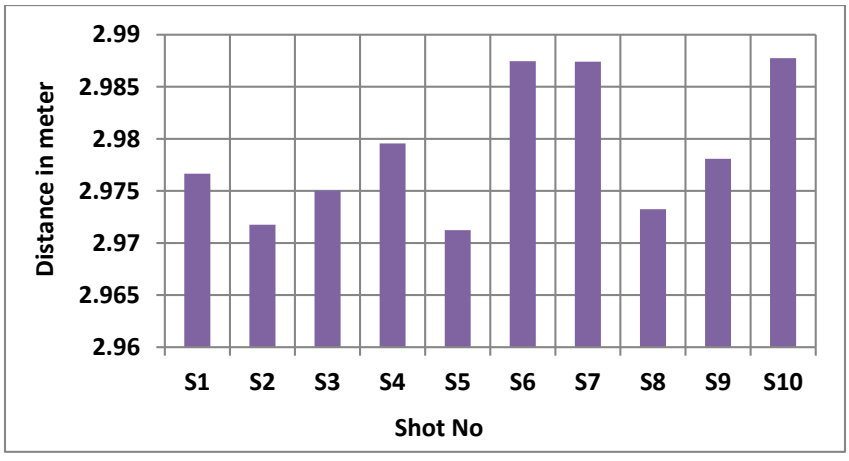

Figure 5.12.4: Distances from the firearm to M4 (for 10 shots of Ruger 101-357)

For 357 caliber shot with Sig 239 pistol, the closest prediction was for S8. The highest pressure value at M4 was observed at S9 in spite the fact that it was the largest distant shot from that azimuth (figure 5.12.5).

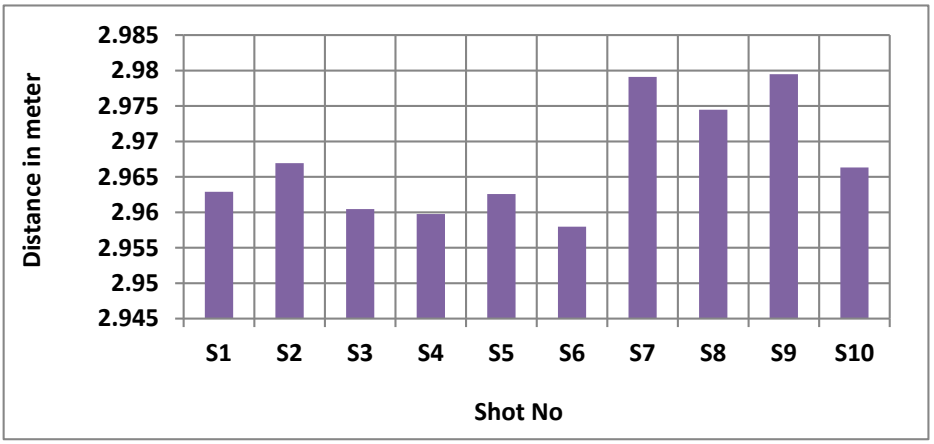

Figure 5.12.5: Distances from the firearm to M4 (for 10 shots of Sig 239-357)

For 12ga, only 3 shots were observed. For S2, the prediction was higher. For that shot, the firearm might be at higher distance than other shots from M4. But observing the displacement data (figure 5.12.6), it is not proven that the shot was the most distant shot from the firearm to M4.

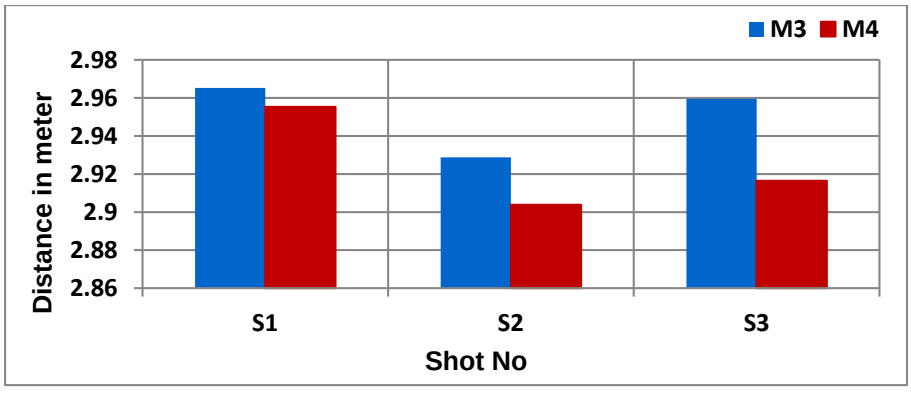

Figure 5.12.6: Distances from the firearm to M4 (for 3 shots of 12ga)

5.13 Relationship between Parameters

The location of the 12ga shotgun on the figure 4.14.1 is at the rightmost side, the total mass of the pellets from a single shot is much higher than other single round bullet. The bullet mass for AR 15 is much lower compare to 12 ga, but generates higher pressure value at receivers. From our analysis, it is hard to conclude regarding any dependency of muzzle peak pressure with the bullet mass.

The way the bullet diameter affected the peak pressure outputs is observed with polynomial and exponential relationships. From figure 4.14.2 and 4.14.3, we can observe there were bullets of nearly the same diameter that generated different pressure values. 12ga pellets have a larger diameter compare to others and generate a very high peak pressure; but lower than rifle bullets. From polynomial relationship, it is seen that there is a reduced peak pressure for bullet diameter around 0.6 mm, the reason behind which could not be explored here. From such small number of observations, it is hard to decide whether such relationship are actually present in real life and whether bullet mass regulates the pressure level at microphones.

From 4.14.4, we can see that the speed of rifle bullets were the highest and they also generate higher pressure values, but why there is a rise of pressure at 2000 feet is not realizable. Perhaps such values only appeared from the fact of fitting the points in polynomial fashion. The logarithmic seems much conclusive, as there is a rise of pressure for bullets having greater speed.

From the linear relationship model, we observe that such linear model cannot predict the pressure levels with same accuracy for different categories of firearm. The pressure prediction errors were the lowest for the rifle category, apart from 0.22 calibers. The highest error was observed for Glock 19/135 JHP. It is hard to conclude with this analysis that whether the relationship between the output peak pressure value and the input parameters are actually linear in nature.

5.14 Future Work

As we have seen through this paper, muzzle blast signals are directional, and the pressure amplitude depends on the azimuth. At higher azimuths, the pressure amplitude tends to decrease. Keeping that in mind, we would like to reorient our microphone array for our next experiments to maximize the dynamic range of the recording system. The microphones will be deployed in such a fashion that microphones having higher sensitivity will be placed where the pressure amplitude is lower (high azimuths behind the shooter) and the less-sensitive microphones will be used in front of the firearm where the sound level is higher.

One of the concerns for our analysis was the hand-held positioning of the firearms. If the muzzle is repositioned for successive shots, this may create pressure variations at the microphones from one shot to the next. Our future plan is to keep the position of the firearm more precisely fixed for successive shots. In addition, we will investigate the use of a certified firearm mount so that repeatable shots can be made without hand-held positioning.

Based on the observed shot-to-shot variations, a question arises about whether the physical variation among bullets was responsible. In the future, it will be useful to repeat the tests with “match grade” ammunition so that the physical variability is minimized. Gunshot sound characteristics presumably depend upon the internal details of the ammunition load, the firing chamber, and the gun barrel. Measuring and matching the physical properties of each ammunition cartridge prior to shooting will be the standard practice.

The speed of the bullets was also a very important factor. As seen from our study, if all the conditions were same for consecutive shots, the variation of the speed of the traveling bullets from one shot to other could cause pressure variation at the microphones. We have plans to use a speed measuring apparatus (chronograph) to record the speed of the bullet during each shot.

The gunshots from the CZ452 rifle using 0.22 caliber rim fire bullets were too quiet for analysis because the microphone sensitivities and preamplifier gain settings were adjusted to accommodate the very high peak pressures from the other firearms. In the future, we plan to observe those signals with higher gain settings, thereby utilizing the maximum dynamic range of the recording system for each type of firearm.

The attenuators we used with G.R.A.S. 12AG amplifiers were mini circuit 20dB attenuators having a characteristic impedance of 75 ohms. However, the effective attenuation was not exactly 20dB for each channel, due to differences in the input impedance of each channel of the audio amplifier system. In our next experiment, we would like to match the attenuators with the amplifier to get precise attenuation.

Both the methods we used for calculating the Muzzle blast duration have their own limitations. In times to come, we would like to develop a more advanced and reliable method to determine durations more precisely and repeatedly.

Our experiment was limited to nine types of firearms and ten types of ammunition. The only firearm that was used with two different types of bullets was the Ruger SP 101 revolver. Our future endeavor will include covering a larger variety of firearms with different types of ammunition.

Finally, this experiment was focused upon experimental recording and analysis of empirical data. In the future, analytical and theoretical work will be needed to provide an explanation of the observed acoustical phenomena.

6. CONCLUSIONS

Acoustic gunshot signals show variations in acoustical attributes depending on the azimuth of the recording microphone and the particular type of firearm. In general, the peak sound pressure decreased with increasing azimuth, although for some shots the decline in level with increasing azimuth was not monotonic. In all cases the peak pressure behind the shooter (approaching 180° azimuth) was lower than in front of the shooter (near 0° azimuth).

There was a detectable variation from one shot to another in successive shots from the same firearm. Shot-to-shot differences may be due to differences in the ammunition cartridge, differences in the exact location of the hand-held firearm that was manually repositioned between shots, and possibly the chaotic nature of the combustion and muzzle blast production details.

Different types of firearms have different acoustical features which also vary with the type and size of ammunition used with that firearm. The acoustical energy of the muzzle blast is directional, and the directionality depends on the firearm and the type of ammunition.

Observing the peak pressure values, it can be concluded that the rifle and shotgun muzzle blasts generate higher pressure values at the microphones than the handguns (pistol and revolver), but again this depends on the type and size of ammunition that was being used. For example, the 22 caliber rifle with rim fire bullets generates the lowest peak sound pressure among all of the firearms tested.

When we tried to determine the duration of the muzzle blast signals using time waveform observation, we saw high frequency fluctuations, apparently random in nature, which resulted in shot-to-shot variability. As the fluctuating pressure values were high enough to overcome low amplitude background noise, it cannot be concluded whether the fluctuations were innate acoustical signatures of that particular firearm and ammunition, or if they were attributable to some aspect of the microphones and recording system.

To find out the relation of between gunshot recordings, linear relationship based analysis was used. In this study, we have only tried to make an observation, no hypothesis or theory has not been tried to prove. Based on our observation, we have seen that when we correlated a particular gunshot signal recorded at a particular azimuth with signals recorded at other azimuths, the correlation factor showed azimuthal variation for successive shots. In some cases, the correlation factors were higher when comparing signals from different firearms than for the same firearm, so higher correlation factors do not necessarily indicate that two highly-correlated signals were from the same firearm. The azimuthal variations of correlation factors were similarly inconclusive. Our experimental data and real life modeled gunshot recording data (comparison made after bandlimited down sampling and then filtering) have a considerable amount of correlation. But again, in some cases, the correlation was higher in different firearms than the similar one. Higher sampling rate does not ensure better correlation, as seen from our analysis. Although one of the prime goals of this study was to answer how similar were the successive shots, what are the resemblances of gunshot recordings for different firearms etc., we conclude that the attempts to use linear correlation to compare and contrast

different firearms and recordings from different azimuths are not recommended. How to correlate different gunshot signals may require a different method of investigation, like wavelet analysis.

The accuracy of muzzle blast peak pressure predictions at a particular azimuth was not same in all the cases, as seen from our comparison with experimental data. Based on our analysis, we can at least have an idea of the directionality of the gunshot muzzle blast. We had our acoustical data from the other 11 microphones to make that prediction. In real life, the availability of recordings may not be sufficient for such analysis.

Comparing the output muzzle blast peak pressure values with variables such as the bullet size, weight, and velocity, we have seen that there is no simple linear relationship between the output and input variables. There are likely additional governing factors, like barrel length and other firearm details that govern the muzzle blast peak pressure and other acoustical features of gunshot signals.

REFERENCES CITED

American Private Inverstigator, 2013. Paul Jaeb With Guests Dr. Rob Maher, Treyce Montoya, Hal Humphreys, Jim McCloud and Alan Goodman. Available at: http://americanprivateinvestigator.com/2013.

Anon, Remington Express Ammunition 12 Gauge 3" 00 Buckshot 15 Pellets Box of 5. Available at: https://www.midwayusa.com/product/123030/remington-express-ammunition-12-gauge-3-00-buckshot-15-pellets-box-of-5.

Baker, W.E., 1973. General Phenomenology. In *Explosion in air*. University of Texas Press, Austin & London.

Beck, S.D., Nakasone, H. & Marr, K.W., 2011. Variations in Recorded Acoustic Gunshot Waveforms Generated by Small Firearms. *The Journal of the Acoustical Society of America*, 129(4), pp.1748–59. Available at: http://www.ncbi.nlm.nih.gov/pubmed/21476632.

Blackstone Shooting Sports, Shooting Vocab: The difference between Rimfire and Centerfire ammo. Available at: http://www.blackstoneshooting.com/shooting-vocab-the-difference-between-rimfire-and-centerfire-ammo.

Hamernik, R.P. & Hsueh, K.D., 1991. Impulse noise: some definitions, physical acoustics and other considerations. *The Journal of the Acoustical Society of America*, 90(1), pp.189–196. Available at: http://link.aip.org/link/?JASMAN/90/189/1.

Heard, B. J., 2008. *Handbook of Firearms and Ammunition* 2nd ed., Wiley-Balckwell.

Hirsch, K. & Bertels, W., 2013. Estimation of the Directivity Pattern of Muzzle Blasts. *Progress of acoustics*, pp.2–3.

Hirsch, K.W., 1998. On the influence of local ground reflections on sound levels from distant blasts at large distances. *Noise Control Engineering Journal*, 46(5), p.215. Available at: http://www.ingentaconnect.com/content/ince/ncej/1998/00000046/00000005/art00005.

Http://www.ruger.com, RUGER SP101®. Available at: http://www.ruger.com/products/sp101/models.html.

Klingenberg, G., 1989. Gun Muzzle Blast and Flash. *Propellants, Explosives, Pyrotechnics*, 14(2), pp.57–68. Available at: http://doi.wiley.com/10.1002/prep.19890140204.

Maher, R. C. & Routh, T.K., 2015. Advancing Forensic Analysis of Gunshot Recordings.

In *Audio Engineering Society Convention 131*. New York, pp. 1–8.

Maher, R.C. & Shaw, S.,2010. Directional aspects of forensic gunshot recordings. *39th International Conference: Audio Forensics: Practices and Challenges*, 4(2), pp.1–6. Available at: http://www.aes.org/e-lib/browse.cfm?elib=15491.

Maher, R.C.& Shaw, S., 2014. Gunshot recordings from digital voice recorders. *AES 54th International Conference, London*, pp.1–7. Available at: http://www.coe.montana.edu/ee/rmaher/publications/maher_aesconf_0614_1-7.pdf.

Maher, R.C., 2009. Audio forensic examination. *IEEE Signal Processing Magazine*, 26(2), pp.84–94.

Maher, R.C., 2010. Overview of audio forensics. *Studies in Computational Intelligence*, 282, pp.127–144.

Needham,C.E., 2010. *Blast Waves*, I. G. Ben-Dor, U. F. K. Lu, & U. N. Thadhani, eds., Springer.

Routh,T.K. & Maher,R.C., 2016. Determining the muzzle blast duration and acoustical energy of quasi-anechoic gunshot recordings. *AES 141st Convention*. Los Angeles.

Sigsauer.com, P239 product details. Available at: http://www.sigsauer.com/CatalogProductDetails/p239.aspx.

Snow, W., 1967. Survey of Acoustic Characteristics of Bullet Shock Waves. *IEEE Transactions on Audio and Electroacoustics*,(3),pp.161–176.

Tachibana, H., Hiroo Yano & Yoshihisa, K., 1987. Definition and measurement of sound energy level of a transient sound source. *Journal of the Acoustical Society of Japan (E)*, 8(6), pp.235–240. Available at: http://ci.nii.ac.jp/naid/110003105806.

Thai, D.Z., Hashemi-sakhtsari, A. & Pattison, T., Speaker Localisation Using Time Difference of Arrival.,1994, *Science And Technology*, pp.1–6.

University of Iowa, 2004. Basic Statistics. ,1(3), pp.153–173. Available at: http://doi.org/10.1007/978-3-662-09621-5_9.

www.bayoushooter.com, Glock 19 gen 3 Homeland Defender edition with night sights. Available at: http://www.bayoushooter.com/forums/showthread.php?92250-SOLD-Glock-19-gen-3-Homeland-Defender-edition-with-night-sights.

www.luckygunners.com, 308 - 175 Grain HP-BT - Federal Premium Sierra Match King Gold Meda. Available at: http://www.luckygunner.com/308-175-gr-hp-bt-federal-premium-sierra-match-king-200-rounds.

www.luckygunners.com, 357 Mag - 158 Grain JSP - Federal American Eagle - 50 Rounds. Available at: http://www.luckygunner.com/federal-357-mag-ammo-for-sale-357mag158jspfederal-50#info.

www.luckygunners.com, 357 Sig - 125 Grain JHP - Winchester USA - 50 Rounds. Available at: http://www.luckygunner.com/winchester-357-sig-ammo-for-sale-357sig125sjhpwinusa-50#info.

www.luckygunners.com, 5.56 NATO - 62gr Lake City M855 Ball FMJ. Available at: http://www.luckygunner.com/5-56x45mm-62gr-fmj-xm855-90-rounds.

www.luckygunners.com, 9mm - +P - 135 gr FlexLock JHP - Critical Duty - Hornady. Available at: http://www.luckygunner.com/9mm-135-gr-p-jhp-flexlock-hornady-critical-duty-250-rounds.

www.midwayusa.com, Fiocchi Ammunition 22 Long Rifle 40 Grain Plated Lead Round Nose. Available at: https://www.midwayusa.com/product/1836418274/fiocchi-ammunition-22-long-rifle-40-grain-plated-lead-round-nose.

www.remington.com, Remington 870. Available at: https://www.remington.com/shotguns/pump-action/model-870.

www.usacarry.com, Does a 38 Cal. hollow points vs 357 Cal. 9.07 mm 38 special have same power ? Available at: http://www.usacarry.com/forums/handgun-discussion/47155-does-38-cal-hollow-points-vs-357-cal-9-07-mm-38-special-have-same-power.html.